



HAL
open science

Effets Zeeman dans les supraconducteurs à électrons lourds

Vincent P. Michal

► **To cite this version:**

Vincent P. Michal. Effets Zeeman dans les supraconducteurs à électrons lourds. Matière Condensée [cond-mat]. Université de Grenoble, 2012. Français. NNT : 2012GRENY043 . tel-01466162

HAL Id: tel-01466162

<https://theses.hal.science/tel-01466162>

Submitted on 13 Feb 2017

HAL is a multi-disciplinary open access archive for the deposit and dissemination of scientific research documents, whether they are published or not. The documents may come from teaching and research institutions in France or abroad, or from public or private research centers.

L'archive ouverte pluridisciplinaire **HAL**, est destinée au dépôt et à la diffusion de documents scientifiques de niveau recherche, publiés ou non, émanant des établissements d'enseignement et de recherche français ou étrangers, des laboratoires publics ou privés.

THÈSE

Pour obtenir le grade de

DOCTEUR DE L'UNIVERSITÉ DE GRENOBLE

Spécialité : **Physique de la matière condensée**

Arrêté ministériel : 7 août 2006

Présentée par

Vincent P. Michal

Thèse dirigée par **Vladimir P. Mineev**

préparée au sein du **CEA Grenoble - Service de Physique Statistique, Magnétisme et Supraconductivité - Groupe Théorie**
et de l'**Ecole Doctorale de Physique de Grenoble**

Zeeman effects in heavy electron superconductors

Thèse soutenue publiquement le **31 Octobre 2012**,
devant le jury composé de :

Pr. Laurent Levy

Institut Néel Grenoble, Président

Pr. Andrei Chubukov

University of Wisconsin Madison, Rapporteur

Pr. Manfred Sigrist

ETH Zürich, Rapporteur

Pr. Alexandre Bouzdine

Université Bordeaux 1, Examinateur

Dr. Stéphane Raymond

CEA Grenoble & ILL, Examinateur

Pr. Vladimir Mineev

CEA Grenoble, Directeur de thèse



Acknowledgments

Many of my thanks go to my family and friends for constant support throughout the years. My director Vladimir Mineev also fully deserves my gratitude for invaluable advice and education.

I acknowledge my colleagues at CEA, both fellow students and staff scientists with whom I shared profitable moments at work and aside. Engaged debates with some of the CEA theoreticians were wonderful and maintaining connection with experimentalists was a memorable experience.

I'm also grateful to people of the physics community I've met at work, in conferences or summer schools, and with whom I shared insights over the past three years.

All sources of inspiration I had in my thesis in the domain of physics or elsewhere were fundamental. I would like to give a lot of my thanks to people driven by curiosity and inhabited by the desire of sharing this.

Abstract

Understanding the properties of newly discovered strongly correlated electron compounds is a considerable challenge for both fundamental matters and long-term industrial impact. Experimental activity on heavy electron metals and superconductors has lead to highlighting effects that depart from current knowledge. The thesis is aimed at modelling effects that have been observed in response to magnetic field in the heavy electron superconductor CeCoIn_5 . This consists of two parts.

In the first time we deal with the vortex lattice state anomalous local magnetic field space variations as highlighted by small angle neutron scattering and muon spin rotation experiment. On the basis of the Ginzburg-Landau theory with account of spin effect, we analyse the local field inhomogeneity in the vortex lattice and derive expressions for the neutron scattering form factors and muon spin rotation static linewidth. The anomalous experimental data are shown to be result of spin driven supercurrents which circulate around the vortex cores and lead to an increase with external field in the internal field inhomogeneity on a distance of the order of the superconducting coherence length from the vortex axis. The importance of the effect is controlled by a single quantity (the Maki parameter).

The second part is on nearly commensurate spin density wave transition in a quasi two-dimensional superconductor. It is motivated by observation of the confinement of spin density wave ordering inside the superconducting state of CeCoIn_5 in magnetic field. In the frame of the spin-fermion formu-

lation we propose a mechanism for the ground state transition consisting in the field-induced slowing down of a collective spin density fluctuation mode (spin-exciton) to static ordering. This represents a scenario by which the transition to spin ordering is intrinsically related to superconductivity.

Contents

1	Background material	14
I	Vortex lattice anomalous local magnetic field variations	21
2	Vortex lattice electrodynamics	22
2.1	Experimental facts	22
2.2	Qualitative considerations at zero temperature	26
2.3	Neutron scattering form factors and muon spin rotation static linewidth	28
2.4	Ginzburg-Landau free energy and equations	29
2.4.1	Free energy	30
2.4.2	Ginzburg-Landau equations and characteristic lengths .	31
2.4.3	Discussion	32
2.5	Addendum: Derivation of the Ginzburg-Landau free energy . .	34
3	Independent vortex regime	39
3.1	Critical fields in the vicinity of T_c	40
3.2	Independent vortex limit	41
3.3	Charge driven diamagnetic currents and orbital form factors .	43
3.3.1	Clem variational gap structure for a single vortex . . .	43
3.3.2	Discussion	44

3.4	Spin driven currents and Zeeman effect in neutron scattering form factors and muon spin rotation static linewidth	45
3.4.1	Derivation of the single-vortex local field	45
3.4.2	Neutron scattering form factors and muon spin rota- tion static linewidth	51
3.4.3	Discussion	55
4	Proximity to critical field	56
4.1	Abrikosov's solution of the linearised Ginzburg-Landau equation	57
4.2	Vortex lattice form factors and static line-width	58
4.3	Discussion	60
5	T-dependent Ginzburg-Landau parameter	63
5.1	The critical field temperature derivative	65
5.2	Comparison with previous results	66
6	Conclusion part I	69
II	Field-induced spin-exciton condensation	71
7	Superconductivity and magnetism	72
7.1	Background information	74
7.2	Model considerations	78
7.2.1	Electronic structure quasi two-dimensionality and su- perconductor $d_{k_a^2-k_b^2}$ -wave pairing symmetry	78
7.2.2	Spin-fermion model	80
7.3	Addendum: Fermion excitation energy spectrum for a super- conductor in Zeeman magnetic field	85
8	Spin-exciton slowing-down	87
8.1	Analytic approach	88
8.2	Numerics	96

8.3	Discussion	102
8.4	Addendum: Derivation of the spin polarisation function Eq. (8.14)	105
9	Conclusion part II	107
10	Résumé	124
11	Conclusion de la première partie	126
12	Conclusion de la deuxième partie	128

List of Figures

1.1	Ce115 phase diagram	18
1.2	CeCoIn ₅ crystal structure	19
2.1	Anomalous experimental form factor (Bianchi)	23
2.2	Anomalous experimental muon spin rotation static linewidth (Spehling)	24
2.3	CeCoIn ₅ phase diagram ($H \parallel c$)	25
2.4	Sketch of vortex lattice section	26
3.1	Local field profile around a single vortex	50
3.2	μSR static linewidth dependence on internal field	53
3.3	Experimental form factor data fit	54
4.1	Abrikosov μSR static linewidths	59
4.2	Abrikosov form factors	61
4.3	Experimental form factors (White)	62
7.1	High-field-low-temperature phase (Kenzelmann)	73
7.2	Spin resonance (Stock)	76
7.3	de-Haas-van-Alphen oscillation frequencies (Settai)	79
7.4	$d_{k_a^2-k_b^2}$ -wave symmetry order parameter	81
7.5	Fermi pockets in Zeeman magnetic field	86
8.1	Model Fermi line	88

8.2	Particle-hole decay threshold	92
8.3	Spin polarisation function	93
8.4	Spin-exciton dispersion	95
8.5	Static polarisation functions dependence on internal field . . .	98
8.6	Dynamic spin susceptibility spectral function	100
8.7	Fit of experimental resonance energy dependence on field . . .	101

List of Symbols

Below is a list of symbols most often used in the text. Throughout we consider units where the reduced Planck constant $\hbar = 1$ and the velocity of light $c = 1$.

Symbol Meaning

α_{M0}	Zero temperature Maki parameter
α_M	Finite temperature Maki parameter
$\mathbf{A}(\mathbf{r})$	Electromagnetic vector potential
B	Induction or norm of superconductor internal field spatial average
B_0	Tricritical point field
β_A	Abrikosov parameter
\mathbf{D}	Gauge invariant gradient
$\Delta_k(\mathbf{r})$	Superconductor local order parameter
$\Delta(\mathbf{r})$	Isotropic part of local superconductor order parameter
Δ_∞	Single vortex gap asymptotic magnitude far from axis
e	Electron charge absolute value
E_F	Fermi energy
F_{mn}	Fourier coefficients of the local field
$F_d[h]$	d-dimensional Fourier transform of function h
g	Electron gyromagnetic ratio

γ_μ	Muon gyromagnetic ratio
γ_d	Landau damping parameter in layered metal
$\mathbf{h}(\mathbf{r})$	Vortex lattice local internal magnetic field
$\mathbf{h}_v(\mathbf{r})$	Single vortex local magnetic field
H	Norm of external magnetic field
H_{c10}	Zero temperature lower critical field
H_{c20}	Zero temperature upper critical field
H_{c20}^{orb}	Scale of zero temperature orbital critical field
H_{c20}^{p}	Scale of zero temperature Pauli critical field
H_{c2}	Ginzburg-Landau upper critical field
H_{c2}^{orb}	Ginzburg-Landau orbital critical field
H_{c2}^{p}	Ginzburg-Landau Pauli critical field
$\mathbf{j}(\mathbf{r})$	Total local electron current density
$\mathbf{j}^{\text{orb}}(\mathbf{r})$	Orbital electron current density
$\mathbf{j}^{\text{Z}}(\mathbf{r})$	Zeeman electron current density
$\mathbf{j}_v(\mathbf{r})$	Current density for a single vortex
κ	Ginzburg-Landau parameter
κ_{eff}	Effective Ginzburg-Landau parameter
K_n	n^{th} -order MacDonald function
k_F	Fermi wave-vector
ℓ_{ab}, ℓ_c	Tetragonal crystal lattice parameters
λ_L	London penetraton depth
λ	Ginzburg-Landau penetration depth
$L(B)$	Spacing between vortices in the square vortex lattice
m	Electron bare mass
m^*	Heavy electron effective mass
\mathbf{M}	Diamagnetic magnetization
μ	Electron magnetic moment absolute value
μ_B	Bohr's magneton
n	Electron density in the layered metal

n_s	Superconductor electron density
N_0	Layered metal density of states (for one spin)
$\Omega_0(\mathbf{q})$	Particle-hole decay threshold energy dispersion
$\Omega_{\text{res}}(\mathbf{q})$	Resonance energy dispersion
ϕ_0	Superconductor vortex flux quantum
$\psi(\hat{k})$	Anisotropic part of local superconductor order parameter
\mathbf{q}_{mn}	Vortex lattice reciprocal wave-vectors ($q_{mn} = \mathbf{q}_{mn} $, $q = q_{01}$)
\mathbf{Q}	Antiferromagnetic wave-vector
σ	Electron pseudo-spin
σ_s^{VL}	Muon spin rotation vortex lattice static line-width
r_e	Classical radius of the electron
T	Temperature
T_c	Superconductor critical temperature
T^*	Spin density wave instability temperature
T_0	Tricritical point temperature
T^\times	Crossover temperature from orbital limiting to Pauli limiting
T_K	Kondo temperature
T_{coh}	Kondo lattice coherence temperature
v_F	Fermi velocity
ξ_0	Scale of superconductor coherence length at zero temperature
ξ	Ginzburg-Landau coherence length
ξ_v	Single vortex gap structure variational parameter
ξ_m	Magnetic coherence length
$\zeta(z)$	Riemann zeta function

Chapter 1

Background material

This introductory chapter is intended to briefly recall to the non-specialist reader the basic notions that constitute the core of the thesis. This concerns the vast domain of unconventional (anisotropic) superconductivity, the very active field of heavy electron systems and the way heavy electron superconductors respond to magnetic field. We further present the experimental system CeCoIn₅ that we refer throughout as a prototypical heavy electron superconductor displaying a number of properties that interest us. For any detail on classical superconductivity and derivation of results discussed below, we refer the reader to the core literature listed in the end of the manuscript and cited specialised references.

Superconductivity (Onnes, 1911) is a quantum mechanical ground state that arises upon cooling a metal¹ (*c. f.* [1] for historical review on superconductivity and references therein). At some critical temperature T_c one measures a discontinuity in specific heat, vanishing DC resistivity, perfect diamagnetism below some magnetic field H_{c1} (Meissner effect, 1933)², and

¹Throughout we understand the term metal as the non-superconducting state.

²For magnetic fields between the *lower critical field* H_{c1} and the *upper critical field* H_{c2} , the superconductor incorporates an Abrikosov's [2] *vortex lattice* consisting of lines parallel to the external field where the order parameter vanishes and around which electron currents circulate. At field greater than H_{c2} the system transits from superconductor

a gap opening in the electron excitation energy spectrum $E(\mathbf{k})$ with \mathbf{k} the electron momentum. This has been microscopically understood (Bardeen-Cooper-Schrieffer [BCS], 1957) as a consequence of electron binding into pairs (Cooper, 1956) all described by a single two-electron wave-function.

Original description of superconductivity involves Cooper pairing mediated by crystal phonons yielding punctual attraction between electrons and isotropic form of the two-electron wave-function. We refer to the description of classical (isotropic, phonon-mediated) superconductors as *conventional superconductivity*. In contrast, in new superconductors [including heavy electrons (Steglich, 1979), organics (Bechgaard, 1979), high- T_c cuprates (Bednorz and Muller, 1986), Sr_2RuO_4 (Maeno *et. al.*, 1994), and iron-pnictides (Hosono group, 2008)] and superfluid ^3He (Osheroff, Richardson and Lee, 1972), the center of mass two-spin-1/2-particle wave-function written in term of relative coordinate (consider first translationally invariant system)

$$\Psi_{\alpha\beta}(\mathbf{r}) = \langle \psi_{\alpha}(\mathbf{r})\psi_{\beta}(\mathbf{0}) \rangle \quad (1.1)$$

is anisotropic in space. Anisotropy of the Cooper pair wave-function in novel superconductors is a feature of *unconventional superconductivity* [MineevSamokhin], [3]. Here α and β are pseudo-spin projection quantum numbers (we shall consider throughout systems of spin-1/2 fermions)³, $\psi_{\sigma}(\mathbf{r})$ is the electron annihilation operator in coordinate representation, $\langle \cdot \rangle$ can be understood as ground state average at zero temperature or Gibbs average at finite temperature.

The wave-function Eq. (1.1) can be written as a product of an orbital part and a spin part

$$\Psi_{\alpha\beta}(\mathbf{r}) = \phi(\mathbf{r})\Sigma_{\alpha\beta}. \quad (1.2)$$

to metal.

³In system with spin-orbit coupling electron spin is not a good quantum number but electron states remain two-fold degenerate if time-reversal symmetry is preserved. As a consequence electron states still can be classified in term of pseudo-spin. In the following we will often use the word spin to implicitly refer to pseudo-spin.

The Pauli principle requires $\Psi_{\beta\alpha}(-\mathbf{r}) = -\Psi_{\alpha\beta}(\mathbf{r})$. One can distinguish two cases depending on the parity symmetry of $\phi(\mathbf{r})$ [*c. f.* footnote⁴]. If the spatial part is even $\phi(-\mathbf{r}) = \phi(\mathbf{r})$ then $\Sigma_{\alpha\beta} = -\Sigma_{\beta\alpha}$ (we choose $\Sigma_{\uparrow\downarrow} = 1$ where \uparrow denotes the spin projection of the first electron *etc.*), and $\Psi_{\alpha\beta}(\mathbf{r})$ is referred to as spin-singlet superconducting state (classical, Ce-based with space-inversion symmetry, high- T_c , iron-based superconductors belong to this class). On the contrary if the spatial part is odd $\phi(-\mathbf{r}) = -\phi(\mathbf{r})$ then $\Sigma_{\alpha\beta} = \Sigma_{\beta\alpha}$, and we are dealing with a spin-triplet state (superfluid ^3He and some Uranium-based superconductors are of this class). In what follows we focus on singlet superconductivity. In crystals pair wave-functions are classified according to irreducible representations⁵ of the point symmetry group of the non-superconducting phase [4]. In particular the isotropic state that transforms according to the A_{1g} irreducible representation (corresponding to the identity element) is called s -wave while the anisotropic state that transforms according to the B_{1g} irreducible representation is called d -wave. These notations are borrowed from orbital quantum state labelling in atomic physics.

A central role is played by the order parameter $\Delta_k(\mathbf{r})$, the index k accounting for the space anisotropy of the state and the coordinate giving its space-inhomogeneity. Inspired by the early work of London (1937), Landau and Ginzburg (1950) introduced this complex function to phenomenologically describe persistent currents (or *supercurrents*) and Meissner effect from the superconductor free energy expressed as a polynomial of $\Delta_k(\mathbf{r})$ and its gauge-invariant gradient. The complex modulus $|\Delta_k(\mathbf{r})|$ in addition represents the

⁴There can be a superposition of the two in system with no space-inversion symmetry where the electron excitation spectrum $\epsilon_{-k\sigma} \neq \epsilon_{k\sigma}$.

⁵A set of functions $\phi_i(\mathbf{r})$ constitute a basis of an irreducible representation Γ of a symmetry group G if any function of this set transforms under operation of an element of this group as $\phi_i^\Gamma(g\mathbf{r}) = \sum_{j=1}^d c_{ij}^\Gamma \phi_j^\Gamma(\mathbf{r})$ with d the dimension of the irreducible representation. Each state corresponding to an irreducible representation has a different critical temperature T_c^Γ .

gap in the fermion excitation energy spectrum in the BCS theory⁶. We shall see next how Gor'kov's Green's function formalism allows computation of the coefficients of the Ginzburg-Landau free energy.

The experimental systems that concern us are heavy electron (or heavy fermion) compounds (Andres, Graebner and Ott, 1975) and Ce based CeMIn₅ [5, 6, 7, 8] in particular [*c. f.* Fig. (1.1)]. Before describing their behaviour as superconductors we state some of their properties at temperatures $T > T_c$ [9]. Rare earth atoms containing unfilled f-electron shells (Ce, Yb, U, or Pu for instance) form an array of localized spins interacting with conduction s-p-d electrons. While a single magnetic impurity gives rise to Kondo effect (resistivity minimum at Kondo temperature scale T_K with screening of the impurity spin), the Kondo lattice has a regime (depending on the localized electron band energy level with respect to the Fermi energy of the itinerant band) where the two bands hybridize with resistivity decrease as temperature lowers to the Kondo lattice energy scale T_{coh} . The obtained electron states are characterized by a large effective mass m^* that can be of the order 100 to 1000 times the bare electron mass m . The formation of heavy electrons as temperature is lowered is observed experimentally [10] and described by mean field theory [9] and dynamical mean field theory [11] of the Anderson model. As displayed by Fig. (1.1) phase diagrams of heavy electron materials are rich with ground state transitions occurring upon doping, applying pressure, or magnetic field. Most often seen is the development of superconductivity in the phase diagram region close to a ground state change [1, 9, 12].

Regarding the superconducting state one approach, justified in the limit $T_c \ll T_{\text{coh}}$, is to consider superconductivity as formed by the heavy electrons.

⁶In the BCS theory the order parameter is introduced as

$$\Delta_k = - \sum_p V(\mathbf{k}, \mathbf{p}) \langle a_{p\uparrow} a_{-p\downarrow} \rangle, \quad (1.3)$$

where $a_{p\sigma} = \int d^d r \psi_\sigma(\mathbf{r}) e^{-i\mathbf{p}\cdot\mathbf{r}}$ is the electron annihilation operator in momentum space (d is dimension), and the energy potential $V(\mathbf{k}, \mathbf{p})$ is included in the model interaction Hamiltonian as $H_{\text{int}} = \sum_{k,p} V(\mathbf{k}, \mathbf{p}) a_{k\uparrow}^\dagger a_{-k\downarrow}^\dagger a_{-p\downarrow} a_{p\uparrow}$.

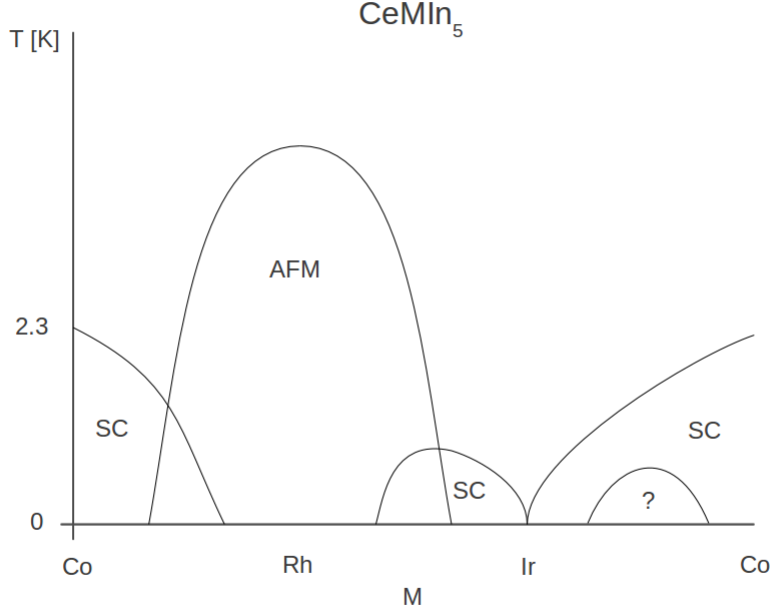


Figure 1.1: (Adapted from [7]) Phase diagram of Cerium 115 compounds CeMIn_5 in temperature and chemical composition (M can be Cobalt (Co), Rhodium (Rh), Iridium (Ir) or stoichiometric composition of two of them). SC is for d-wave superconductivity and AFM means antiferromagnetism. Remarkable regions are those where the domains overlap yielding coexisting orders. Observe appearance of superconductivity near chemical compositions where antiferromagnetic ground state transition occurs.

This quasiparticle effective mass theory yields novel qualitative behaviour when the superconductor is subject to magnetic field. The basic reason comes from comparison of energy scale of the energy of a charge in magnetic field

$$E^{\text{orb}} \sim \omega_c, \quad (1.4)$$

$\omega_c = 2eB/m^*$ being the heavy electron cyclotron frequency, with energy scale

of a spin

$$E^Z \sim \mu_B B, \quad (1.5)$$

$\mu_B = e/(2m)$ being Bohr's magneton. Hence $E^Z/E^{\text{orb}} \sim m^*/m$ as a consequence of quenching of the heavy electron orbital motion. The system loses superconductivity in magnetic field greater than H_{c2} . In the next part this upper critical field is explicitly evaluated in two limits yielding the orbital limiting field H_{c2}^{orb} (field coupling to charge) and the Pauli limiting field H_{c2}^{p} (field coupling to spin).

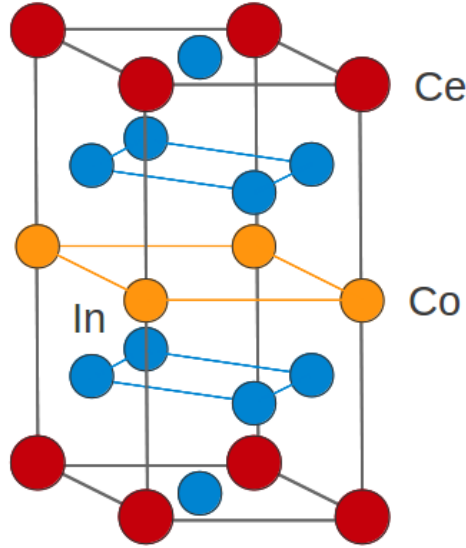


Figure 1.2: Sketch of CeCoIn_5 tetragonal crystal structure where cerium (Ce) atoms sitting on the lattice corners are represented in red, cobalt (Co) atoms are in yellow, and indium (In) atoms in blue. The lattice parameters are as follows [5]: the in-plane spacing is $\ell_{ab} \approx 4.62\text{\AA}$ while the distance between Ce layers is $\ell_c \approx 7.56\text{\AA}$.

An interesting example of a heavy electron superconductor is CeCoIn_5 , part of the Ce115 family. CeCoIn_5 crystallizes in a tetragonal lattice [*c. f.* Fig. (1.2)], it is a semi-metal (a multiband metal with both electron-like and hole-like Fermi surfaces) with non-Fermi liquid resistivity exponent (the re-

sistivity $\rho = \rho_0 + AT^n$, with $n \neq 2$) a common consequence of proximity to a transition to a new ground state [13]. The Kondo temperature $T_K \sim 7\text{K}$ while the Kondo lattice coherence temperature $T_{\text{coh}} \sim 50\text{K}$ [14]. Grown samples are in the clean limit [15] with $k_F\ell \sim 10^2$, ℓ being the electron mean free path, and the electronic structure displays remarkable two-dimensionality [16, 17]. The system becomes a superconductor below the temperature $T_c \approx 2.3\text{K}$ [5]. Passing from the cubic structure of CeIn_3 to the tetragonal crystal structure of CeCoIn_5 has given an increase of one order of magnitude for the superconductor critical temperature in accordance with the prediction [18] that reduction of dimensionality favours unconventional superconductivity. The order parameter symmetry in the system is likely to be $d_{k_a^2-k_b^2}$ -wave⁷ [19, 20, 21], a form which is often observed close to antiferromagnetism and can be analysed [22, 23, 24, 12] as a result of antiferromagnetic spin density fluctuation mediated pairing. Another particularity of the system is the low value of the Kondo temperature in comparison with the superconductor critical temperature. From this observation it has been developed a phenomenological two-fluid model [25, 26, 27, 28] (see also [29]) for explaining susceptibility and Knight shift data in superconducting CeCoIn_5 . From this point of view one electron component consists of fractions of unscreened Ce^{3+} localized magnetic moments while the other includes itinerant heavy electrons which form superconductivity. Superconducting heavy quasiparticle description has yielded good correspondence with BCS theory [27].

⁷In a two-dimensional system, such an order parameter has point nodes on the diagonals of the first Brillouin zone. We adopt the notation $d_{k_a^2-k_b^2}$ instead of the more commonly used $d_{x^2-y^2}$ to avoid confusion with a choice of a frame in part II where the x-axis is in the crystal c-axis direction.

Part I

Vortex lattice anomalous local magnetic field variations

Chapter 2

Pauli limited superconductor vortex lattice electrodynamics

This chapter consists in motivating the need for extending the original description of superconductor vortex lattice electrodynamics to the case of Pauli limited superconductivity. Experimental results are reviewed and a qualitative discussion with characteristic orders of magnitudes for heavy electron superconductors follows. The zero temperature Maki parameter $\alpha_{M0} = H_{c20}^{\text{orb}}/H_{c20}^{\text{P}}$ which plays a central role in this part is also introduced. After defining the experimentally relevant neutron scattering form factors and muon spin rotation static linewidth, we establish the basic equations of the Ginzburg-Landau theory with account of Pauli paramagnetism. The results included in chapters 2, 3, and 4 have been published in [30] and accepted for publication to [31].

2.1 Experimental facts

The motivation for looking at local magnetic field variations in the vortex lattice of heavy electron superconductors came from experiment on CeCoIn_5 with magnetic field applied perpendicularly to the tetragonal crystal layers.

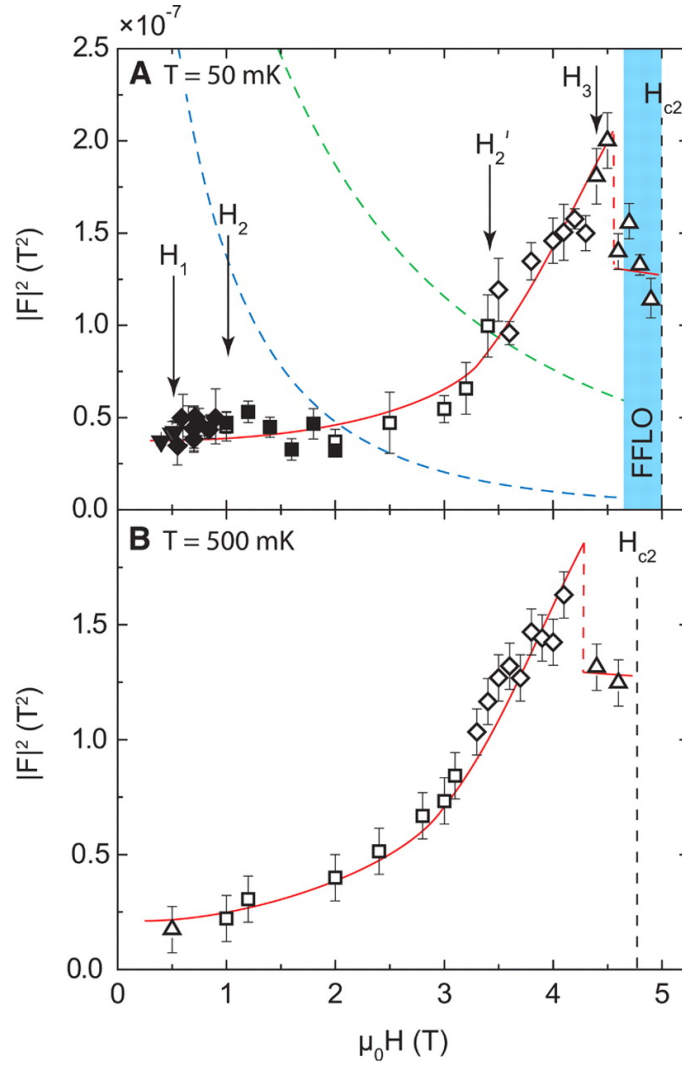


Figure 2.1: (from [32]) Anomalous external field dependence of the squared first form-factor F_{10} and comparison with existing form factor theory [33] (theoretical curves are dashed blue and green, red lines are guides to the eye).

The first set [35, 32, 36] [Fig. (2.1)] consisted in the measurement of the first component of vortex lattice form factors (these are the two-dimensional Fourier coefficients of the local magnetic field in the vortex lattice) with

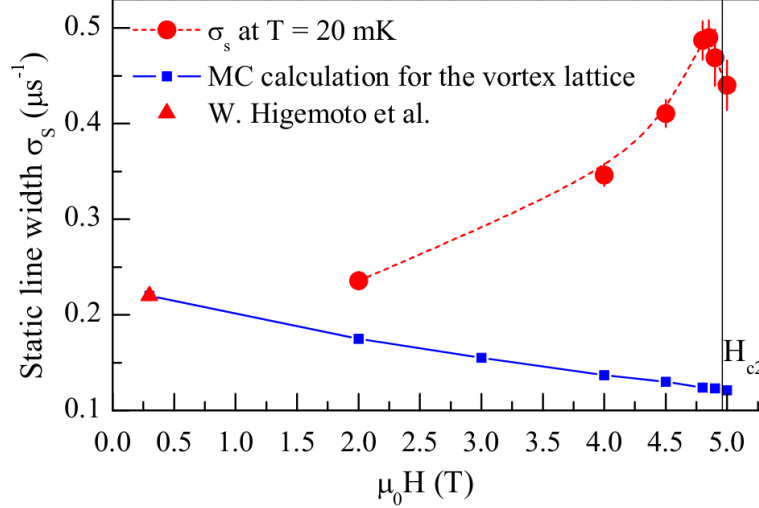


Figure 2.2: (from [34]) Anomalous muon spin rotation static linewidth dependence with applied field measured at temperature $T = 20\text{mK}$ compared with numerical simulation. The latter considered the characteristic lengths $\lambda = 5500\text{\AA}$ and $\xi = 46.84\text{\AA}$.

Small Angle Neutron Scattering (SANS). The second set [34] [Fig. (2.2)] was measurement of vortex lattice static linewidth (this is proportional to the root mean square deviation of the field variations in space, see definition below) with Muon Spin Rotation (μSR) technique. The two methods have clearly shown an increase with external magnetic field in both the form factor and the static linewidth and a fall down just before the upper critical field [*c. f.* Figs. (2.1) and (2.2)]. Because these two quantities are usually observed as monotonously decreasing function of the applied magnetic field, this suggested anomalous local magnetic field variations in the vortex lattice of the system.

In magnetic field directed along the crystal c -axis the metal to superconductor transition is second order for temperature between $T_0 \approx 0.3T_c \approx 0.7\text{K}$ and T_c , and becomes first order below T_0 [37] [Fig. (2.3)]. The system has moreover generated great interest because of hints for existence of the Fulde-

Ferrell-Larkin-Ovchinnikov (FFLO) phase¹ for magnetic field parallel to the ab plane (and possibly to the c -axis) [40]. We demonstrate below that such a behaviour in response to magnetic field can be understood as a consequence of *Pauli limiting* [41, 42] of heavy electron superconductivity in magnetic field.

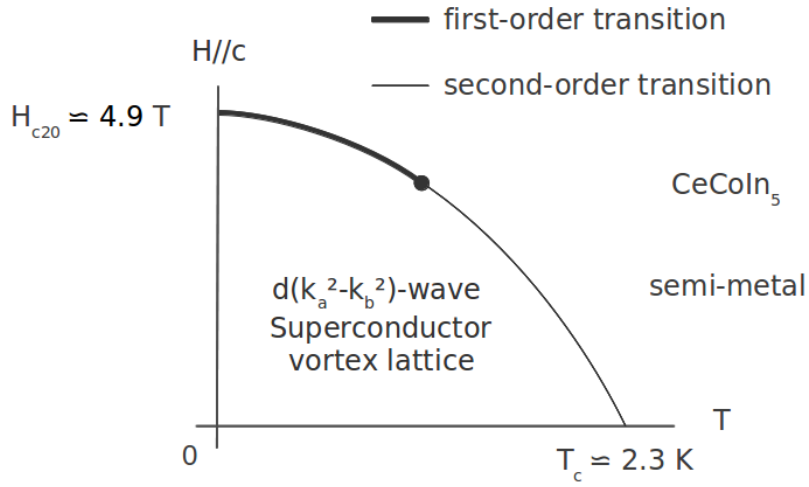


Figure 2.3: Sketch of the CeCoIn₅ phase diagram as determined experimentally in temperature and magnetic field perpendicular to the planes of the tetragonal crystal. The transition from the metal to the superconductor is second-order between the temperatures T_0 and T_c , and becomes first-order below T_0 . The zero temperature upper critical field is $H_{c20} \approx 4.9$ T.

¹The FFLO phase is predicted [38, 39] in strong magnetic field and consists in Cooper pairing with finite centre of mass momentum yielding superconductor order parameter modulated along the field direction with planes where it vanishes.

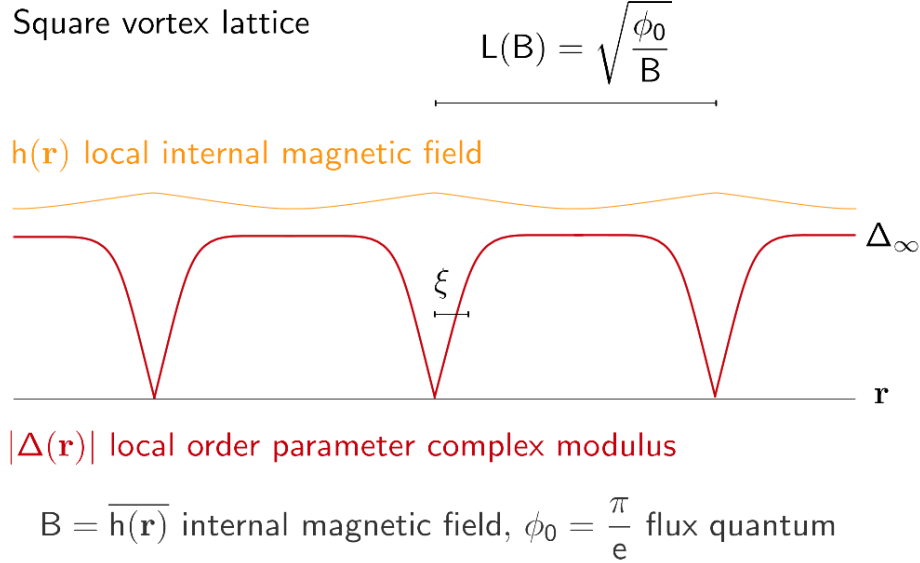


Figure 2.4: Sketch of the section of a vortex lattice. Relevant quantities are indicated for a square lattice including the field-dependent inter-vortex distance $L(B)$, the coherence length ξ , and the gap magnitude far from vortex centre Δ_∞ .

2.2 Qualitative considerations at zero temperature

Let us first discuss in a qualitative way the general properties of Pauli limited heavy electron superconductors [41, 42, 43, 44, 30]. This class is characterized by a greater-than-one zero temperature Maki parameter which we define here $\alpha_{M0} = H_{c20}^{\text{orb}}/H_{c20}^{\text{p}}$ (an alternative definition includes a $\sqrt{2}$ factor which we don't assume). We set $H_{c20}^{\text{orb}} = \phi_0/\xi_0^2$ and $H_{c20}^{\text{p}} = T_c/\mu$ the zero temperature scales for orbital and Pauli limiting fields respectively (we put throughout $\hbar = c = 1$). $\phi_0 = \pi/e \approx 2.07 \times 10^7 \text{G.cm}^2$ is the vortex fluxoid quantum, e the absolute value of the electron charge, $\xi_0 = v_F/T_c$ the $T = 0$ Cooper pair radius or coherence length, $v_F = k_F/m^*$ the Fermi velocity, k_F the Fermi

momentum, m^* the renormalized electron mass, $\mu = g\mu_B/2$ the electron magnetic moment absolute value, g the Landé factor, $\mu_B = e/(2m)$ the Bohr magneton, and m the electron bare mass.

There are three characteristic lengths in the problem: the zero temperature coherence length ξ_0 defined above, $L(H_{c20}^p) = \sqrt{\mu\phi_0/T_c}$ the inter-vortex distance of a square vortex lattice in the Pauli limit at temperature $T = 0$ and field H_{c20}^p (more generally we note

$$L(B) = \sqrt{\frac{\phi_0}{B}} \quad (2.1)$$

the inter-vortex spacing of a square vortex lattice with internal field B , see [45] for vortex lattice in general geometry), and the London penetration depth $\lambda_L = \sqrt{m^*/(4\pi n_s e^2)}$ with n_s the electron density in the superconductor (at $T=0$ and for a cylindrical Fermi surface this is the electron density in the layered metal $n = k_F^2/(2\pi\ell_c)$ with ℓ_c the spacing between the planes of the tetragonal crystal). Hence

$$\alpha_{M0} = \left[\frac{L(H_{c20}^p)}{\xi_0} \right]^2 = \frac{\mu\phi_0 T_c}{v_F^2} \sim \frac{m^* T_c}{m E_F}, \quad (2.2)$$

and we define the zero-temperature Ginzburg-Landau parameter

$$\kappa = \frac{\lambda_L}{\xi_0} \sim \sqrt{\frac{m^*}{m(k_F r_e)}} \frac{T_c}{E_F}, \quad (2.3)$$

where $r_e = e^2/m$ is the classical radius of the electron and $k_F r_e \sim 10^{-5}$.

The orders of magnitudes are as follows. In a classical, non-heavy electron superconductor, $m^* \sim m$ and $E_F \sim 10^3 T_c$ give $\kappa \sim 1$ and $\alpha_{M0} \sim 10^{-3}$. In CeCoIn₅ however, $T_c \approx 2.3\text{K}$, $\xi_0 \sim 50\text{\AA}$, $\lambda_L \sim 5000\text{\AA}$ yield $m^* \sim 100m$, $E_F \sim 50T_c$, $\kappa \sim 100$, and $\alpha_{M0} \sim 1 - 5$, which is the origin of special magnetic response in the superconductor vortex lattice state. The large Ginzburg-Landau parameter implies [deGennes] the ratio between the field

at which the first vortex nucleates in the bulk of the sample and the orbital upper critical field $H_{c10}/H_{c20}^{\text{orb}} \sim \ln(\kappa)/\kappa^2 \ll 1$, hence

$$B = H + 4\pi M \lesssim H, \quad (2.4)$$

for a broad magnetic field range, M being the diamagnetic magnetization of the superconductor. In a Pauli limited superconductor,

$$H_{c10}/H_{c20}^{\text{p}} \sim (k_F r_e)(E_F/T_c) \ln(\kappa) \sim 10^{-3} \quad (2.5)$$

and the same property applies.

2.3 Neutron scattering form factors and muon spin rotation static linewidth

We aim at studying the electrodynamics of the vortex lattice which results from large values for the parameters (2.2) and (2.3). Experimentally relevant quantities are the Fourier coefficients F_{mn} of the component of the internal local field $h(\mathbf{r})$ parallel to the external field H which are called vortex lattice *form factors* [30, 32, 36, 35]. For a square vortex lattice they are defined by the relation

$$h(\mathbf{r}) = \sum_{m,n=-\infty}^{+\infty} F_{mn} e^{i2\pi mx/L(B)} e^{i2\pi ny/L(B)}, \quad (2.6)$$

where x and y are the space coordinates in the plane perpendicular to the magnetic field, and $L(B)$ the inter-vortex distance given by Eq. (2.1). The square of the form factors are related in the Born approximation to the intensity of Bragg peaks [deGennes] observed in neutron scattering experiments.

In view of muon spin rotation experiment sensitive to local field inhomogeneity [deGennes] we define the vortex lattice *static linewidth*, proportional

to the local field root mean square deviation,

$$\sigma_s^{\text{VL}} = \frac{\gamma_\mu}{\sqrt{2}} \left[\overline{(h(\mathbf{r}) - B)^2} \right]^{1/2} = \frac{\gamma_\mu}{\sqrt{2}} \left[\sum_{(m,n) \neq (0,0)} F_{mn}^2 \right]^{1/2}, \quad (2.7)$$

where $\gamma_\mu = 2\pi \times 135.5342 \text{MHz/T}$ is the muon gyromagnetic ratio, the macroscopic internal field $B = \overline{h(\mathbf{r})}$, and overline means averaging over a vortex lattice unit cell. Parseval's theorem was used in the second equality of Eq. (2.7).

2.4 Ginzburg-Landau free energy and equations

We would like to determine the evolution with applied magnetic field and temperature of the local field $h(\mathbf{r})$ and evaluate the form factors and static linewidth in order to compare with experiment [35, 32, 36]. To do so we adopt the Ginzburg-Landau approach [Abrikosov, deGennes, MineevSamokhin]. Let us consider a singlet superconducting state with order parameter

$$\Delta_k(\mathbf{r}) = \psi(\hat{k})\Delta(\mathbf{r}), \quad (2.8)$$

where \hat{k} is the unit vector pointing to the electron momentum direction,

$$\psi(\hat{k}) = \begin{cases} 1 & \text{for } s\text{-wave pairing,} \\ \sqrt{2} \cos(2\varphi) & \text{for } d_{k_a^2 - k_b^2}\text{-wave pairing,} \end{cases} \quad (2.9)$$

φ being the angle between \hat{k} and the axis $k_b = 0$ in reciprocal space.

2.4.1 Free energy

The free energy of the condensate is given by the Ginzburg-Landau functional

$$\mathcal{F} = \int d^2r \left(\frac{\mathbf{h}(\mathbf{r})^2}{8\pi} + \alpha|\Delta(\mathbf{r})|^2 + \varepsilon[h(\mathbf{r}) - B]|\Delta(\mathbf{r})|^2 + \gamma|\mathbf{D}\Delta(\mathbf{r})|^2 + \beta|\Delta(\mathbf{r})|^4 \right), \quad (2.10)$$

where $\mathbf{D} = -i\nabla - 2e\mathbf{A}(\mathbf{r})$ is the gauge-invariant gradient and $\mathbf{A}(\mathbf{r})$ the potential vector related to the local field by $\mathbf{h}(\mathbf{r}) = h(\mathbf{r})\hat{z} = \nabla \times \mathbf{A}(\mathbf{r})$. The coefficients in the functional depend on both temperature T and induction B . In the clean limit they read [43, 44, 30] (*c. f.* addendum for derivation)

$$\alpha = -N_0 \left[\ln \left(\frac{T_c}{T} \right) + \Psi \left(\frac{1}{2} \right) - \Re \mathfrak{e} \Psi \left(\frac{1}{2} - \frac{i\mu B}{2\pi T} \right) \right], \quad (2.11)$$

$$\varepsilon = \frac{\partial \alpha}{\partial B} = \frac{N_0 \mu}{2\pi T} \Im \mathfrak{m} \Psi^{(1)} \left(\frac{1}{2} - \frac{i\mu B}{2\pi T} \right), \quad (2.12)$$

$$\beta = -\frac{N_0}{8(2\pi T)^2} \langle |\psi(\hat{k})|^4 \rangle \Re \mathfrak{e} \Psi^{(2)} \left(\frac{1}{2} - \frac{i\mu B}{2\pi T} \right), \quad (2.13)$$

$$\gamma = \frac{v_F^2 \langle |\psi(\hat{k})|^2 \cos^2(\varphi) \rangle}{\langle |\psi(\hat{k})|^4 \rangle} \beta, \quad (2.14)$$

where $\Psi(w)$ is the digamma function, $\Psi^{(m)}(w)$ are its derivatives called the polygamma functions [AbramowitzStegun], and $\langle \cdot \rangle$ means averaging in momentum space over the Fermi surface.

We shall consider s and d -wave superconducting states in a crystal with a nearly cylindrical Fermi surface. For the d -wave order parameter given above the averages are $\langle |\psi(\hat{k})|^4 \rangle = 3/2$ and $\langle |\psi(\hat{k})|^2 \cos^2(\varphi) \rangle = 1/2$ while for s -wave superconductivity they are 1 and 1/2.

2.4.2 Ginzburg-Landau equations and characteristic lengths

We wish to minimize the free energy Eq. (2.10) with suitable choice of fields $\Delta(\mathbf{r})$ and $\mathbf{A}(\mathbf{r})$. These are solutions of the Ginzburg-Landau equations. The *first Ginzburg-Landau equation* is

$$\frac{\delta\mathcal{F}}{\delta\Delta^*(\mathbf{r})} = 0, \quad (2.15)$$

or

$$\alpha\Delta(\mathbf{r}) + 2\beta|\Delta(\mathbf{r})|^2\Delta(\mathbf{r}) + \gamma[-i\nabla - 2e\mathbf{A}(\mathbf{r})]^2\Delta(\mathbf{r}) = 0. \quad (2.16)$$

We have omitted here the ε term of the Ginzburg-Landau free energy Eq. (2.10) quadratic in $|\Delta|$. We shall verify *a posteriori* that this gives negligible contribution so that the length and energy scales in this sections are consistently defined. Eq. (2.16) firstly gives the *Ginzburg-Landau coherence length*

$$\xi = \sqrt{\frac{\gamma}{|\alpha|}}, \quad (2.17)$$

and secondly yields the asymptotic gap magnitude at large radius from the vortex centre

$$\Delta_\infty = \sqrt{\frac{|\alpha|}{2\beta}}. \quad (2.18)$$

The two are related as

$$\Delta_\infty^2 \xi^2 = \frac{v_F^2}{4\langle|\psi(\hat{k})|^4\rangle}. \quad (2.19)$$

Neglecting the non-linear term in Eq. (2.16) with respect to $\Delta(\mathbf{r})$, the solution becomes a linear combination of Landau wave functions with level $n = 0$ (lowest Landau level) [Abrikosov, deGennes] and provides us with the equation

$$\alpha + 2e\gamma B = 0, \quad (2.20)$$

whose solution in B gives the *upper critical field* $H_{c2}(T)$. The *second Ginzburg-Landau equation*

$$\frac{\delta\mathcal{F}}{\delta\mathbf{A}(\mathbf{r})} = \mathbf{0}, \quad (2.21)$$

is equivalent to Maxwell's equation

$$\nabla \times \mathbf{h}(\mathbf{r}) = 4\pi\mathbf{j}(\mathbf{r}), \quad (2.22)$$

and determines the vortex lattice field distribution. The current density

$$\mathbf{j}(\mathbf{r}) = \mathbf{j}_{\text{orb}}(\mathbf{r}) + \mathbf{j}_Z(\mathbf{r}) \quad (2.23)$$

consists of two parts originating from two different terms in the free energy. The *orbital current* is [Abrikosov, deGennes]

$$\mathbf{j}_{\text{orb}}(\mathbf{r}) = -2e\gamma \left[\Delta^*(\mathbf{r}) \left(-i\nabla - 2e\mathbf{A}(\mathbf{r}) \right) \Delta(\mathbf{r}) + \text{complex conjugate} \right], \quad (2.24)$$

while the *Zeeman current* writes [44]

$$\mathbf{j}_Z(\mathbf{r}) = -\varepsilon \nabla \times (|\Delta(\mathbf{r})|^2 \hat{z}). \quad (2.25)$$

Eq. (2.22) together with Eqs. (2.18) and (2.24) yield the *Ginzburg-Landau penetration depth*

$$\lambda = \sqrt{\frac{\beta}{16\pi e^2 \gamma |\alpha|}}. \quad (2.26)$$

2.4.3 Discussion

From the point of view of the Ginzburg-Landau theory in the Pauli limit, that is when the orbital effects brought about by the gauge invariant gradient term of the free energy are neglected, the transition from the metallic to the superconducting state takes place at the critical field $H_{c2}^p(T)$ (or alternatively the critical temperature $T_c(B)$) defined by equation $\alpha(T, B) = 0$. Along this

transition line, the coefficients $\beta(T, B)$ and $\gamma(T, B)$, which are positive near T_c , become negative at $T < T_0^{\text{GL}} \approx 0.56T_c$. This defines the tricritical point $(T_0^{\text{GL}}, B_0^{\text{GL}})$ of the phase diagram with $B_0^{\text{GL}} = H_{c2}^{\text{p}}(T_0^{\text{GL}}) \approx 1.07T_c/\mu$. At the tricritical point, the sign change of the coefficient γ signals an instability toward the FFLO state with spatial modulation of the order parameter Δ with wave-vector $q = 2\mu B/v_F$ [38, 39, 46, 47, 48], while the sign change of the coefficient β signals a change of the order of the transition from the non-superconducting to the superconducting state. Including the orbital effects and the higher order terms in the GL functional [43, 44] results in the following effects: (i) the upper critical field is slightly reduced by value of the order $H_{c2}^{\text{p}}(T)/\alpha_{M0}$; (ii) the temperature where the change of the order of the transition occurs and the one where the FFLO state arises are decreased by values of the order T_c/α_{M0} with respect to T^* . Below we consider only the temperatures above T_0 where the β and γ coefficients are positive.

In the case of a large Maki parameter the Ginzburg-Landau expansion of the free energy in powers of the order parameter and its gradients is applicable near the critical field which is mainly determined by the paramagnetic depairing effect [43, 44]. At small field the Ginzburg-Landau theory is justified in the vicinity of the superconducting critical temperature T_c .

In what follows we shall demonstrate that the Ginzburg-Landau theory predicts an increasing behaviour of the form factors and static linewidth. This results from the Zeeman interaction of the electron spin with the superconductor internal field, which dominates over the usual charge response supercurrents. The existence of the effect was pointed out [44] in the context of magnetism of the FFLO (Fulde-Ferrel-Larkin-Ovchinnikov) state. As a result the field distribution is modified on a distance $\sim \xi$ (ξ is the coherence length of the Ginzburg-Landau theory) from the centre of each vortex [30]. In parallel to this, a numerical approach to Eilenberger equations was undertaken [49, 50] and effects of strong Pauli paramagnetism were highlighted in the vortex lattice state of Pauli limited superconductors.

2.5 Addendum: Derivation of the Ginzburg-Landau free energy

This supplementary section follows the appendix of [43] where the Ginzburg-Landau free energy expansion is obtained considering disorder by impurities with both the Green function approach used here and the Eilenberger formalism.

We consider the interaction Hamiltonian²

$$H_{\text{int}} = - \sum_{k, k', q} V \psi(\hat{k}) \psi^*(\hat{k}') a_{k\uparrow}^\dagger a_{-k+q\downarrow}^\dagger a_{-k'+q\downarrow} a_{k'\uparrow} \quad (2.28)$$

where $\psi(\hat{k})$ carries the momentum anisotropy of the superconducting state with average over Fermi surface $\langle |\psi(\hat{k})|^2 \rangle = 1$. The condensate free energy (difference between superconductor and normal state free energies) can be introduced [51] in the frame of the path integral by first decoupling the interaction Hamiltonian with introduction of an auxiliary bosonic field and then integrating out fermions. In the BCS approximation the free energy reads

$$\mathcal{F} = \sum_q \frac{|\Delta_q|^2}{V} - \frac{T}{2} \text{Tr} \ln[1 - \hat{G}^{(0)} \hat{\Delta}] \quad (2.29)$$

where $\Delta_{kq} = \psi(\hat{k}) \Delta_q$ is the mean field of the superconductor and the trace is understood as the matrix trace in particle-hole space, and Feynman diagram loop summation over spin, momentum and frequency with superconductor

²In the case of boson mediated pairing the interaction potential energy in the singlet channel can be written as

$$V^g(\mathbf{k}, \mathbf{k}') = \frac{1}{2} [D(\mathbf{k} - \mathbf{k}') + D(\mathbf{k} + \mathbf{k}')], \quad (2.27)$$

where g is from the German *gerade* [even]. For general boson propagator $D(\mathbf{k})$, $V^g(\mathbf{k}, \mathbf{k}')$ can be decomposed into channels corresponding to different pairing symmetry and factorisable forms. Here we focus on the d-wave channel.

order parameter as vertices. The metal fermion Green function matrix writes

$$\hat{G}^{(0)} = \begin{pmatrix} G_{\sigma}^{(0)}(\mathbf{k}, i\omega_m) & 0 \\ 0 & -G_{-\sigma}^{(0)}(-\mathbf{k}, -i\omega_m) \end{pmatrix}, \quad (2.30)$$

with $[G_{\sigma}^{(0)}(\mathbf{k}, i\omega_m)]^{-1} = i\omega_m - \epsilon_k - \sigma\mu B$, $\omega_m = \pi T(2m + 1)$ the fermion Matsubara frequencies (m are integer), $\epsilon_k = \mathbf{v} \cdot \mathbf{k}$ the electron excitation dispersion measured from the Fermi surface, and the gap matrix (*c. f.* part II)

$$\hat{\Delta} = \begin{pmatrix} 0 & \Delta_{kq} \\ \Delta_{kq}^* & 0 \end{pmatrix}. \quad (2.31)$$

The first non-vanishing terms are quadratic and quartic

$$\mathcal{F} = \mathcal{F}_2 + \mathcal{F}_4. \quad (2.32)$$

The first one in the clean limit equals

$$\begin{aligned} \mathcal{F}_2 &= \sum_q \frac{|\Delta_q|^2}{V} \\ &\quad -T \sum_{\omega_m, k, \sigma, q} G_{\sigma}^{(0)}(\mathbf{k}, i\omega_m) \Delta_{k,q}^* G_{-\sigma}^{(0)}(-\mathbf{k} + \mathbf{q}, -i\omega_m) \Delta_{k,q}. \end{aligned} \quad (2.33)$$

First ignore the q -dependence in the Green function. The second term in \mathcal{F}_2 becomes in the first approximation

$$\begin{aligned} &-T \sum_{\omega_m, k, \sigma, q} G_{\sigma}^{(0)}(\mathbf{k}, i\omega_m) \Delta_{k,q}^* G_{-\sigma}^{(0)}(-\mathbf{k}, -i\omega_m) \Delta_{k,q} \\ &= - \sum_q |\Delta_q|^2 N_0 \Re \sum_{m=0}^{\Lambda} \frac{1}{m + 1/2 - i\mu B/(2\pi T)}, \end{aligned} \quad (2.34)$$

where we have used the average over Fermi surface $\langle |\psi(\hat{k})|^2 \rangle = 1$, N_0 is the volumic density of states at Fermi energy and Λ is an energy cut-off. By

using the regularization

$$\frac{1}{N_0V} = \ln(T/T_c) + \sum_{n=0}^{\Lambda} \frac{1}{n+1/2} \quad (2.35)$$

and Fourier transforming $\Delta_q = \int d^3r e^{-i\mathbf{q}\cdot\mathbf{r}} \Delta(\mathbf{r})$ so $\sum_q |\Delta_q|^2 = \int d^3r |\Delta(\mathbf{r})|^2$, we obtain the coefficient α of Eq. (2.10) with the digamma function defined as [AbramowitzStegun]

$$\Psi(z) = -C + \sum_{n=0}^{\infty} \left(\frac{1}{n+1} - \frac{1}{n+z} \right), \quad (2.36)$$

where $C \approx 0.577$ is the Euler constant and we have let the cutoff go to infinity.

Now developing $G_{-\sigma}^{(0)}(-\mathbf{k} + \mathbf{q}, -i\omega_m)$ with respect to \mathbf{q} we have (implicit summation over repeated indices)

$$G_{-\sigma}^{(0)}(-\mathbf{k} + \mathbf{q}, -i\omega_m) \approx q_\mu \frac{\partial G_{-\sigma}^{(0)}(-\mathbf{k}, -i\omega_m)}{\partial q_\mu} + \frac{1}{2} q_\mu q_\nu \frac{\partial^2 G_{-\sigma}^{(0)}(-\mathbf{k}, -i\omega_m)}{\partial q_\mu \partial q_\nu}. \quad (2.37)$$

Only the second term remains after averaging over Fermi surface, this writes

$$\delta G_{-\sigma}^{(0)}(-\mathbf{k} + \mathbf{q}, -i\omega_m) = -\frac{(\mathbf{q} \cdot \mathbf{v})^2}{(i\omega_m - \sigma\mu B + \epsilon_k)^3}. \quad (2.38)$$

The corresponding correction to the free energy is

$$\delta\mathcal{F}_2 = \frac{\pi}{2} \sum_q \langle |\psi(\hat{k})|^2 (\mathbf{q} \cdot \mathbf{v})^2 \rangle |\Delta_q|^2 N_0 T \Re \sum_{\omega_m > 0} \frac{1}{(\omega_m - i\mu B)^3}. \quad (2.39)$$

Again using the Fourier transform of Δ_q and introducing the vector potential by substituting $-i\nabla \rightarrow -i\nabla - 2e\mathbf{A}(\mathbf{r})$, we obtain the gradient term in Eq. (2.10) with expression of the γ coefficient. The polygamma function of order

n is defined as [AbramowitzStegun]

$$\Psi^{(n)}(z) = (-1)^{n+1} n! \sum_{m=0}^{\infty} \frac{1}{(m+z)^{n+1}}. \quad (2.40)$$

The quartic term expresses as

$$\begin{aligned} \mathcal{F}_4 = & \frac{T}{2} \sum_{\omega_m, k, \sigma, -q_1+q_2-q_3+q_4=0} G_{\sigma}^{(0)}(\mathbf{k}, i\omega_m) \Delta_{k, q_1}^* \\ & \times G_{-\sigma}^{(0)}(-\mathbf{k} + \mathbf{q}_1, -i\omega_m) \Delta_{k, q_2} \\ & \times G_{\sigma}^{(0)}(\mathbf{k} - \mathbf{q}_1 + \mathbf{q}_2, i\omega_m) \Delta_{k, q_3}^* \\ & \times G_{-\sigma}^{(0)}(-\mathbf{k} + \mathbf{q}_4, -i\omega_m) \Delta_{k, q_4}. \end{aligned} \quad (2.41)$$

Here we ignore the q -dependence in the Green functions which gives corrections of the order $1-T/T_c$ and $\mu B/(\alpha_{M0} T_c)$ in comparison with the quadratic gradient term above [44]. The coefficient β thus evaluates to

$$\beta = \frac{\pi}{2} \langle |\psi(\hat{k})|^4 \rangle N_0 T \sum_{\omega_m > 0} \frac{1}{[m + 1/2 - i\mu B/(2\pi T)]^3}, \quad (2.42)$$

with the sum over momenta $\sum_{q_1, q_2, q_3} \Delta_{q_1}^* \Delta_{q_2} \Delta_{q_3}^* \Delta_{q_3+q_1-q_2} = \int d^3 r |\Delta(\mathbf{r})|^4$.

The term that accounts for the local field inhomogeneity is found as follows. In an inhomogeneous system the free energy part that corresponds to the loop diagram including two order parameter vertices is

$$-T \sum_{\omega_m, k, k', \sigma, q, q'} G_{\sigma}(\mathbf{k}, \mathbf{k}', i\omega_m) \Delta_{k, q}^* G_{-\sigma}(-\mathbf{k} + \mathbf{q}, -\mathbf{k}' + \mathbf{q}', -i\omega_m) \Delta_{k', q'}. \quad (2.43)$$

This brings the first correction

$$\delta \mathcal{F}_{\delta h} =$$

$$\begin{aligned}
& -T \sum_{\omega_m, \mathbf{k}, \mathbf{k}', \sigma, \mathbf{q}, \mathbf{q}'} \left[G_{\sigma}^{(0)}(\mathbf{k}, \mathbf{k}', i\omega_m) \Delta_{\mathbf{k}, \mathbf{q}}^* G_{-\sigma}^{(1)}(-\mathbf{k} + \mathbf{q}, -\mathbf{k}' + \mathbf{q}', -i\omega_m) \Delta_{\mathbf{k}', \mathbf{q}'} \right. \\
& \quad \left. + G_{\sigma}^{(1)}(\mathbf{k}, \mathbf{k}', i\omega_m) \Delta_{\mathbf{k}, \mathbf{q}}^* G_{-\sigma}^{(0)}(-\mathbf{k} + \mathbf{q}, -\mathbf{k}' + \mathbf{q}', -i\omega_m) \Delta_{\mathbf{k}', \mathbf{q}'} \right], \quad (2.44)
\end{aligned}$$

where the Green functions

$$G_{\sigma}^{(0)}(\mathbf{k}, \mathbf{k}', i\omega_m) = G_{\sigma}^{(0)}(\mathbf{k}, i\omega_m) \delta(\mathbf{k} - \mathbf{k}'), \quad (2.45)$$

and

$$G_{\sigma}^{(1)}(\mathbf{k}, \mathbf{k}', i\omega_m) = -G_{\sigma}^{(0)}(\mathbf{k}, i\omega_m) \sigma \mu \delta h_{\mathbf{k}-\mathbf{k}'} G_{\sigma}^{(0)}(\mathbf{k}', i\omega_m). \quad (2.46)$$

Here $\delta h_{\mathbf{k}-\mathbf{k}'} = \int d^3r e^{-i\mathbf{r} \cdot (\mathbf{k}-\mathbf{k}')} \delta h(\mathbf{r})$ and $\delta h(\mathbf{r}) = h(\mathbf{r}) - B$ is the local field projection deviation from average. Again discarding the \mathbf{q} -dependence in Eq. (2.44) which gives extra gradient negligible in Pauli limited superconductivity we obtain

$$\delta \mathcal{F}_{\delta h} = \int d^3r \mu \delta h(\mathbf{r}) \frac{N_0}{2\pi T} \Im \sum_{m=0}^{\infty} \frac{1}{[m + 1/2 - i\mu B / (2\pi T)]^2}, \quad (2.47)$$

hence the coefficient ε in Eq. (2.10).

Chapter 3

Analysis of the equations I: independent vortex regime

On the basis of the Ginzburg-Landau equations established in the previous chapter we now focus on the field regime $\mu B \ll 2\pi T_c$ near the superconductor critical temperature T_c . In this limit we start with deriving the orbital upper critical field H_{c2}^{orb} and the paramagnetic upper critical field H_{c2}^{p} together with their temperature dependence. We then consider the limit $L(B) \gg \xi$ so that each vortex can be treated as having cylindrical symmetry (independent vortex regime) and present in this case expressions for the form factors and results of the Ginzburg-Landau theory. The variational gap structure for an isolated vortex introduced by Clem is presented and applied to the resolution of the Maxwell equation determining the single vortex field profile, neutron scattering form factors and muon spin rotation static linewidth with full account of the Zeeman effect.

3.1 Critical fields in the vicinity of T_c

In the field regime $\mu B \ll 2\pi T_c$ the coefficients of the Ginzburg-Landau free energy become

$$\alpha = -N_0 \left[\frac{T_c - T}{T_c} - 7\zeta(3) \left(\frac{\mu B}{2\pi T_c} \right)^2 \right], \quad (3.1)$$

$$\varepsilon = \frac{7\zeta(3)N_0\mu^2 B}{2\pi^2 T_c^2}, \quad (3.2)$$

$$\beta = \frac{7\zeta(3)N_0}{16\pi^2 T_c^2} \langle |\psi(\hat{k})|^4 \rangle, \quad (3.3)$$

$$\gamma = \frac{7\zeta(3)N_0 v_F^2}{32\pi^2 T_c^2} \quad (3.4)$$

where $\zeta(z)$ is the Riemann zeta function, $\zeta(3) \approx 1.2021$. Considering Eq. (2.20) with the coefficients Eqs. (3.1) and (3.4) gives the critical field

$$H_{c2} = \frac{e\gamma(2\pi T_c)^2}{7\zeta(3)N_0\mu^2} \left[-1 + \sqrt{1 + \frac{7\zeta(3)N_0^2\mu^2}{(2\pi e\gamma T_c)^2} (1 - T/T_c)} \right]. \quad (3.5)$$

Here we recognise $7\zeta(3)N_0^2\mu^2/(2\pi e\gamma T_c)^2 \sim \alpha_{M0}^2$, α_{M0} being the Maki parameter defined at zero temperature by Eq. (2.2). Thus in the limit $\alpha_{M0}^2(1 - T/T_c) \ll 1$ one obtains the *orbital critical field*

$$H_{c2}^{\text{orb}} = \frac{N_0}{2e\gamma} (1 - T/T_c), \quad (3.6)$$

while in the limit $\alpha_{M0}^2(1 - T/T_c) \gg 1$ one has the *Pauli critical field*

$$H_{c2}^{\text{p}} = \frac{2\pi T_c}{\sqrt{7\zeta(3)\mu}} \sqrt{1 - T/T_c}. \quad (3.7)$$

We introduce the temperature Maki parameter

$$\alpha_M = \alpha_{M0} \sqrt{1 - T/T_c}, \quad (3.8)$$

with α_{M0} given by Eq. (2.2). Hence $H_{c2}^{\text{orb}}/H_{c2}^{\text{P}} \sim \alpha_M$ and the crossover temperature T^\times from orbital limiting in the vicinity of T_c to Pauli limiting is of the order $1 - T^\times/T_c \sim 1/\alpha_{M0}^2$. As a consequence the near- T_c Ginzburg-Landau regime is accessible in the Pauli limit $\alpha_{M0} \gg 1$.

In addition with the coefficients (3.1), (3.3), and (3.4) we get expressions for the coherence length Eq. (2.17)

$$\frac{1}{\xi^2} = \frac{32\pi^2 T_c^2}{7\zeta(3)v_F^2} \left[\frac{T_c - T}{T_c} - 7\zeta(3) \left(\frac{\mu B}{2\pi T_c} \right)^2 \right], \quad (3.9)$$

and the penetration depth Eq. (2.26)

$$\frac{1}{\lambda^2} = \frac{8\pi e^2 v_F^2 N_0}{\langle |\psi(\hat{k})|^4 \rangle} \left[\frac{T_c - T}{T_c} - 7\zeta(3) \left(\frac{\mu B}{2\pi T_c} \right)^2 \right], \quad (3.10)$$

which diverge at the Pauli critical field.

3.2 Independent vortex limit

Consider a square vortex lattice formed in a type II superconductor in magnetic field directed along the z-axis. For small external field, where the distance between the vortices is much larger than the core radius, the local magnetic field can be approximated as the superposition of fields solutions of the Ginzburg-Landau equations for single vortices

$$h(\mathbf{r}) = \sum_{m,n=-\infty}^{+\infty} h_v(\mathbf{r} - \mathbf{r}_{mn}), \quad (3.11)$$

where $\mathbf{r}_{mn} = L(B)(m\hat{x} + n\hat{y})$, m and n are integer, \hat{x} and \hat{y} are orthogonal unit vectors of the plane perpendicular to the magnetic field, and $L(B)$ is given by Eq. (2.1). Thus, with reference to Poisson summation formula [Abrikosov]¹, the form factors are proportional to the magnetic field Fourier transform around a single vortex evaluated at a vector of the reciprocal lattice

$$F_{mn} = \frac{B}{\phi_0} F_2[h_v](\mathbf{q}_{mn}), \quad (3.12)$$

with $\mathbf{q}_{mn} = 2\pi/L(B)(m\hat{x} + n\hat{y})$ and $h_v(\mathbf{r})$ the field solution of Maxwell's equation Eq. (2.22) for a single vortex. The two-dimensional Fourier transform of a function h with cylindrical symmetry reads

$$F_2[h](q) = \int d^2r h(r) e^{-i\mathbf{q}\cdot\mathbf{r}} = 2\pi \int_0^\infty dr r J_0(qr) h(r), \quad (3.13)$$

with the norm of the reciprocal lattice wave-vector $q = |\mathbf{q}|$. This is referred to as zeroth order Hankel's transform. In the square vortex lattice we have

$$q_{mn} = 2\pi \sqrt{\frac{B}{\phi_0} (m^2 + n^2)}. \quad (3.14)$$

The general order parameter expression for an isolated vortex is

$$\Delta(\mathbf{r}) = \Delta_\infty f(r) e^{-i\theta}, \quad (3.15)$$

where θ is the azimuthal angle in the plane perpendicular to the vortex axis. The function of the radius f must behave as $f(r) \rightarrow 1$ as $r \rightarrow \infty$ and

¹Poisson summation formula in two-dimensions reads

$$\sum_{m,n=-\infty}^{+\infty} h(\mathbf{r} - L(m\hat{x} + n\hat{y})) = \frac{1}{L^2} \sum_{m,n=-\infty}^{+\infty} F_2[h]\left(\frac{2\pi}{L}(m\hat{x} + n\hat{y})\right) e^{i2\pi mx/L} e^{i2\pi ny/L},$$

where we define the Fourier transform $F_2[h](\mathbf{q}) = \int d^2r h(\mathbf{r}) e^{-i\mathbf{q}\cdot\mathbf{r}}$, the integral being performed over the entire plane.

assuming singly quantized vortex $f(r) \sim r/\xi$ as $r \rightarrow 0$. This gives the orbital current Eq. (2.24)

$$\mathbf{j}_v^{\text{orb}}(\mathbf{r}) = -8e^2\gamma \left[A_v(r) - \frac{\phi_0}{2\pi r} \right] |\Delta|^2 \hat{\theta}, \quad (3.16)$$

with $\hat{\theta}$ the azimuthal unit vector and the vector potential $\mathbf{A}_v(\mathbf{r}) = A_v(r)\hat{\theta}$. The Zeeman current Eq. (2.25) becomes

$$\mathbf{j}_v^{\text{Z}}(\mathbf{r}) = \varepsilon \frac{d}{dr} |\Delta|^2 \hat{\theta}. \quad (3.17)$$

Equations (2.16) and (2.22) constitute a system of coupled differential equations for the vector potential and the superconductor order parameter which are not analytically solvable. To go further one has to bring input into the problem and one idea is to use a variational form for the gap dependence on radius for a single vortex. The next section shows how this has been previously done with consideration of orbital currents Eq. (3.16).

3.3 Charge driven diamagnetic currents and orbital form factors

3.3.1 Clem variational gap structure for a single vortex

The Ginzburg-Landau theory for the vortex lattice form factor with current Eq. (3.16), valid in the limit $\kappa \gg 1$ was developed by J. Clem [33]. Starting from the superconductor order parameter Eq. (3.15), J. Clem proposed to model $f(r)$ by the trial function

$$f(r) = \frac{r}{R}, \quad (3.18)$$

with $R = \sqrt{r^2 + \xi_v^2}$. The *variational parameter* ξ_v is constrained to minimize the vortex total energy and is found to be in the large κ limit $\xi_v = \sqrt{2}\xi$, where ξ is the Ginzburg-Landau coherence length. By application of Maxwell's equation Eq. (2.22) for a single vortex with the gap structure Eq. (3.18) and the orbital current Eq. (3.16), Clem has calculated the field distribution

$$h_v^{\text{orb}}(r) = \frac{\phi_0 K_0(R/\lambda)}{2\pi\lambda\xi_v K_1(\xi_v/\lambda)}, \quad (3.19)$$

and has obtained the Hankel transform Eq. (3.13)

$$F_2[h_v^{\text{orb}}](q) = \frac{\phi_0 K_1(Q\xi_v)}{Q\lambda K_1(\xi_v/\lambda)}, \quad (3.20)$$

where $Q = \sqrt{q^2 + \lambda^{-2}}$, $q = 2\pi\sqrt{B/\phi_0}$, $K_1(z)$ is the modified Bessel function of the first order [AbramowitzStegun], and λ is the London penetration depth. Notice the vortex flux quantum is given by $F_2[h_v^{\text{orb}}](0) = \phi_0$, and one can approximate Eq. (3.20) by

$$F_2[h_v^{\text{orb}}](q) \approx \frac{\phi_0 \xi_v}{q\lambda^2} K_1(q\xi_v) \quad (3.21)$$

in the limits $\kappa \gg 1$ and $q \gg \lambda^{-1}$.

3.3.2 Discussion

The form factors Eq. (3.12) derived with Clem's solution slowly decrease with magnetic field. The formal application of Eq. (3.20) up to $H \lesssim H_{c2}$, where $q\xi_v \approx \sqrt{2\pi}$, gives their exponential decrease. In fact in the vicinity of H_{c2} the approximation of independent vortices does not work. The proper calculation should be done within an approach in the spirit of Abrikosov's [Abrikosov] which is the subject of the next chapter and leads to the vanishing of the form factors as $H_{c2} - H$.

The magnetic field profile derived in this section considers coupling of the

field with the electron charge through the gauge-invariant gradient in the Ginzburg-Landau free energy Eq. (2.10). The dependence with induction of the form factors is not in correspondence with observation on the system CeCoIn₅. The previous chapter however shows important role played by electron spin. We therefore wish to include Zeeman effect into the Ginzburg-Landau approach to vortex lattice electrodynamics in order to confront predictions with anomalous experimental data discussed in introduction. This is developed in the next section.

3.4 Spin driven currents and Zeeman effect in neutron scattering form factors and muon spin rotation static linewidth

3.4.1 Derivation of the single-vortex local field

The field distribution is determined by the Maxwell equation Eq. (2.22) for a single vortex

$$\nabla \times \mathbf{h}_v(\mathbf{r}) = 4\pi[\mathbf{j}_v^{\text{orb}}(\mathbf{r}) + \mathbf{j}_v^Z(\mathbf{r})]. \quad (3.22)$$

By considering the order parameter Eq. (3.15) with cylindrical vortex gap structure, the currents Eq. (3.16) and Eq. (3.17), and the field $\mathbf{h}_v(\mathbf{r}) = (\hat{z}/r)d[rA_v(r)]/dr$, we come to the equation that determines the potential vector component $A_v(r)$

$$\frac{d}{dr} \left[\frac{1}{r} \frac{d}{dr} (rA_v) \right] - \frac{f^2}{\lambda^2} A_v = -\frac{\phi_0 f^2}{2\pi\lambda^2 r} - 4\pi\varepsilon\Delta_\infty^2 \frac{df^2}{dr}, \quad (3.23)$$

where λ is the penetration depth Eq. (2.26) and Δ_∞ the asymptotic gap Eq. (2.18). Let us introduce the auxiliary function

$$v_s(r) = \frac{\phi_0}{2\pi r} - A_v(r) \quad (3.24)$$

which plays the role of the superfluid velocity [Abrikosov] and substitute it into Eq. (3.23). We obtain the differential equation with an inhomogeneous term of Zeeman origin

$$\frac{d}{dr} \left[\frac{1}{r} \frac{d}{dr} (rv_s) \right] - \frac{f^2}{\lambda^2} v_s = 4\pi\varepsilon\Delta_\infty^2 \frac{df^2}{dr}. \quad (3.25)$$

The general solution of Eq. (3.25)

$$v_s(r) = v_s^i(r) + v_s^h(r) \quad (3.26)$$

consists of the sum of a particular solution of the inhomogeneous equation and a solution of the corresponding homogeneous equation. Following Clem's procedure we consider an isolated vortex with real-space gap structure given by Eq. (3.18) such that a solution of the inhomogeneous equation is

$$v_s^i(r) = -\frac{R}{r} K_1(R/\lambda) C(R/\lambda), \quad (3.27)$$

where

$$C(z) = -\frac{8\pi\varepsilon\Delta_\infty^2\xi_v^2}{\lambda} \int_{\xi_v/\lambda}^z \frac{dz}{zK_1^2(z)} \int^z \frac{K_1(z)}{z^2} dz, \quad (3.28)$$

chosen such that $v_s^i(0) = 0$ and $v_s^i(\infty) = 0$. The latter condition is assured by letting the constant be zero in the primitive $\int^z K_1(z)/z^2 dz$. The solution of the homogeneous equation falling to zero at $r \rightarrow \infty$

$$v_s^h(r) = \frac{\phi_0}{2\pi\xi_v} \frac{RK_1(R/\lambda)}{rK_1(\xi_v/\lambda)} \quad (3.29)$$

meets the requirement that the vector potential

$$A_v(r) = \frac{\phi_0}{2\pi r} - v_s^h(r) - v_s^i(r) \quad (3.30)$$

vanishes on the vortex axis. Then one can split the total vector potential into the orbital part and the Zeeman part

$$A_v(r) = A_v^{\text{orb}}(r) + A_v^Z(r), \quad (3.31)$$

where the first

$$A_v^{\text{orb}}(r) = \frac{\phi_0}{2\pi r} - v_s^h(r) = \frac{\phi_0}{2\pi r} \left[1 - \frac{RK_1(R/\lambda)}{\xi_v K_1(\xi_v/\lambda)} \right] \quad (3.32)$$

is the solution of Eq. (3.23) without the Zeeman term and was found in [33]. The corresponding magnetic field $\mathbf{h}^{\text{orb}}(r) = h^{\text{orb}}(r)\hat{z}$ is Eq. (3.19) and the first form factor is Eq. (3.20) with Eq. (3.12) for $(m, n) = (1, 0)$.

The Zeeman part of the vector potential on the other hand is

$$A_v^Z(r) = -v_s^i(r) = \frac{R}{r} K_1(R/\lambda) C(R/\lambda), \quad (3.33)$$

and the corresponding magnetic field projection $h_v^Z(r) = \mathbf{h}_v^Z(r) \cdot \hat{z}$ reads

$$h_v^Z(r) = \frac{1}{\lambda} \left[-K_0(R/\lambda) C(R/\lambda) + K_1(R/\lambda) C'(R/\lambda) \right]. \quad (3.34)$$

This additional term does not spoil the basic properties of the Abrikosov vortex. Namely the total magnetic flux through the surface perpendicular to the vortex axis is equal to the flux quantum

$$2\pi \int_0^\infty dr r [h_v^{\text{orb}}(r) + h_v^Z(r)] = 2\pi \lim_{r \rightarrow \infty} r [A_v^{\text{orb}}(r) + A_v^Z(r)] = \phi_0. \quad (3.35)$$

To show this property, one may consider the asymptotic form

$$K_1(z) \approx \sqrt{\frac{\pi}{2z}} e^{-z}, \quad z \gg 1, \quad (3.36)$$

and

$$C(z) \approx \frac{8\sqrt{2\pi\varepsilon}\Delta_\infty^2\xi_v^2}{\lambda} \frac{e^z}{z^{5/2}}, \quad z \gg 1, \quad (3.37)$$

so that we observe the Zeeman part of the vector potential $A_v^Z(r)$ Eq. (3.33) behaves as $\propto 1/r^3$ for $r \gg \lambda$. At small distances $r \ll \lambda$ on the other hand these functions comport as

$$K_1(z) \approx \frac{1}{z}, \quad z \ll 1, \quad (3.38)$$

and

$$C(z) \approx \frac{4\pi\varepsilon\Delta_\infty^2\xi_v^2}{\lambda} \ln\left(\frac{\lambda z}{\xi_v}\right), \quad z \ll 1. \quad (3.39)$$

The superfluid velocity given by

$$v_s(r) = \frac{\phi_0}{2\pi r} \left(\frac{RK_1(R/\lambda)}{\xi_v K_1(\xi_v/\lambda)} - \frac{2\pi}{\phi_0} RK_1(R/\lambda)C(R/\lambda) \right) \quad (3.40)$$

thus becomes

$$v_s(r) \approx \frac{\phi_0}{2\pi r} \left[1 - \frac{8\pi^2\varepsilon\Delta_\infty^2\xi_v^2}{\phi_0} \ln\left(\frac{R}{\xi_v}\right) \right]. \quad (3.41)$$

The magnitude of the dimensionless combination $8\pi^2\varepsilon\Delta_\infty^2\xi_v^2/\phi_0$ is estimated as follows. Using the relation Eq. (2.19) and Eq. (3.2) one obtains

$$\frac{8\pi^2\varepsilon\Delta_\infty^2\xi_v^2}{\phi_0} \sim k_F r_e \frac{E_F}{T_c} \frac{\mu B}{T_c} \sim 10^{-3} \frac{\mu B}{T_c}. \quad (3.42)$$

Then we recover the usual expression for the superfluid velocity

$$v_s(r) \approx \frac{\phi_0}{2\pi r}, \quad (3.43)$$

which is valid at $r \ll \lambda$. The total field amplitude

$$h_v(r) = h_v^{\text{orb}}(r) + h_v^Z(r) \quad (3.44)$$

differs from the orbital part $h^{\text{orb}}(r)$ Eq. (3.19) only within a distances $\sim \xi_v$ from the vortex axis. In the high- κ limit we can therefore find a simple form for the Zeeman internal field by looking at its asymptotic behaviour at radius $r \ll \lambda$. By using Eqs. (3.38) and (3.39) we find the dominant term in Eq. (3.34)

$$h_v^Z(r) \approx 4\pi\varepsilon\Delta_\infty^2 \frac{\xi_v^2}{R^2}. \quad (3.45)$$

The local field amplitude is proportional to ε and hence proportional to B in the limit $\mu B \ll T_c$. The formula (3.45) may be derived by directly considering the equation $\nabla \times \mathbf{h}_v^Z = 4\pi\mathbf{j}_v^Z$, which is valid in the absence of orbital current. From Eq. (3.34) one can find the correction to Eq. (3.45), $\delta h_v^Z = -4\pi\varepsilon\Delta_\infty^2 K_0(R/\lambda) \ln(R/\xi_v)/\kappa^2$, namely $\delta h_v^Z/h_v^Z \sim 1/\kappa^2$ for $r \sim \xi_v$. The local field deviation from average at the vortex centre is

$$\frac{h(0) - B}{B} \approx \frac{h_v^Z(0)}{B} \sim \frac{m^*}{m} k_F r_e (1 - T/T_c), \quad (3.46)$$

with $k_F r_e m^*/m \sim 10^{-3}$, and the Zeeman free energy density $\varepsilon(h - B)|\Delta|^2$ of Eq. (2.10) compared with the regular free energy density $\alpha|\Delta|^2$ estimates

$$\frac{\varepsilon[h(0) - B]}{\alpha} \sim \left(\frac{\mu B}{T_c}\right)^2 \frac{m^*}{m} k_F r_e. \quad (3.47)$$

Therefore for $H_{c1} < B < H_{c2}$ the Zeeman term of the first Ginzburg-Landau equation is dominated over by the regular one (with coefficient α) which means that the solution of the equation for the isolated vortex depends on radius as

$$\frac{|\Delta(r)|}{\Delta_\infty} \sim \begin{cases} r/\xi, & r \ll \xi \\ 1 - \xi^2/r^2, & r \gg \xi \end{cases} \quad (3.48)$$

as it is in the absence of the Zeeman interaction [Abrikosov]. This justifies the variational approach that makes use of the order parameter given by Eqs. (3.15) and (3.18). The minimization of the energy of a single vortex

gives the variational parameter $\xi_v = \sqrt{2}\xi$ as in the orbitally limited case [33]. The lower critical field moreover keeps the usual value determined with logarithmic accuracy as $H_{c1} \approx \phi_0/(4\pi\lambda^2) \ln \kappa$.

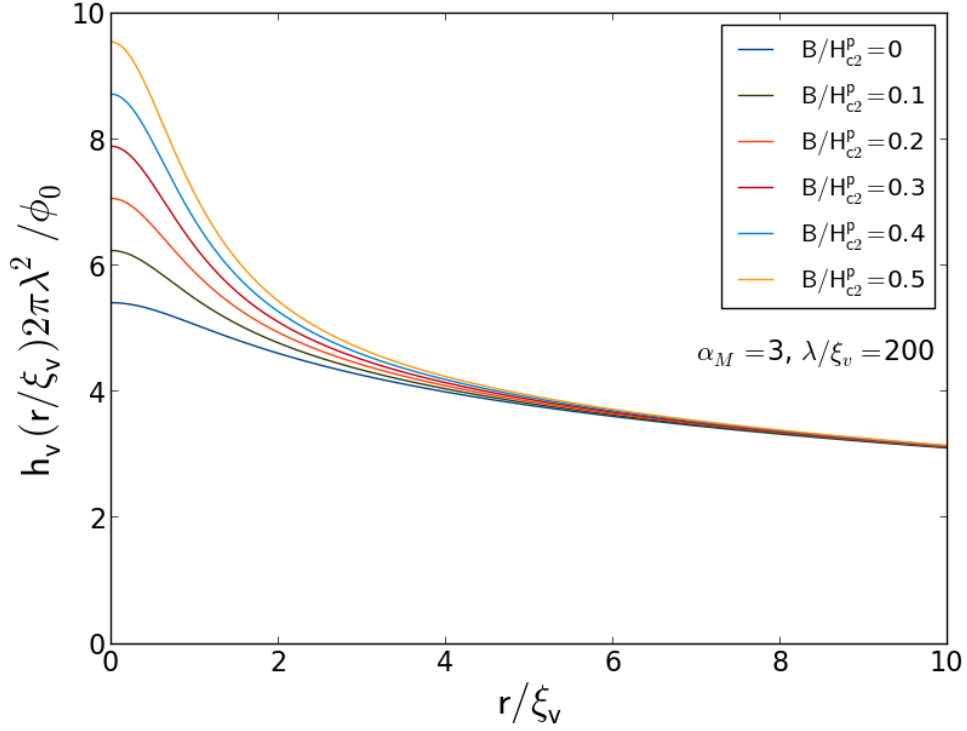


Figure 3.1: Plot of the radial dependence of the dimensionless local magnetic field $2\pi h_v \lambda^2 / \phi_0$ around a single vortex for various inductions and with fixed temperature Maki parameter $\alpha_M = 3$ and parameter $\lambda/\xi_v = 200$. The first (blue) curve represents the orbital part of the local magnetic field alone. The other curves show the addition of the Zeeman contribution with length-scale ξ for different inductions which goes upon the orbital background. We have verified that at large distance $r > \lambda$ the field $h_v^Z(r)$ becomes negative such that the total flux for single vortex is equal to the flux quantum (see discussion in text).

At this point it is useful scaling the internal field B with H_{c2}^p of Eq. (3.7)

so that

$$b = \frac{B}{H_{c2}^p} \quad (3.49)$$

is a dimensionless variable. Together with the temperature Maki parameter in Eq. (3.8), the single vortex local field in the region $r \ll \lambda$ Eqs. (3.19), (3.44), and (3.45) evaluates to

$$h_v(r) = \frac{\phi_0}{2\pi\lambda^2} \left[K_0 \left(\frac{\xi_v}{\lambda} \sqrt{1 + r^2/\xi_v^2} \right) + \frac{8\alpha_M b}{\sqrt{7\zeta(3)}(1 + r^2/\xi_v^2)} \right], \quad (3.50)$$

which is shown in Fig. (3.1). The order of magnitude of Eq. (3.50) is

$$\frac{\phi_0}{\lambda^2} \sim (\phi_0 k_F^2)(k_F r_e) \left(\frac{m}{m^*} \right) (1 - T/T_c) \sim 1 \text{ Tesla} \left(\frac{m}{m^*} \right) (1 - T/T_c), \quad (3.51)$$

which is reduced when the electron effective mass is large. The ratio between the two terms in Eq. (3.50) taken at the vortex center writes

$$\frac{h_v^Z(0)}{h_v^{\text{orb}}(0)} \sim \alpha_M \frac{B}{H_{c2}^p} = \alpha_{M0} \frac{B}{H_{c20}^p} = \alpha_{M0}^2 \frac{B}{H_{c20}^{\text{orb}}}, \quad (3.52)$$

which is of the order unity when α_M is of the order unity and (quadratically) small in an orbitally limited superconductor, *i. e.* where $\alpha_{M0} < 1$.

3.4.2 Neutron scattering form factors and muon spin rotation static linewidth

Eq. (3.45) can be used in the form factors derivation since the contribution to the Hankel transform brought by the region $r > \lambda$ is negligible when $q^{-1} \ll \lambda$, that is when the distance between the vortices is much smaller than the penetration depth. We have validated the accuracy of approximation Eq. (3.45) to calculate the form factors by numerical integration of the full expression Eq. (3.34). Thus in the large- κ limit the form factors can be

decomposed as a sum of two contributions

$$F_{mn} = F_{mn}^{\text{orb}} + F_{mn}^Z. \quad (3.53)$$

By considering the form factors for a dilute array of vortices Eq. (3.12), the orbital part in dimensionful form becomes

$$F_{mn}^{\text{orb}} = \frac{B\xi_v}{q_{mn}\lambda^2} K_1(q_{mn}\xi_v), \quad (3.54)$$

with q_{mn} given in Eq. (3.14), while the part which follows from the Zeeman effect is

$$F_{mn}^Z = \frac{8\pi^2\varepsilon\Delta_\infty^2\xi_v^2}{\phi_0} BK_0(q_{mn}\xi_v). \quad (3.55)$$

After substitution of the near- T_c and low-field limit of ε Eq. (3.2) and using the relation Eq. (2.19) this becomes

$$F_{mn}^Z = \frac{14\zeta(3)N_0v_F^2}{\langle|\psi(\hat{k})|^4\rangle\phi_0} \left(\frac{\mu B}{T_c}\right)^2 K_0(q_{mn}\xi_v). \quad (3.56)$$

We again use the scaled internal field Eq. (3.49), temperature Maki parameter Eq. (3.8), and introduce

$$x = q_{mn}\xi_v = \sqrt{\frac{\pi\sqrt{7\zeta(3)}}{2} \frac{b}{\alpha_M} (m^2 + n^2)}, \quad (3.57)$$

such that Eq. (3.53) in the limit $B \ll H_{c2}^p$ simply evaluates to

$$F_{mn} = \frac{\phi_0}{(2\pi\lambda)^2} \left[\frac{x}{m^2 + n^2} K_1(x) + 4\pi b^2 K_0(x) \right]. \quad (3.58)$$

In the vicinity of T_c the dimensionless form factors $f_{mn} = (2\pi\lambda)^2 F_{mn}/\phi_0$ Eq. (3.58) have a universal form where only remains the parameter α_M that controls the relative contribution of the spin effect with respect to the charge effect. The static linewidth Eq. (2.7) variations with dimensionless internal

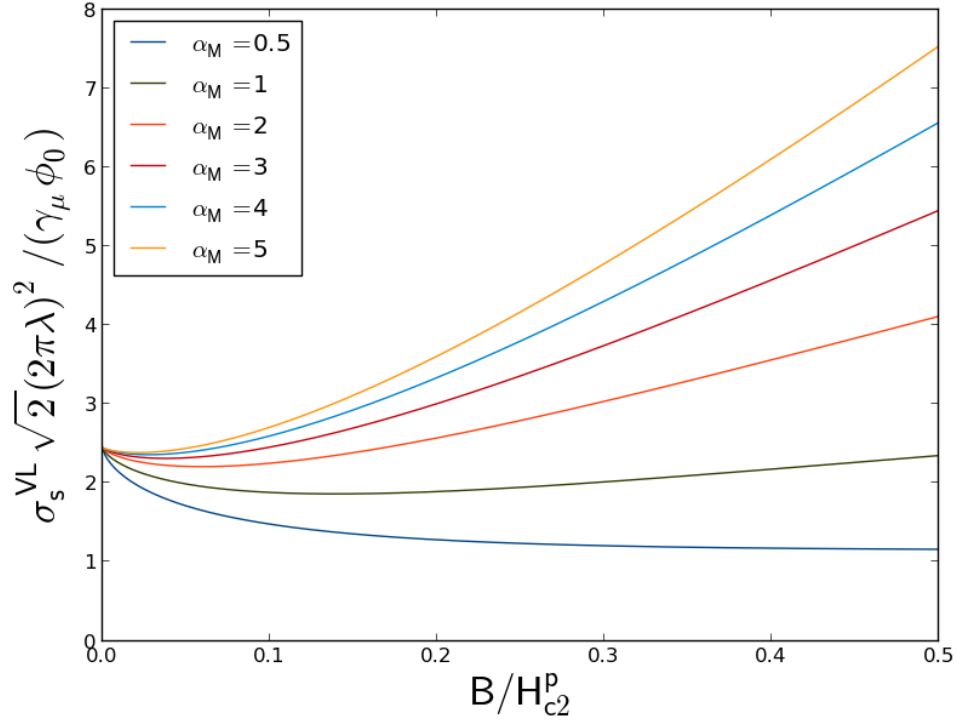


Figure 3.2: Dimensionless μSR static linewidth [Eqs. (2.7) and (3.58)] dependence with induction scaled with Pauli critical field H_{c2}^P . Different values for the temperature Maki parameter were used as indicated in the inset.

field b in the independent vortex limit and for different values for α_M are shown in Fig. (3.2). Observe in Fig. (2.7) the low field regime where all curves meet which follows from the limit

$$\sqrt{\sum_{(m,n) \neq (0,0)} (f_{mn})^2} \rightarrow \sqrt{\sum_{(m,n) \neq (0,0)} \frac{1}{(m^2 + n^2)^2}} \approx 2.455 \text{ as } b \rightarrow 0. \quad (3.59)$$

The MacDonald functions assume the limits $K_0(z) \rightarrow -\ln(z/2) - C$ and Eq. (3.38) as $z \rightarrow 0$ where $C \approx 0.5772$ is the Euler constant. With Small Angle Neutron Scattering experiment in mind in the large- α_M limit it is

useful considering Eq. (3.58) with $(m, n) = (1, 0)$

$$F_{10} = \frac{\phi_0}{(2\pi\lambda)^2} \left[1 - 2\pi b^2 \ln \left(\frac{\pi \sqrt{7\zeta(3)}}{8\alpha_M} b e^{2C} \right) \right]. \quad (3.60)$$

The effect of temperature on the form factors is also transparent from Eqs. (3.58) and (3.57). The overall form factor amplitude proportional to $1/\lambda^2$ decreases linearly with temperature and the temperature Maki parameter defined by Eq. (3.8) has square-root non-analyticity at T_c .

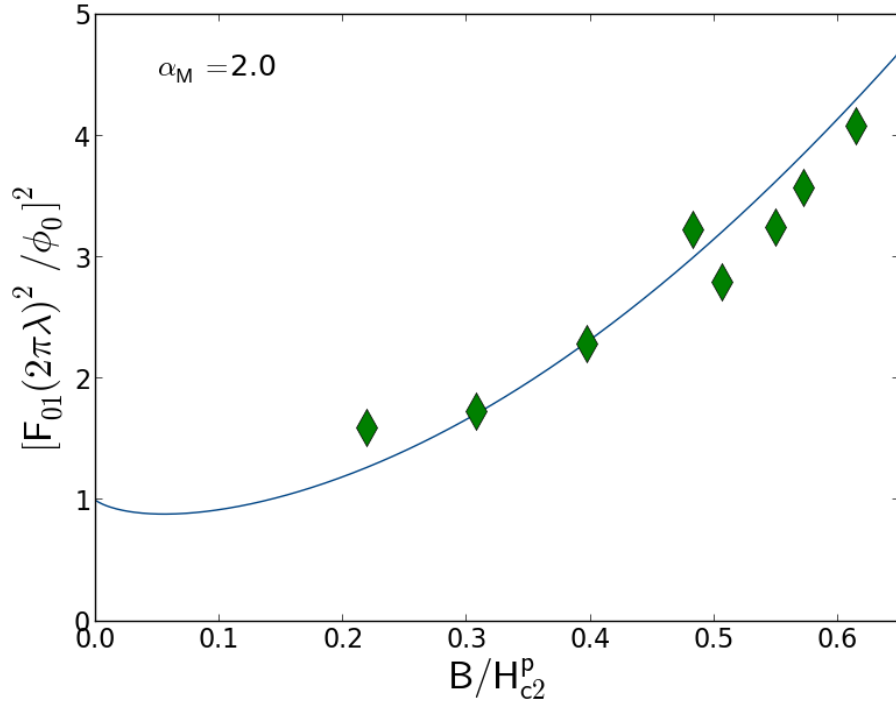


Figure 3.3: Comparison between experimental data (from [36]) at temperature $T = 1\text{K}$ and the theoretical squared first form factor Eq. (3.58). The parameters taken are $\alpha_M = 2$, $H_{c2}^P = 4.5\text{T}$ and $\lambda = 6480\text{\AA}$.

3.4.3 Discussion

The Zeeman effect significantly changes the form factor dependence on B for parameter α_M larger than unity. The origin of the effect is the local magnetic field inhomogeneity on the length-scale ξ from the vortex axis developing linearly with B [*c. f.* Fig. (3.1)]. In the vortex lattice this field inhomogeneity is small [*c. f.* Eq. (3.46)] but builds upon a B -independent background which sensibly varies on the scale λ . A fit of experimental squared first form factor measured at temperature $T = 1\text{K}$ [36] by formula Eq. (3.12) is shown in Fig. (3.3). Notice the experiment is realised beyond the Ginzburg-Landau regime. As temperature in Eq. (3.58) only enters through penetration depth λ and Maki parameter α_M , extension of the Ginzburg-Landau theory to lower temperature merely consists in renormalisation of these parameters. The comparison between the model and experiment leads to good agreement.

As shown by Eq. (3.12) the pairing symmetry of the singlet superconductor does not affect the ratio between the orbital and the Zeeman terms but represents an overall factor [*c. f.* the penetration depth dependence on the gap symmetry in Eq. (2.26)]. Assuming other parameters unchanged, the form factor is larger in the s-wave case than in the d-wave case by a factor $3/2$. Similar anomalous form factor variations were observed in experiment on the s-wave superconductor $\text{TmNi}_2\text{B}_2\text{C}$ [52].

A phenomenological model connected to anomalous vortex lattice magnetism has been recently developed [53]. It consists of a Ginzburg-Landau free energy coupling superconductivity with magnetisation of localised spins. The result is substitution of external field $H \rightarrow H[1 + \gamma_M/A(T)]$ where γ_M accounts for localised spin contribution to the field acting on the superconducting electron spin and $A(T)$ is the localised magnetism inverse susceptibility. In connection with the present model this leads to the increase in the coupling between superconducting electron magnetic moment and the internal field with Maki parameter enhancement. This additional effect is relevant to leading to strongly Pauli limited superconductors.

Chapter 4

Analysis of the equations II: Abrikosov solution in the Pauli limit close to critical field

The form factors as given by Eq. (3.58) are found in the isolated vortex approximation. The derivation does not work near the transition to the metal. Near to $H_{c2}^p(T)$ (the curve solution of $\alpha = 0$) we instead take the point of view of Abrikosov [Abrikosov] by using the solution of the linearised first Ginzburg-landau equation Eq. (2.16) to determine the field inhomogeneity in the Pauli limit and temperature above the tricritical point.

At large Maki parameter and in the vicinity of the critical field $H_{c2}^p(T)$ the main cause of magnetic field inhomogeneity in the vortex lattice comes from the Zeeman spin response [44, 30]

$$\delta h(\mathbf{r}) = -4\pi\varepsilon(|\Delta(\mathbf{r})|^2 - \overline{|\Delta(\mathbf{r})|^2}), \quad (4.1)$$

where ε is given by Eq. (2.12) and by overlining we again mean averaging over a vortex lattice unit cell. Thus the form factors are proportional to the Fourier coefficients of $|\Delta|^2$, which needs to be determined from the linearised

first Ginzburg-Landau equation (2.16).

4.1 Abrikosov's solution of the linearised Ginzburg-Landau equation

The gap solves the linearised Ginzburg-Landau equation Eq. (2.16). For a square vortex lattice with period $L(B) = \sqrt{\phi_0/B}$ this is [Abrikosov, de-Gennes]

$$\Delta(\mathbf{r}) = C \sum_{n=-\infty}^{+\infty} (-1)^n e^{i2\pi ny/L(B)} e^{-\pi(x/L(B)-n+1/2)^2}, \quad (4.2)$$

so that $|\Delta(mL(B), nL(B))| = 0$ (m and n are integer). Multiplying the expression by its complex conjugate we obtain

$$\begin{aligned} |\Delta(\mathbf{r})|^2 &= C^2 \sum_{m,n=-\infty}^{+\infty} (-1)^{n+m} e^{-\pi(x/L(B)-n+1/2)^2} \\ &\quad \times e^{-\pi(x/L(B)-m+1/2)^2} e^{i2\pi(n-m)y/L(B)}. \end{aligned} \quad (4.3)$$

Now, putting the dummy index $n' = n - m$, and using one-dimensional Poisson's summation formula [Abrikosov]

$$\sum_{m=-\infty}^{+\infty} f(x - mL) = \frac{1}{L} \sum_{m=-\infty}^{+\infty} F_1[f]\left(\frac{2\pi m}{L}\right) e^{2\pi i m x/L}, \quad (4.4)$$

where $F_1[f](q) = \int_{-\infty}^{+\infty} dz f(z) e^{-iqz}$, we have the desired expression

$$|\Delta(\mathbf{r})|^2 = \frac{C^2}{\sqrt{2}} \sum_{m,n=-\infty}^{+\infty} (-1)^{m+n+mn} e^{-\frac{\pi}{2}(m^2+n^2)} e^{i2\pi(mx+ny)/L(B)}. \quad (4.5)$$

The average is

$$\overline{|\Delta(\mathbf{r})|^2} = \frac{C^2}{\sqrt{2}}. \quad (4.6)$$

4.2 Vortex lattice form factors and static linewidth

By Eqs. (4.1), (4.5) and (4.6), the form factors corresponding to the Bragg peaks with indices $(m, n) \neq (0, 0)$ become

$$F_{mn}^A = -4\pi\varepsilon \overline{|\Delta(\mathbf{r})|^2} (-1)^{m+n+mn} e^{-\frac{\pi}{2}(m^2+n^2)}. \quad (4.7)$$

and the vortex lattice static linewidth simply reads

$$\sigma_s^{\text{VL}} = \frac{4\pi s}{\sqrt{2}} \gamma_\mu \varepsilon \overline{|\Delta(\mathbf{r})|^2}, \quad (4.8)$$

where

$$s = \sqrt{\left(\sum_{n=-\infty}^{+\infty} e^{-\pi n^2} \right)^2 - 1} \approx 0.4247. \quad (4.9)$$

Eqs. (4.7) and (4.8) explicitly show that the vortex lattice form factors and static linewidth vanish when the transition is of the second order but shows a discontinuity where the transition is of the first order. In the former case, the gap average is [44, 30]

$$\overline{|\Delta(\mathbf{r})|^2} = \frac{|\alpha|}{2\beta_A\beta}, \quad (4.10)$$

where α and β of Eqs. (2.11) and (2.13) are the quadratic and quartic coefficients of the Ginzburg-Landau free energy Eq. (2.10). The Abrikosov parameter

$$\beta_A = \overline{|\Delta(\mathbf{r})|^4} / \overline{|\Delta(\mathbf{r})|^2}^2 \quad (4.11)$$

is $\beta_A^\square = 1.18$ for a square vortex lattice and $\beta_A^\triangle = 1.16$ for a triangular lattice. Then it follows

$$\sigma_s^{\text{VL}} = \frac{2\pi s \gamma_\mu}{\sqrt{2}\beta_A} \frac{|\alpha|\varepsilon}{\beta}, \quad (4.12)$$

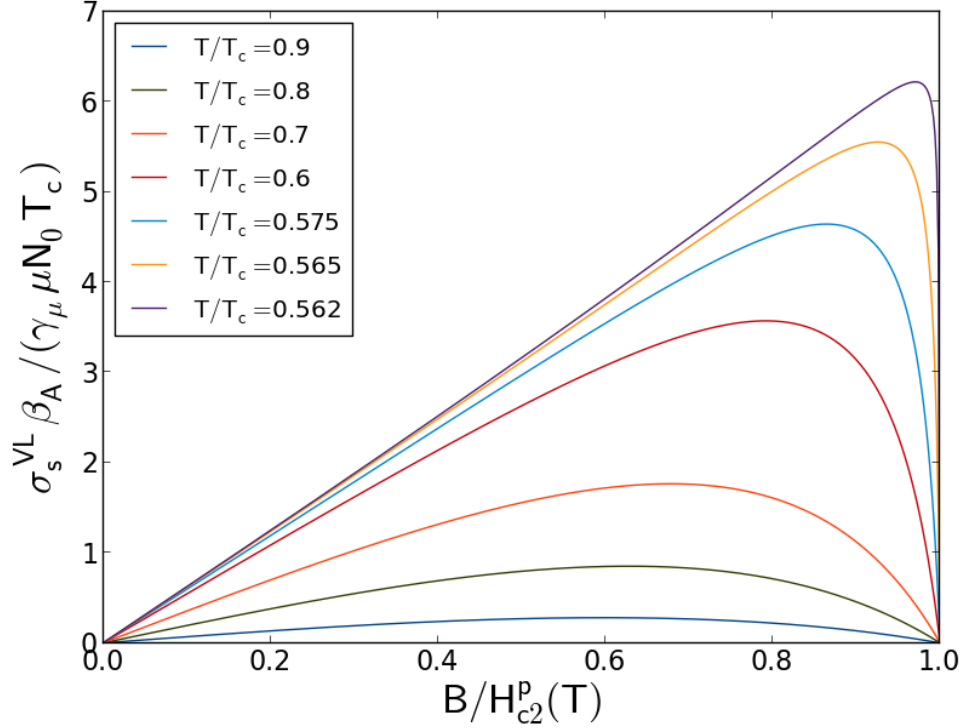


Figure 4.1: μ SR static linewidth as obtained from Abrikosov's analysis in the Pauli limit Eq. (4.8) for a temperature range from the tricritical point temperature T_0 to the superconductor critical temperature T_c . We have scaled the internal field with respect to $H_{c2}^p(T)$. Note the rapid increase in the absolute value of the slope of $\sigma_s^{VL}(B)$ while approaching the first order transition at $T/T_c \approx 0.5615$ and $\mu H_{c2}^p/T_c \approx 1.0728$.

which is shown in Fig. (4.1).

In the immediate vicinity of $B \sim H_{c2}^p(T)$ we can linearise $\alpha \approx \varepsilon(H_{c2}^p)(B - H_{c2}^p)$ so that we see that the form factors Eq. (4.7) collapse linearly below the critical field and that the slope absolute value diverge as $T \rightarrow T_0^{\text{GL}}$ where $\beta \rightarrow 0$. Below are shown plots of the squared form factor $(F_{10}^A)^2$ Eq. (4.7) together with experimental curves from [36].

4.3 Discussion

We have derived the evolution with internal magnetic field of the vortex lattice form factors and static linewidth in the Pauli (large Maki parameter) limit from the solution of the linearised first Ginzburg-Landau equation close to the transition temperature $T_c(B)$. We observe a linear collapse of the static linewidth close to the transition line and a crossover from continuous vanishing to discontinuous behaviour when approaching the tricritical point temperature. At lower field the static linewidth shows linear increase consistent with what was found in the previous chapter except in the very low-field limit where the solution in the independent vortex limit yields $\propto B^2 \ln(B)$ variations. Computed squared first form factor is displayed in Fig. (4.2) followed by corresponding experimental curves [36] in Fig. (4.3). Inspection of the two figures leads us to assert reasonable agreement between measurement and the present analysis.

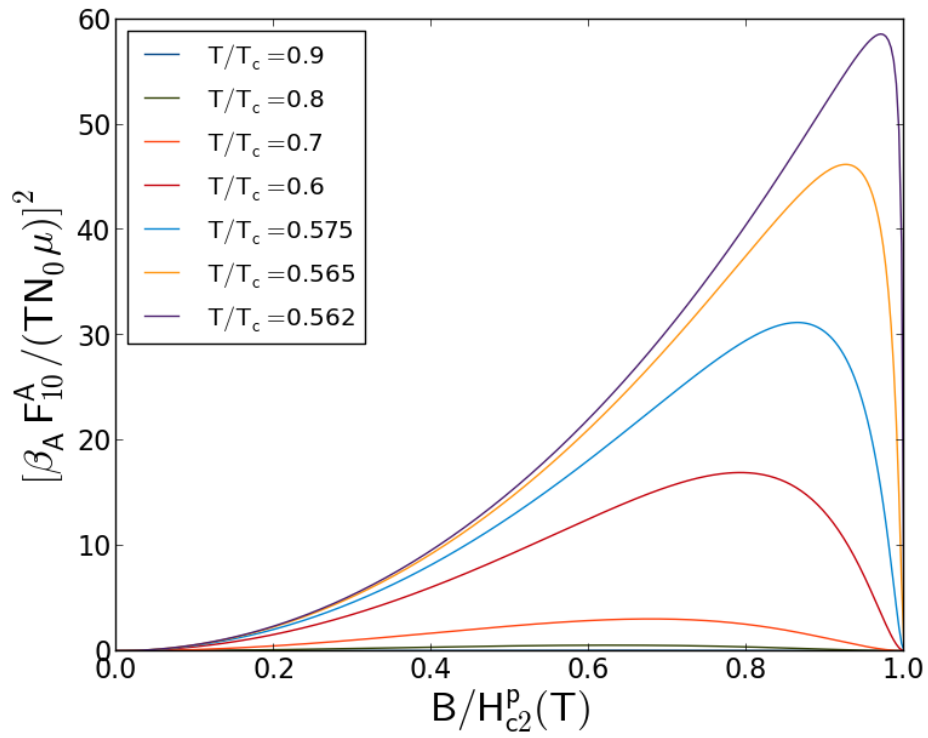


Figure 4.2: Dimensionless squared form factor Eq. (4.7) dependence on induction evaluated for a temperature range between T_0^{GL} and T_c .

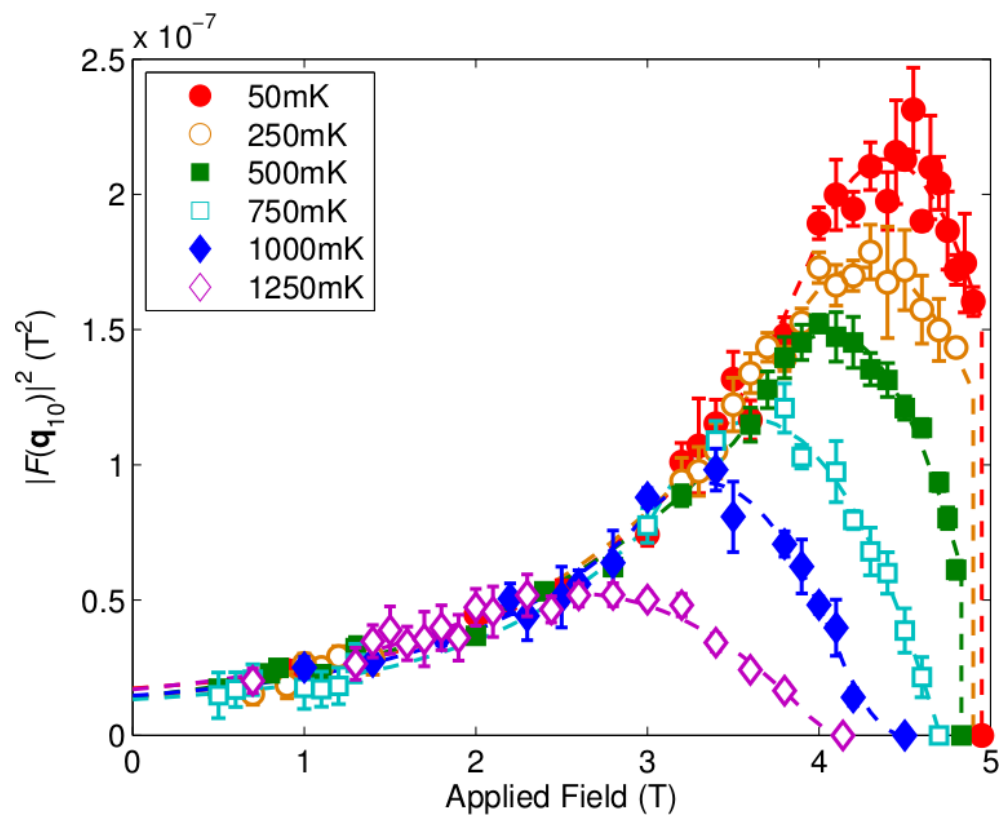


Figure 4.3: (from [36]) Experimental squared first form factor for a temperature range as indicated in inset.

Chapter 5

Temperature-dependent effective Ginzburg-Landau parameter

It was recently observed [54, 55] anomalous magnetic field-dependence of the effective Ginzburg-Landau parameter κ_{eff} . This parameter is defined through magnetisation dependence on external magnetic field (see below) and corresponds to the usual Ginzburg-Landau parameter $\kappa_{\text{GL}} = \lambda/\xi$ in orbitally limited superconductors, where λ is the Ginzburg-Landau penetration depth and ξ the Ginzburg-Landau coherence length. In this chapter we show that the Ginzburg-Landau-Abrikosov theory for type II superconductors near the upper critical field predicts significant effective Ginzburg-Landau temperature dependence if the zero temperature Maki parameter α_{M0} is large. This method allows identifying a number of heavy electron systems as strongly Pauli limited superconductors. Material included in this chapter has been published in [56].

The effective tool for the experimental determination of the Ginzburg-Landau parameter κ_{eff} near the critical temperature is given by the famous Abrikosov formula [2] for the field derivative of magnetisation near the upper

critical field in the type-II superconductors

$$\left. \frac{dM}{dH} \right|_{H=H_{c2}} = \frac{1}{4\pi(2\kappa_{\text{eff}}^2 - 1)\beta_A}. \quad (5.1)$$

Here β_A is the Abrikosov parameter Eq. (4.11). In practice, it is convenient to use the Ehrenfest formula which relates the slope of magnetisation curve near H_{c2} to the specific heat jump at $T = T_c(H_{c2})$

$$\frac{\Delta C}{T} = \left(\frac{dH_{c2}}{dT} \right)^2 \left(\frac{dM}{dH} \right). \quad (5.2)$$

From Eqs. (5.1) and (5.2) we obtain

$$\kappa_{\text{eff}} = \frac{1}{\sqrt{2}} \sqrt{1 + \frac{T}{4\pi\beta_A\Delta C} \left(\frac{dH_{c2}}{dT} \right)^2}. \quad (5.3)$$

For type II superconductors with large κ_{eff} ,

$$\kappa_{\text{eff}} \approx \left| \frac{dH_{c2}}{dT} \right| \sqrt{\frac{T}{8\pi\beta_A\Delta C}}. \quad (5.4)$$

The slope of the upper critical field in the vicinity of T_c is temperature-independent. The same is true for the ratio $T/\Delta C$. In several heavy fermionic compounds however there was revealed a fast drop of the effective Ginzburg-Landau parameter with decreasing temperature [57, 54]. So, κ_{eff} proved to be a function of temperature. Already in the earliest experimental study there was suggested [57] that this temperature dependence is an effect of Pauli de-pairing. Then the temperature dependence of the effective Ginzburg-Landau parameter has been discussed theoretically in the paper [58] from numerical solution of the Eilenberger equations with account of both the orbital and the Zeeman effects. Later the analytical expression for the parameter below $T_c(H)$ in the large α_{M0} limit has been found in the paper [44]. Here

we give in a straightforward way a simple analytic formula for the effective Ginzburg-Landau parameter valid near the phase transition line taking into account both the paramagnetic and the orbital depairing dependence. Then we compare this with results of the paper [44].

5.1 The critical field temperature derivative

We saw in chapter 3 that in the field regime $\mu B \ll 2\pi T_c$ the solution of the linearised Ginzburg-Landau equation as the linear combination of Landau wave functions with level $n = 0$ yields the equation for the upper critical field

$$N_0 \frac{T - T_c}{T_c} + a \left(\frac{\mu B}{T_c} \right)^2 + 2e\gamma B = 0, \quad (5.5)$$

where we recall T_c is the superconductor critical temperature at zero field and N_0 the metal volumic density of states at the Fermi level. This formula is valid for any type of superconducting state with singlet pairing or not equal spin triplet pairing and one component order parameter from a metal with arbitrary Fermi surface shape. The value of coefficients can of course have different values in concrete materials with different purities or different field orientation with respect to crystallographic axes. In a d-wave superconductor the coefficient $a = 7\zeta(3)N_0/(4\pi^2)$.

Solving Eq. (5.5) we obtain the critical field Eq. (3.5) and the orbital and Pauli limits Eqs. (3.6) and (3.7). By differentiating Eq. (3.5) with respect to temperature, substituting the orbital critical field Eq. (3.6) this becomes in a clean superconductor

$$-\frac{dH_{c2}}{dT} = \frac{N_0/(2e\gamma T_c)}{\sqrt{1 + C\alpha_{M0}^2(1 - T/T_c)}}, \quad (5.6)$$

with C a constant of the order of unity and α_{M0} the zero temperature Maki parameter Eq. (2.2). In the limit of small Maki parameters the critical

field temperature derivative is determined by the orbital effect only, it is temperature-independent and given by the numerator of Eq. (5.6). In a superconductor with strong paramagnetic effect however that is at large enough Maki parameter the value of $|dH_{c2}/dT|$ rapidly decreases with decreasing temperature, which leads to the fast decrease in the Ginzburg-Landau parameter (5.4).

5.2 Comparison with previous results

We have found the temperature dependence of the Ginzburg-Landau parameter on the basis of the Ehrenfest relation (5.2). As we have already pointed out there was derived an expression for κ_{eff} valid in the limit of strong paramagnetic depairing in [44]. To compare these results it is convenient to begin with the general formula¹ for the spatial average of the superconductor free energy density

$$\overline{\mathcal{F}_s} = \mathcal{F}_{n0} + \frac{B^2}{8\pi} - \frac{(\overline{\mathcal{F}_2(\Delta, \mathbf{A}_0)})^2}{4 \left[\overline{\mathcal{F}_4(\Delta, \mathbf{A}_0)} - \overline{\mathbf{h}_1^2}/(8\pi) \right]}, \quad (5.7)$$

where \mathcal{F}_{n0} is the free energy density in the normal state in absence of magnetic field, and \mathcal{F}_2 and \mathcal{F}_4 collect together quadratic and quartic terms with respect to Δ respectively. Just below the upper critical line $H_{c2}(T)$, the magnetic field is partially screened by supercurrents and we decompose $\mathbf{h} = \mathbf{B} + \mathbf{h}_1$, such that $\overline{\mathbf{h}_1} = 0$, and correspondingly $\mathbf{A} = \mathbf{A}_0 + \mathbf{A}_1$.

Starting with this formula one can derive a general expression for κ_{eff} at arbitrary Maki parameter value. However, to escape cumbersome formulæ we consider only the situations with $\alpha_{M0} \ll 1$ and $\alpha_{M0} \gg 1$. In the first case

$$\overline{\mathcal{F}_2(\Delta, \mathbf{A}_0)} = 2e\gamma[(B - H_{c2}^{\text{orb}}(T))|\overline{\Delta}|^2], \quad (5.8)$$

¹The general expression for the spatially averaged energy is derived exactly in the same manner as Eq. (20) in the paper [44] where it was done for $\alpha_{M0} \gg 1$.

while in the second case

$$\overline{\mathcal{F}_2(\Delta, \mathbf{A}_0)} = \varepsilon[(B - H_{c2}^p(T))|\Delta|^2]. \quad (5.9)$$

Here,

$$\varepsilon = \left(\frac{\partial \alpha}{\partial B} \right)_{B=H_{c2}^p} = \frac{2a\mu^2 H_{c2}^p}{T_c^2}. \quad (5.10)$$

In any case

$$\overline{\mathcal{F}_4(\Delta, \mathbf{A}_0)} = \beta\beta_A(|\Delta|^2)^2. \quad (5.11)$$

Then, taking into account the screening current term $\overline{\mathbf{h}_1^2}/(8\pi)$ in the denominator of Eq. (5.7) we come [44] to the equation

$$\overline{\mathcal{F}_s} = \mathcal{F}_{n0} + \frac{B^2}{8\pi} - \frac{(B - H_{c2}(T))^2}{8\pi[1 + \beta_A(2\kappa_{\text{eff}}^2 - 1)]}, \quad (5.12)$$

valid for any Maki parameter value. But for $\alpha_{M0} \ll 1$ one must put here the upper critical field as determined by Eq. (3.6) and then the Ginzburg-Landau parameter writes

$$\kappa_{\text{eff}} = \kappa_{\text{GL}} = \frac{\sqrt{\beta}}{4\sqrt{\pi e\gamma}}. \quad (5.13)$$

Whereas for $\alpha_{M0} \gg 1$ and $1 - T/T_c > 1/\alpha_{M0}^2$ one must use the upper critical field as determined by Eq. (3.7) and the Ginzburg-Landau parameter becomes

$$\kappa_{\text{eff}} = \frac{\sqrt{\beta}}{2\sqrt{\pi\varepsilon}}. \quad (5.14)$$

The latter for a clean superconductor can be rewritten as

$$\kappa_{\text{eff}} \approx \frac{\kappa_{\text{GL}}}{\alpha_{M0}\sqrt{1 - T/T_c}}. \quad (5.15)$$

This expression is in obvious correspondence with Eqs. (5.6) and (5.4).

The derived temperature dependence of the Ginzburg-Landau parameter is consistent with experimental observations [54] in several heavy fermionic

superconductors CeCoIn_5 , URu_2Si_2 , NpPd_5Al_2 . In all of these compounds the phase transition to the superconducting state becomes of the first order in the low-temperature-high-field region [37, 59, 60], which directly demonstrates the dominant role played by paramagnetic Clogston, Chandrasekhar [41, 42] depairing mechanism.

Similar observations have been recently made [55] in heavy fermionic compound UBe_{13} . This case demands further investigation because it seems that this material with extremely high upper critical field [61] and T^3 behaviour of specific heat at low temperature [62] belongs to triplet superconductors with point nodes in the quasiparticle spectrum.

Chapter 6

Conclusion part I

On the basis of the Ginzburg-Landau expansion for the superconductor free energy including both electron charge and spin coupling to the internal magnetic field, we have studied the evolution with field of anomalous local magnetic field inhomogeneity as measured by vortex lattice form factors and muon spin rotation static linewidth both in the limit of independent vortices near T_c , and in the near $H_{c2}^p(T)$ regime on the other hand.

In the first case, relying on a variational function for the gap structure of an isolated vortex we have found a simple expression for the form factors which is a function of the internal field scaled with the temperature dependent upper critical field in the Pauli limit and includes a single parameter $\alpha_M = \alpha_{M0} \sqrt{1 - T/T_c}$ with $\alpha_{M0} = \mu\phi_0 T_c / v_F^2$ the zero-temperature Maki parameter. We have found a crossover between two regimes depending on the value of α_M . In the orbitally limited regime ($\alpha_M < 1$) the static linewidth (this also stands for the form factor F_{10}) decreases with respect to internal field as previously known. The Pauli limited regime ($\alpha_M > 1$) however yields static linewidth increase (first in a non-analytic way, then linearly) because of local field inhomogeneity increase in the vortex core region due to Zeeman effect. Comparison between the derived formula and experimental data gives good agreement.

In the regime near $H_{c_2}^p(T)$ we have applied the Abrikosov solution of the linearised first Ginzburg-Landau equation to determine the magnetic field inhomogeneity in the Pauli limit. We recovered the form factor linear increase and found form factor linear collapse at the critical field $H_{c_2}^p$. We described the approach from second-order to first-order transition to the metal (this occurs at $T/T_c \approx 0.56$ and $\mu H_{c_2}^p/T_c \approx 1.07$) with a sudden raise in the absolute value of the slope of $\sigma_s^{\text{VL}}(B)$ while approaching $H_{c_2}^p(T)$.

The additional chapter discusses the effective Ginzburg-Landau parameter dependence on temperature in the vicinity of the upper critical field. We have contrasted expected behaviour in the orbital limit ($\alpha_{M0} \ll 1$) leading to constant effective Ginzburg-Landau parameter with the Pauli limit ($\alpha_{M0} \gg 1$) leading to sudden increase in the parameter when raising temperature to $T_c(B)$ with $B < T_c/(\mu\alpha_{M0})$ (vicinity of T_c). This provides additional signature of Pauli-limited superconductivity allowing identification of a number of experimental systems such as URu₂Si₂, NpPd₅Al₂ and possibly UBe₁₃ as being elements of this class.

Part II

Field-induced spin-exciton condensation

Chapter 7

Heavy electron superconductivity and antiferromagnetism

We now turn to the issue of the relation between superconductivity and antiferromagnetism in heavy electron compounds. This is supported by long-term experimental investigation on superconducting CeCoIn₅ with magnetic field applied in the tetragonal crystal plane ($H_{c20} \approx 11.7\text{T}$). Crucial experimental facts [63, 64, 48, 65, 66, 67] proved the confinement of magnetism (incommensurate spin density wave¹ close to antiferromagnetism) within the superconductor. This raised the questions of how magnetism emerges from superconductivity in high magnetic field. First we state experimental evidence on the nature of the system ground state and review theoretical ideas on interaction between heavy electron superconductivity and antiferromagnetism in magnetic field. Second we present complementary information provided by inelastic neutron scattering with description of spin collective

¹Here we use the terminology spin density wave to denote static quasi long range spin correlations with finite wave-vector \mathbf{q} . In particular the commensurate case with doubling of lattice period is referred to as antiferromagnetism.

mode. Third we recall how spin correlations and superconductivity are considered in the spin-fermion model and how such an approach relates inelastic and ground state properties.

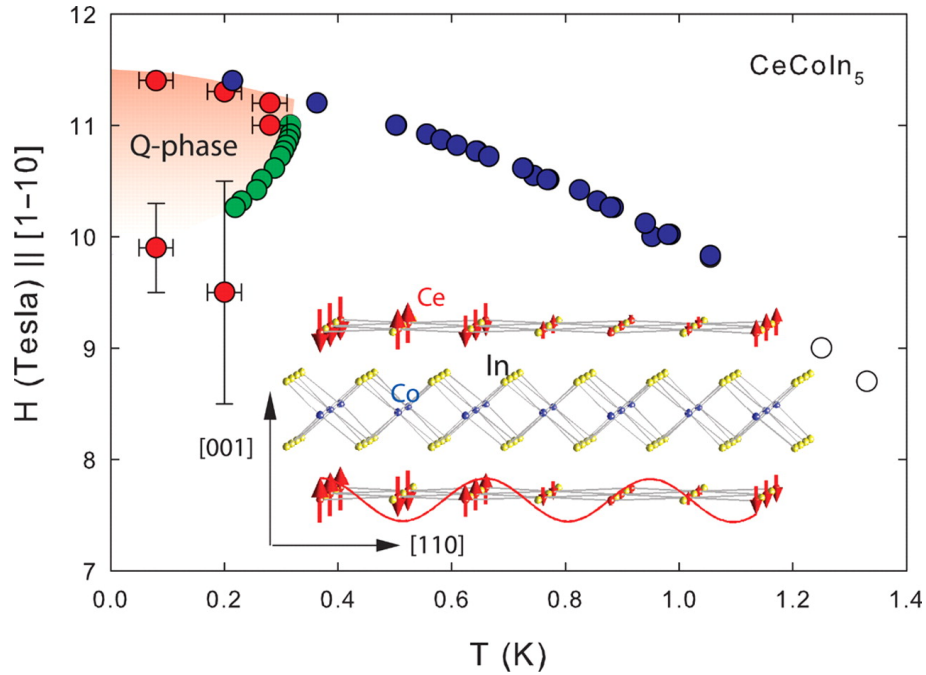


Figure 7.1: (From [48]) CeCoIn₅ phase diagram in temperature and magnetic field directed in the plane of the tetragonal crystal structure ([1,-1,0] direction). The magnetically ordered phase is colored in red. The blue and open circles signal first- and second-order transition respectively between the metal and the superconductor as revealed by specific heat measurement [40]. The green circles represent the boundary of the high-field-low-temperature magnetic phase as measured by specific heat [40] and red circles are results of neutron diffraction experiment [48]. The inset shows the crystal and magnetic structures with static magnetic moments on the Ce³⁺ ions.

7.1 Background information

Original measurement [40] in CeCoIn₅ phase diagram of a line of discontinuity in the specific heat highlighted a second-order transition to a high-field-low-temperature phase ($10\text{T} < H < 11.5\text{T}$, $T < 0.4\text{K}$) inside the superconductor with magnetic field applied in the basal plane of the tetragonal crystal structure [*c. f.* Fig. (7.1)]. In such a configuration the upper critical field in CeCoIn₅ is mostly determined by Pauli limiting ($H_{c20} \approx 11.7\text{T}$) and due to this the phase transition to the superconducting state below $T \approx 0.4T_c \approx 1\text{K}$ is of the first order [37]. This phase transition of the superconductor was initially interpreted as a realisation of the Fulde-Ferrel-Larkin-Ovchinnikov (FFLO) state [40].

An important finding was later achieved by Kenzelmann and collaborators [48, 65] [Fig. (7.1)] while using elastic neutron scattering to probe magnetism in this low-temperature and high-field region of the superconductor. It was observed a spin density wave order with wave-vector $\mathbf{Q} = (q, q, \pi)$ (*c. f.* footnote²). $q \approx 0.9\pi$ is incommensurate and almost independent of the field magnitude. The appearance of the magnetic phase coincides with the transition line determined by thermodynamical measurement which gives evidence that the phase previously detected at high-field has a magnetic character with magnetic coherence length $\sim 3000\text{\AA}$ [48] extending well beyond the vortex cores. The value of the magnetic moment on Cerium sites $m = 0.15\mu_B$ is small and oriented along the *c*-axis of the tetragonal crystal structure. It was remarkable there that incommensurate spin density wave was confined within the superconducting phase, meaning that superconductivity is an essential ingredient for spin density wave to develop. The existence of the transition in the superconductor was earlier detected by magnetisation measurement [63], magnetic order was revealed by Nuclear Magnetic Resonance (NMR) [64, 66], further NMR experiment [67] lead to characterisation of magnetic

²In this part we express lengths in units of the in-plane lattice constant ℓ_{ab} .

order evolution with field, and neutron diffraction [68] showed the phase disappearance when the field is rotated with angle $> 17^\circ$ with respect to the crystal basal plane.

From a theoretical point of view these coexisting orders were discussed within models which can be divided into three classes. In the first one [48, 69, 70, 71, 72, 73] theories rely on coupling between spin density wave, superconductivity and superconductivity with Cooper pairs having non-zero center of mass momentum (FFLO phase, Pair Density Wave (PDW), or π -triplet superconductivity), which stabilises spin density wave and superconductivity at high-field and low-temperature. In particular the model [70, 71] considers the magnetic transition as an extrinsic property of the superconductor which is an effect of the density of state increase due to bound state formation in the planes of the FFLO phase where the superconductor gap vanishes. A second point of view [74] also put forward an extrinsic mechanism with the role played by the vortex lattice in a $d_{k_a^2 - k_b^2}$ -wave superconductor which increases the density of states in the nodal direction of the gap and triggers a magnetic instability. In the third class [75, 76, 77] it was emphasised the importance of Pauli limiting in d-wave superconductors for stabilizing spin density wave order in the case where the two-dimensional fermion excitation energy spectrum presents nesting features of the metal Fermi surface. In [75, 76] the Fermi surface is considered to be analogous to the one in ferropnictides high-critical-temperature superconductors and there was moreover conjectured that the low-temperature-high-field superconducting phase in CeCoIn_5 consists of coexisting FFLO and incommensurate spin density wave orders. The model [77] proposed the enhancement of nesting due to pockets formed by the d-wave superconductivity order parameter in nodal region of the energy spectrum.

Another key observation was made on CeCoIn_5 by Inelastic Neutron Scattering. Stock and collaborators [78] measured a spin resonance that was sharp in energy ($\Omega_{\text{res}} = 0.60 \pm 0.03 \text{ meV}$) with wave-vector distribution centered

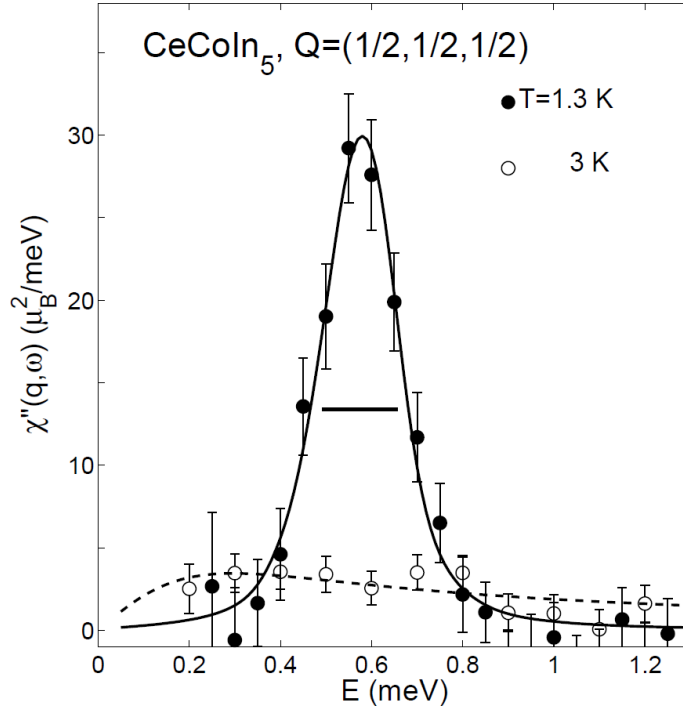


Figure 7.2: (From [78]) Spin resonance measured by Stock and collaborators by inelastic neutron scattering (the experiment extracts the imaginary part of the spin dynamical susceptibility). This is taken at commensurate wave-vector $\mathbf{Q} = (\pi, \pi, \pi)$, which is the point in momentum space where the resonance intensity is maximum. The experimental convention is to take the dimensions of the Brillouin zone as units for expressing wave-vectors. Our convention is different as stated in text.

on $\mathbf{Q} = (\pi, \pi, \pi)$ and width $\approx 0.3\pi$. Thereafter Panarin and collaborators [79] examined the evolution of the resonance in magnetic field applied in the $[1, -1, 0]$ direction. They observed a decrease in the resonance energy and a broadening in its lineshape with increasing field. They were able to measure it up to the field $\approx 0.5H_{c20}$ at which point the resonance signal was lost in the incoherent part of the neutron diffusion spectrum.

Interpreting the inelastic neutron scattering data has given rise to debate. Eremin and collaborators [80] have attributed the resonance to the proximity

to the threshold of particle-hole excitation of a $d_{k_a^2-k_b^2}$ -wave superconductor in the same line as the discussion of experiment in the original paper [78] and by analogy with analysis of resonances in cuprate high- T_c superconductors [81, 82, 83, 84, 12, 85]. We refer to this interpretation as the *spin-exciton* scenario. The particle-hole decay threshold energy at antiferromagnetic wave-vector $\mathbf{Q} = (\pi, \pi, \pi)$ writes [80]

$$\Omega_0 = \min_k (|\Delta_k| + |\Delta_{k+Q}|), \quad (7.1)$$

where the wave-vector k belongs to the Fermi surface in the crystal first Brillouin zone and so does $k + \mathbf{Q}$ (c . f. footnote³). $|\Delta_k|$ and $|\Delta_{k+Q}|$ are the order parameter complex moduli at these points of wave-vector space. The spin-exciton interpretation [81, 82, 83, 84, 12, 85] requires the symmetry of the superconductor order parameter to be $d_{k_a^2-k_b^2}$ -wave which follows from the necessity the order parameter changes sign from one hot-spot to the other. Observation of the resonance therefore represents the proof for the order parameter symmetry in CeCoIn₅ according to [78, 80].

Such an interpretation for the spin resonance was however criticised by Chubukov and Gor'kov [86] because of the lack of strict two-dimensionality of the compound. Instead, they proposed a magnon scenario in a three-dimensional system where the presence of the superconducting gap removes Landau damping of the spin collective mode and makes the magnon coherent in energy. From their point of view observation of the resonance is not a probe of the superconductor order parameter symmetry but instead a manifestation of the effect of superconductivity in hindering hybridization between itinerant s-p-d electrons and localized f-electrons.

Here we shall argue in favour of the spin-exciton scenario [87] in a quasi two-dimensional $d_{k_a^2-k_b^2}$ -wave superconductor and show that the ground state

³The set of points of the Fermi surface that are connected by the wave-vector at which the spin susceptibility is maximum [here this is the diagonal antiferromagnetic wave-vector $\mathbf{Q} = (\pi, \pi, \pi)$] are referred to as *hot-lines* in three-dimension and *hot-spots* in two-dimension [12].

transition in magnetic field observed [48] in superconducting CeCoIn₅ can be viewed as an *intrinsic* property of the superconductor and a direct consequence of the existence of the superconductor collective spin excitation mode [78] whose condensation⁴ naturally explains confinement of magnetic ordering within the superconductor. This effect can be understood in the "two-fluid" approach connected with observation [27, 28, 29] on superconducting CeCoIn₅.

7.2 Model considerations

We now give a formulation of the model on the basis of experimental knowledge of the fermion excitation energy spectrum in the non-superconducting state and the pairing symmetry in the superconducting state.

7.2.1 Electronic structure quasi two-dimensionality and superconductor $d_{k_a^2-k_b^2}$ -wave pairing symmetry

Regarding dimensionality a number of de-Haas-van-Alphen and transport measurements [16, 17, 88, 89] have determined the momentum resolved electronic structure in the non-superconducting phase of CeCoIn₅. It was found a multiband system with remarkable two-dimensional character [in particular de-Haas-van-Alphen experiment [16, 17, 88] highlighted strong two-dimensionality displayed by the α electron-15 band, *c. f.* Fig. (7.3)]. In spite of caution [86] on two-dimensional system hypothesis, we argue here that the electronic structure of CeCoIn₅ has sufficient two-dimensional character so that we can consider a model of a two dimensional metal from which superconductivity develops.

On the other hand determining the superconductor pairing symmetry has been a long-standing issue. A method based on the supercurrent Doppler

⁴Here the term *condensation* is used in the sense of a transition of a dynamic collective excitation mode to static ordering.

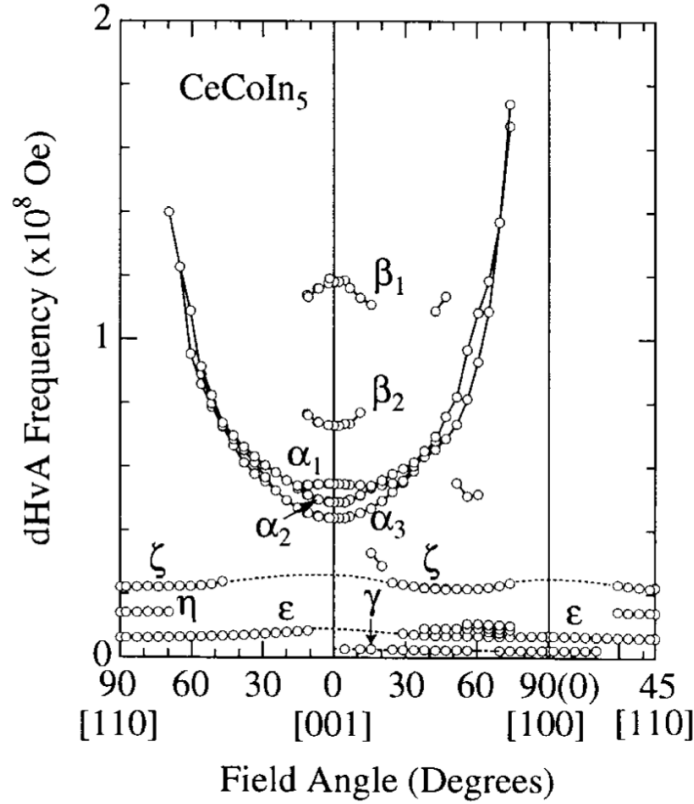


Figure 7.3: (From [16]) de-Haas-van-Alphen oscillation frequencies dependence on the magnetic field orientation with respect to the crystal principal axes. This shows multiband character and alpha band (electron 15-band) with two-dimensional character.

shift effect for characterising the state of unconventional superconductors in magnetic field has been developed in a series of theoretical and experimental papers [90, 19, 20] (for a review see [9]). The principle stands on the modification of the electronic system thermodynamics when a magnetic field is rotated in space due to superconductor gap anisotropy. By measuring thermal conductivity in magnetic field the symmetry of the gap in CeCoIn_5 has been found to be $d_{k_a^2 - k_b^2}$ -wave [19]. Although this result was for some time contradicted by specific heat data of another group [91] indicating $d_{k_a k_b}$ -wave symmetry, $d_{k_a^2 - k_b^2}$ -wave symmetry was later confirmed by Andreev reflection

experiment [92] and by new specific heat measurement [21]. Expression for $d_{k_a^2-k_b^2}$ -wave superconductor order parameter corresponding to the irreducible representation B_{1g} of the tetragonal crystal point group reads [12] (*c. f.* Fig. 7.4)

$$\Delta_k = \frac{\Delta_0}{2} \sum_n a_n [\cos(nk_a) - \cos(nk_b)]. \quad (7.2)$$

From the point of view of the spin-fermion model [12] a feature required for $d_{k_a^2-k_b^2}$ -wave superconductivity pairing in a two-dimensional system close to antiferromagnetic ground state transition is the existence of hot-spots. This gives rise to Landau-damped spin density fluctuations interacting with fermions and leads to superconductivity pairing [12]. Their existence also plays a determinant role for the spin collective excitations in the superconducting state⁵. It was argued [86] that the α -band seen in de-Haas-van-Alphen experiment is large enough to contain hot-spots. In the present model we are considering $d_{k_a^2-k_b^2}$ -wave superconductivity on a single two-dimensional Fermi surface including hot-spots. We shall not study the superconducting transition itself but start with a system in a $d_{k_a^2-k_b^2}$ -wave superconducting ground state and consider static and dynamic uniaxial spin susceptibilities in transverse magnetic field.

7.2.2 Spin-fermion model

We construct our argumentation on the frame of the spin-fermion model in a two-dimensional $d_{k_a^2-k_b^2}$ -wave superconductor [86, 12] which describes interaction between superconductivity and collective spin excitations in a system close to ground state magnetic transition with short-range spin correlations. The two building blocks are fermion excitations and spin density fluctuation

⁵We have earlier introduced hot-spots as special points in wave-vector space defined by the non-superconducting properties of a two-dimensional system. In the $d_{k_a^2-k_b^2}$ -wave superconductor, there is a gap above the hot-spots which yields [86] (*c. f.* below) a dynamic collective spin excitation mode with maximum intensity at antiferromagnetic wave-vector.

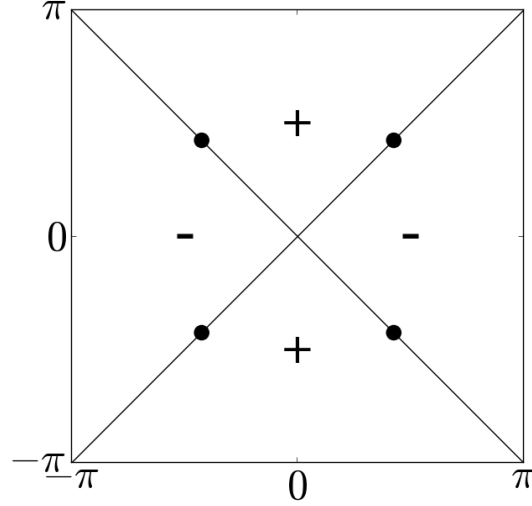


Figure 7.4: Superconductor $d_{k_a^2 - k_b^2}$ -wave symmetry order parameter on first Brillouin zone of a square lattice in the case of zero magnetic field. Diagonals mark the locations where the order parameter vanishes, on each side of which it changes sign. Black circles represent the points (Dirac points) of intersection between the Fermi line and the diagonals. At these discrete locations the fermion energy spectrum remains gapless.

excitations which are part of the action [12]

$$\mathcal{S} = \mathcal{S}_{\text{Fermion}} + \mathcal{S}_{\text{Spin}} + \mathcal{S}_{\text{Int}}. \quad (7.3)$$

We recall the electron part

$$\mathcal{S}_{\text{Fermion}} = -T \sum_{k, \sigma, \omega_m} [G_{\sigma}^{(0)}(\mathbf{k}, i\omega_m)]^{-1} a_{k\sigma}^{\dagger} a_{k\sigma}, \quad (7.4)$$

with the free electron Green function

$$G_{\sigma}^{(0)}(\mathbf{k}, i\omega_m) = \frac{1}{i\omega_m - \sigma\mu B - \epsilon_k}, \quad (7.5)$$

where $\omega_m = \pi T(2m + 1)$ are fermion Matsubara frequencies (m are integer), ϵ_k the fermion excitation energy spectrum measured from chemical potential, σ the electron spin projection, μ the electron magnetic moment and B the superconductor internal magnetic field. The spin part we consider uniaxial⁶ is

$$\mathcal{S}_{\text{Spin}} = \frac{T}{2} \sum_{q, \Omega_n} \chi_0^{-1}(\mathbf{q}, i\Omega_n) S_q^x S_{-q}^x, \quad (7.6)$$

where the free spin excitation propagator has the Ornstein-Zernike form

$$\chi_0(\mathbf{q}, i\Omega_n) = \frac{\chi_0}{\xi_m^{-2} + |\mathbf{q} - \mathbf{Q}|^2 - (i\Omega_n)^2/v_s^2}. \quad (7.7)$$

Here $\Omega_n = 2n\pi T$ are boson Matsubara frequencies (n are integer), χ_0 is a constant, ξ_m a magnetic correlation length in units of the cell parameter, and v_s an energy scale for the spin collective excitations in absence of fermions. The interaction term between the fermions and spins writes

$$\mathcal{S}_{\text{Int}} = g \int_{k, q} a_{k+q\alpha}^\dagger \sigma_{\alpha\beta}^x a_{k\beta} S_{-q}^x. \quad (7.8)$$

The full fermion Green functions are defined as

$$G_\sigma(\mathbf{k}, i\omega_m) = - \int_0^{1/T} d\tau e^{i\omega_m\tau} \langle a_{k\sigma}(\tau) a_{k\sigma}^\dagger(0) \rangle, \quad (7.9)$$

$$F_\sigma(\mathbf{k}, i\omega_m) = - \int_0^{1/T} d\tau e^{i\omega_m\tau} \sigma \langle a_{k\sigma}(\tau) a_{-k-\sigma}(0) \rangle, \quad (7.10)$$

$$F_\sigma^+(\mathbf{k}, i\omega_m) = - \int_0^{1/T} d\tau e^{i\omega_m\tau} \sigma \langle a_{-k-\sigma}^\dagger(\tau) a_{k\sigma}^\dagger(0) \rangle. \quad (7.11)$$

where brackets mean Gibbs averaging, $a_{k\sigma}(\tau)$ are imaginary time-dependent fermion operators in the Matsubara representation [AGD]. In a superconductor with Zeeman magnetic field along the z-axis they evaluate to (*c. f.*

⁶In this part we consider spin excitations along the single axis x which corresponds to the c-axis of the tetragonal crystal.

addendum)

$$G_\sigma(\mathbf{k}, i\omega_m) = \frac{i\omega_m - \sigma\mu B + \epsilon_k}{(i\omega_m - \sigma\mu B)^2 - \epsilon_k^2 - \Delta_k^2}, \quad (7.12)$$

and

$$F_\sigma(\mathbf{k}, i\omega_m) = F_\sigma^+(\mathbf{k}, i\omega_m) = \frac{\Delta_k}{(i\omega_m - \sigma\mu B)^2 - \epsilon_k^2 - \Delta_k^2}, \quad (7.13)$$

where we have fixed the phase of Δ_k so that it is real. The full spin-density fluctuation Green function in the case of uniaxial magnetic anisotropy along the x-axis is defined as

$$\chi(\mathbf{q}, i\Omega_n) = \int_0^{1/T} d\tau \int d^2r e^{-i\mathbf{q}\cdot\mathbf{r} + i\Omega_n\tau} \langle S^x(\mathbf{r}, \tau) S^x(0, 0) \rangle, \quad (7.14)$$

where $S^x(\mathbf{r}, \tau)$ is an imaginary time-dependent boson operator in the Matsubara representation. This can be written as

$$\chi^{-1}(\mathbf{q}, i\Omega_n) = \chi_0^{-1}(\mathbf{q}, i\Omega_n) - \Pi(\mathbf{q}, i\Omega_n), \quad (7.15)$$

which consists of the free part Eq. (7.7) and a self-energy part due to fermions $\Pi(\mathbf{q}, i\Omega_n)$. At one loop level the self energy reads

$$\begin{aligned} & \Pi^{ab}(\mathbf{q}, i\Omega_n) \\ &= -g^2 \chi_0 T \sum_{k, \sigma, \sigma', \omega_m} \left[\sigma_{\sigma\sigma'}^a G_{\sigma'}(\mathbf{k}, i\omega_m) \sigma_{\sigma'\sigma}^b G_\sigma(\mathbf{k} + \mathbf{q}, i\omega_m + i\Omega_n) \right. \\ & \quad \left. + \sigma_{\sigma\sigma'}^a F_{\sigma'}(\mathbf{k}, i\omega_m) \sigma_{\sigma'\sigma}^b F_\sigma^+(\mathbf{k} + \mathbf{q}, i\omega_m + i\Omega_n) \right], \quad (7.16) \end{aligned}$$

with σ^a the Pauli matrices, we note $\Pi(\mathbf{q}, i\Omega_n) = \Pi^{xx}(\mathbf{q}, i\Omega_n)$, and the retarded response function is obtained from analytic continuation $i\Omega_n \rightarrow \Omega + i0^+$ with 0^+ a positive infinitesimal.

Connection between the model Eq. (7.15) and experiment is provided by the fluctuation-dissipation theorem which relates the spin correlations represented by the *dynamic structure factor* in inelastic neutron scattering experiment [78] with the spin excitation *spectral function* (the imaginary part

of the spin excitation retarded Green function)

$$\mathcal{S}(\mathbf{q}, \Omega) = \frac{2}{1 - e^{-\Omega/T}} \Im \chi(\mathbf{q}, \Omega + i0^+). \quad (7.17)$$

In general the spectral function can be written as

$$\Im \chi(\mathbf{q}, \Omega) = \frac{\Im \Pi(\mathbf{q}, \Omega)}{[\chi_0^{-1}(\mathbf{q}, \Omega) - \Re \Pi(\mathbf{q}, \Omega)]^2 + [\Im \Pi(\mathbf{q}, \Omega)]^2} \quad (7.18)$$

which looks like a Dirac delta $\pi \delta[\chi_0^{-1}(\mathbf{q}, \Omega) - \Re \Pi(\mathbf{q}, \Omega)]$ in absence of Landau damping by fermion particle-hole excitations (*i. e.* as $\Im \Pi(\mathbf{q}, \Omega) \rightarrow 0$). In this limit the collective spin excitation mode is a resonance *i. e.* is coherent in energy. This can be re-expressed as

$$\Im \chi(\mathbf{q}, \Omega) = Z \delta(\Omega - \Omega_{\text{res}}), \quad (7.19)$$

which defines the resonance energy Ω_{res} solution of $\chi_0^{-1}(\mathbf{q}, \Omega) - \Re \Pi(\mathbf{q}, \Omega) = 0$ and the spectral weight

$$Z = \pi \text{abs} \left(\frac{\partial}{\partial \Omega} [\chi_0^{-1}(\mathbf{q}, \Omega) - \Re \Pi(\mathbf{q}, \Omega)]_{\Omega = \Omega_{\text{res}}} \right)^{-1}. \quad (7.20)$$

Eq. (7.19) defines a collective mode [pole of the spin Green function Eq. (7.15)] which is in general an inelastic process *i. e.* $\Omega_{\text{res}} \neq 0$. The additional requirement $\Omega_{\text{res}} = 0$ is a condition for a ground state instability also known as Overhauser criterion for spin density wave transition. These relations constitute the basis of the next chapter on collective properties of two-dimensional $d_{k_a^2 - k_b^2}$ -wave superconductors in Zeeman field.

7.3 Addendum: Fermion excitation energy spectrum for a superconductor in Zeeman magnetic field

In this supplementary section we express the fermion excitation energy spectrum for a d-wave singlet superconductor in Zeeman magnetic field starting from the pairing Hamiltonian. In matrix notation the latter reads

$$\mathcal{H} = \frac{1}{2} \sum_{k\sigma} \bar{\Psi}_{k\sigma} \hat{\mathcal{H}}_{k\sigma} \Psi_{k\sigma} \quad (7.21)$$

with

$$\bar{\Psi}_{k\sigma} = \left(a_{k\sigma}^\dagger, \sigma a_{-k-\sigma} \right), \quad \Psi_{k\sigma} = \begin{pmatrix} a_{k\sigma} \\ \sigma a_{-k-\sigma}^\dagger \end{pmatrix} \quad (7.22)$$

and

$$\hat{\mathcal{H}}_{k\sigma} = \begin{pmatrix} \epsilon_k + \sigma\mu B & \Delta_k \\ \Delta_k^* & -\epsilon_k + \sigma\mu B \end{pmatrix}. \quad (7.23)$$

We have assumed space inversion symmetry $\epsilon_{-k} = \epsilon_k$. The fermion Gor'kov-Nambu Green function solves the Dyson equation

$$\hat{G}_\sigma^{-1}(\mathbf{k}, i\omega_m) = i\omega_m - \hat{\mathcal{H}}_{k\sigma}, \quad (7.24)$$

where we recall $\omega_m = \pi T(2m + 1)$ the fermion Matsubara frequency. This directly gives

$$\hat{G}_\sigma(\mathbf{k}, i\omega_m) = \frac{\begin{pmatrix} i\omega_m - \sigma\mu B + \epsilon_k & \Delta_k \\ \Delta_k^* & i\omega_m - \sigma\mu B - \epsilon_k \end{pmatrix}}{(i\omega_m - \sigma\mu B)^2 - \epsilon_k^2 - |\Delta_k|^2}, \quad (7.25)$$

together with the Green functions Eqs. (7.12), (7.13), and (7.11). The later are characterized by the spectrum of fermion excitation in the superconductor

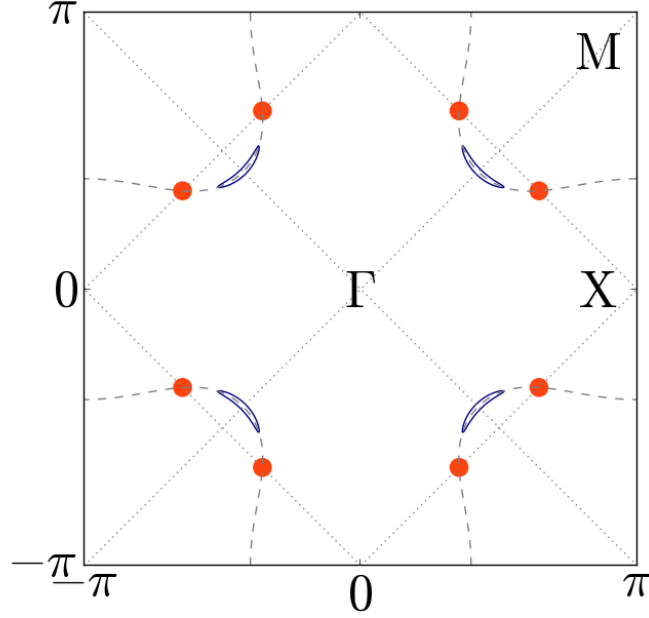


Figure 7.5: Fermi pockets in the first Brillouin zone of a $d_{k_a^2 - k_b^2}$ -wave superconductor in Zeeman magnetic field. The pockets set of momenta which solve $\sqrt{\epsilon_k^2 + \Delta_k^2} = \mu B$ are in blue. Also shown are hot-spots in orange. We took $\mu B = 0.23\Delta_0$ with superconductor and metal spectra defined in the next chapter.

[93]

$$E_{k\sigma}^s = s[\epsilon_k^2 + \Delta_k^2]^{1/2} + \sigma\mu B \quad (7.26)$$

where $s, \sigma = \pm 1$ represents the particle-hole index. In a d-wave superconductor the Zeeman field transforms the gap nodes to pockets [*c. f.* Fig. (7.5)] of gapless quasiparticles.

Chapter 8

From collective spin density fluctuation mode to magnetic ordering of a quasi two dimensional $d_{k_a^2-k_b^2}$ -wave superconductor

The field-induced spin-exciton criticality scenario is presented. The first section consists in the analysis of the properties of the spin polarisation function in the two-dimensional $d_{k_a^2-k_b^2}$ -wave superconductor with Zeeman magnetic field. It shows how the singular behaviour of the response function for nearly commensurate wave-vector arises and how this leads to criticality in magnetic field directed transversally to the easy magnetic direction. The second section provides results from numerical computation of the spin polarisation function with comparison between the static response functions field dependence in the superconductor and in the metal . We then present field dependence of the collective mode energy for comparison with experiment. Discussion of the approach is included in the last section. Part of the results

of this chapter are from the published article [87] and from the SCES 2011 (Strongly Correlated Electron Systems) conference proceeding [94] accepted for publication.

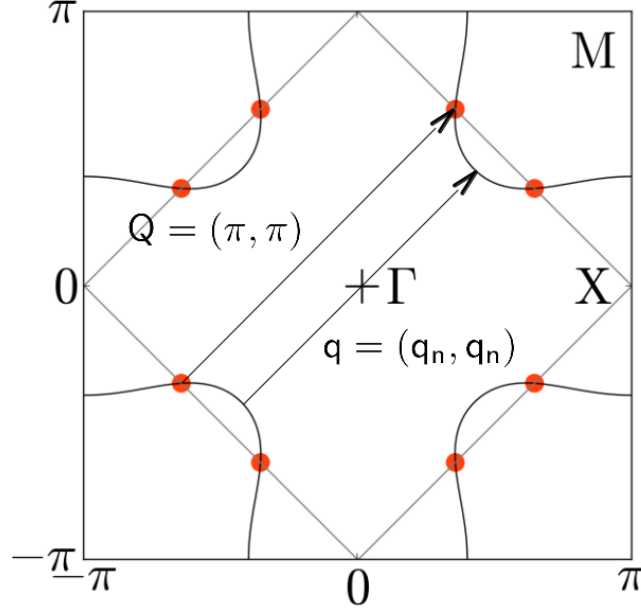


Figure 8.1: Configuration of diagonal antiferromagnetic and nesting wave-vectors in the two-dimensional first Brillouin zone (by nesting wave-vector we mean the wave-vector that connects a pair of points of the Fermi line where Fermi velocities are parallel). Contour plot of the normal-state energy spectrum used for numerics $\epsilon_k = 0$ (the Fermi line) is shown. Points of intersection between the Fermi line and the antiferromagnetic Brillouin zone (diamond included in the Brillouin zone) are hot-spots. The spin-fermion model for the $d_{k_a^2 - k_b^2}$ -wave superconductor instability [12] predicts flat gap at these eight locations.

8.1 Analytic approach

Here we develop the scenario for the occurrence of the phase with coexisting superconductivity and spin density wave in CeCoIn_5 which consists in

the ground state transition [48, 65] as the result of field-induced criticality of the collective mode detected with inelastic neutron scattering [78] at energy $\Omega_{\text{res}} \approx 0.6\text{meV}$ and whose evolution has been observed in magnetic field [79, 95, 96]. The mechanism is an *intrinsic* property of the superconductor and follows from (i) the reduced dimensionality of the system, (ii) the existence of a gap around hot-spots, and (iii) the $d_{k_a^2-k_b^2}$ -wave symmetry order parameter sign change from one hot-spot to the other¹ (flat gap at hot-spots gives rise to logarithmic divergence of the spin polarisation function). This model for a continuous transition is little restrictive as it does not require coexistence with another state like FFLO or pair-density-wave, neither nesting properties of the Fermi surface. This further establishes connection with interpretation of inelastic neutron scattering experiment which is debated [12]: in the interpretation of the resonance as a collective spin density fluctuation excitation of the $d_{k_a^2-k_b^2}$ -wave superconductor, the slowing down of the mode to static ordering in transverse magnetic field naturally accounts for confinement of magnetism in the superconductor. From a static point of view the incommensurate magnetic instability occurs after development of pockets around gap nodes in Zeeman magnetic field with gapless excitations approaching hotspots. Only the weak coupling limit $\xi_m^2 g^2 \chi_0 \rightarrow 0$ yields instability at commensurate wave-vector.

The properties of the self-energy function $\Pi(\mathbf{q}, \Omega)$ is known at one loop level for zero field [86]. We now evaluate $\Pi(\mathbf{q}, \Omega) = \Pi^{xx}(\mathbf{q}, \Omega)$ the uniaxial self energy in transverse Zeeman magnetic field by making use of the Green

¹Pairing symmetry is a determinant element for the resonance to occur [86]: s-wave gap yields negative Π with no divergence in opposition with the $d_{k_a^2-k_b^2}$ -wave case. Dimensionality is also key since the three-dimension case replaces log-divergence by a cusp and then resonance only occurs at strong coupling yielding small peak feature.

functions Eqs. (7.12) and (7.13) (*c. f.* footnote²),

$$\Pi(\mathbf{Q}, i\Omega_n) = -g^2 \chi_0 T \sum_{k, \sigma, \omega_m} \frac{(i\omega_m - \sigma\mu B + \epsilon_k)(i\omega_m + i\Omega_n + \sigma\mu B + \epsilon_{k+q}) + \Delta_k \Delta_{k+q}}{[\epsilon_k^2 + \Delta_k^2 - (i\omega_m - \sigma\mu B)^2][\epsilon_{k+q}^2 + \Delta_{k+q}^2 - (i\omega_m + i\Omega_n + \sigma\mu B)^2]}. \quad (8.1)$$

We consider a pair of hot-spots which are separated by diagonal antiferromagnetic wave-vector, label them by 1 and 2, and linearise the metal energy dispersion about them

$$\epsilon_k = \mathbf{v}_1 \cdot (\mathbf{k} - \mathbf{k}_1), \quad \epsilon_{k+q} = \mathbf{v}_2 \cdot (\mathbf{k} - \mathbf{k}_1). \quad (8.2)$$

Here \mathbf{k}_1 and \mathbf{v}_1 [\mathbf{k}_2 and \mathbf{v}_2] are the Fermi momentum and Fermi velocity at hot-spot 1 [2] respectively. Summation over momenta can be expressed as an integral $\sum_k = \int d^2k / (2\pi)^2$ and performing the latter about hot-spot we obtain

$$\Pi(\mathbf{Q}, i\Omega_n) = -\frac{Ng^2\chi_0}{4|\mathbf{v}_1 \times \mathbf{v}_2|} T \sum_{\sigma, \omega_m} \left[1 + \frac{(i\omega_m - \sigma\mu B)(i\omega_m + i\Omega_n + \sigma\mu B) + \Delta_1 \Delta_2}{\sqrt{\Delta_1^2 - (i\omega_m - \sigma\mu B)^2} \sqrt{\Delta_2^2 - (i\omega_m + i\Omega_n + \sigma\mu B)^2}} \right], \quad (8.3)$$

where N is the number of hot-spots and Δ_1 [Δ_2] the superconductor order parameter value at hot-spot 1 [2] which can be set constant if the gap at hot-spot is flat [12, 86]. The number 1 in parenthesis is introduced for integral regularisation at high energy. As a notation convenience we define the

²Eq. 8.1 includes magnetic field effect in the Pauli limit. The influence of the electron orbital motions on the spin polarisation function can be evaluated [97] in the linearised Doppler shift approximation and gives correction of the order $B/(H_{c20}^p \alpha_{M0})$ which is small in a Pauli-limited superconductor as expected.

parameter (which is responsible for Landau-damping in the metallic state)

$$\gamma_d = \frac{Ng^2\chi_0}{8\pi|\mathbf{v}_1 \times \mathbf{v}_2|}. \quad (8.4)$$

The gap with $d_{k_a^2-k_b^2}$ -wave symmetry has the property $\Delta_1 = -\Delta_2$ which results in singular character of the real part of Eq. (8.3). The next step goes in a similar way as in [AGD] (p. 318). Setting $\Delta = |\Delta_1| = |\Delta_2|$, we obtain after analytic continuation the zero temperature real and imaginary parts

$$\Re\Pi(\mathbf{q}, \Omega) = 2\gamma_d\Delta \sum_{\sigma} f\left(\frac{\Omega + 2\sigma\mu B}{2\Delta}\right), \quad (8.5)$$

$$\Im\Pi(\mathbf{q}, \Omega) = 2\gamma_d\Delta \sum_{\sigma} g\left(\frac{\Omega + 2\sigma\mu B}{2\Delta}\right), \quad (8.6)$$

with the functions

$$f(y) = \int_{\max(0, y-1)}^y dx \frac{-x^2 - x(1-y) + y/2}{\sqrt{x(x+1)(y-x)(x+1-y)}}, \quad (8.7)$$

and

$$g(y) = \int_0^{\max(0, y-1)} dx \frac{-x^2 - x(1-y) + y/2}{\sqrt{x(x+1)(y-x)(y-1-x)}}. \quad (8.8)$$

The behaviour of Eqs. (8.7) and (8.8) is seen [86] as $f(y) \approx \pi y^2/8$ for $y \ll 1$, to logarithmic accuracy $f(y) \approx y \ln(y/|y-1|)/2$ for $|y-1| \ll 1$, and $g(y) \approx \pi y/2$ as $y-1 \ll 1$, which leads to the sketch of the polarisation function in Fig. (8.2). As a check these results are consistent with Kramers-Krönig relations [12]. Also shown in Fig. (8.3) are the dimensionless susceptibilities Eqs. (8.7) and (8.8) at zero and finite magnetic field.

Hence we have a positive spin polarisation function, increasing with energy, and logarithmic divergence of the real part at threshold energy $\Omega_0 = 2\Delta - 2\sigma\mu B$, which is split by magnetic field. Regarding the dynamics of the collective mode given by Eq. (7.15), we consider the energy scale v_s in

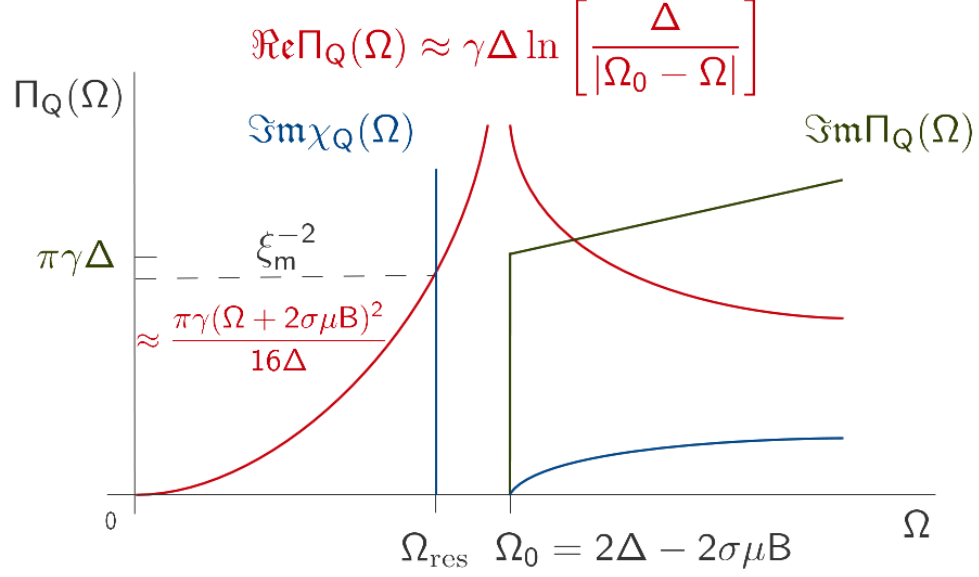


Figure 8.2: Uniaxial dynamic spin polarisation function for antiferromagnetic wave-vector with step discontinuity in the imaginary part associated with logarithmic divergence in the real part [12]. Spin resonance occurs ([86] and references therein) at energy Ω_{res} below the threshold energy Ω_0 , whose position depends on the value of short-range magnetic correlation length ξ_m . The effect of transverse magnetic field is splitting the threshold into two-step discontinuity.

the free spin Green function significantly larger than the threshold energy Ω_0 so that the dynamics is overwhelmed by superconductivity and at commensurate antiferromagnetic wave-vector we can effectively rewrite Eq. (7.15)

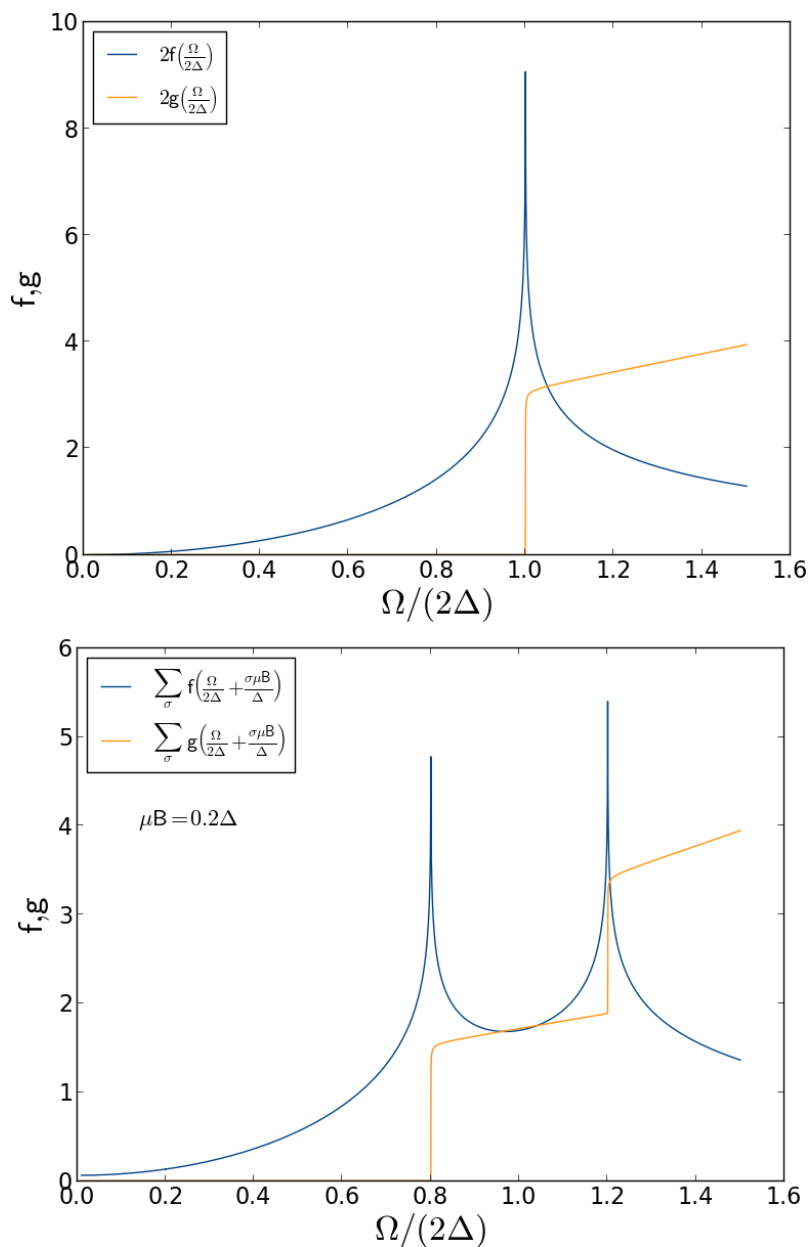


Figure 8.3: Above are real (blue) and imaginary (yellow) part of the dimensionless spin polarisation function Eqs. (8.7) and (8.8) at zero field. Below are the corresponding functions with field $\mu B = 0.2\Delta$.

as³

$$\chi(\mathbf{q}, \Omega) = \frac{\chi_0}{\xi_m^{-2} - \Pi(\mathbf{q}, \Omega)}, \quad (8.9)$$

such that Eq. 8.9 yields the condition

$$\Re \Pi(\mathbf{q}, \Omega_{\text{res}}) = \xi_m^{-2}, \quad (\Omega_{\text{res}} > 0), \quad \Im \Pi(\mathbf{q}, \Omega_{\text{res}})/(\gamma_d \Delta) \ll 1, \quad (8.10)$$

which defines the superconductor resonance represented in Fig. (8.2).

The mode dispersion is schematically represented in Fig. (8.4) at zero field and at the condensation field. The mode spectral weight [99] is maximum at commensurate wave-vector and expresses as $Z = 4\xi_m \sqrt{\pi \Delta / \gamma_d}$. Away from this point the downward dispersion [98] follows from the wave-vector dependence of the d-wave gap. Eventually the mode resonance energy reaches a minimal value at which point the threshold and resonance energy meet. There the dependence of the polarisation function is logarithmic with spectral weight $Z = \pi \exp[-1/(\xi_m^2 \gamma_d \Delta)] / \gamma_d$.

Transverse magnetic field splits the mode into a branch which goes down in energy and an upper part which becomes damped by the continuum of particle-hole excitations⁴. As a consequence the low energy region of the mode becomes critical at field $\mu B^* = \Delta_{\text{min}}$ with Δ_{min} the gap magnitude at Fermi-line points separated by incommensurate wave-vector and corresponding to lowest resonance energy of the mode. From the asymptotic expression of the spin polarisation function near the energy threshold in the static limit

³One mathematically equivalent way of dealing with superconductivity and antiferromagnetism was early put forward by Bulut and Scalapino [83] who dealt with interactions in a Random Phase Approximation susceptibility $\chi(\mathbf{q}, \omega) = \chi_0(\mathbf{q}, \omega) / [1 - U \chi_0(\mathbf{q}, \omega)]$, with $\chi_0(\mathbf{q}, \omega)$ the bare susceptibility in the superconductor and U is an effective repulsion potential. In this approach the conditions for the spin-exciton to occur are $U \Re \chi_0(\mathbf{q}, \omega) = 1$, and $U \Im \chi_0(\mathbf{q}, \omega) \ll 1$.

⁴In recent numerical work [100] consideration of different magnetic anisotropy as given two-fold splitting of the resonance. Magnetic isotropy gives splitting between three undamped modes [101].

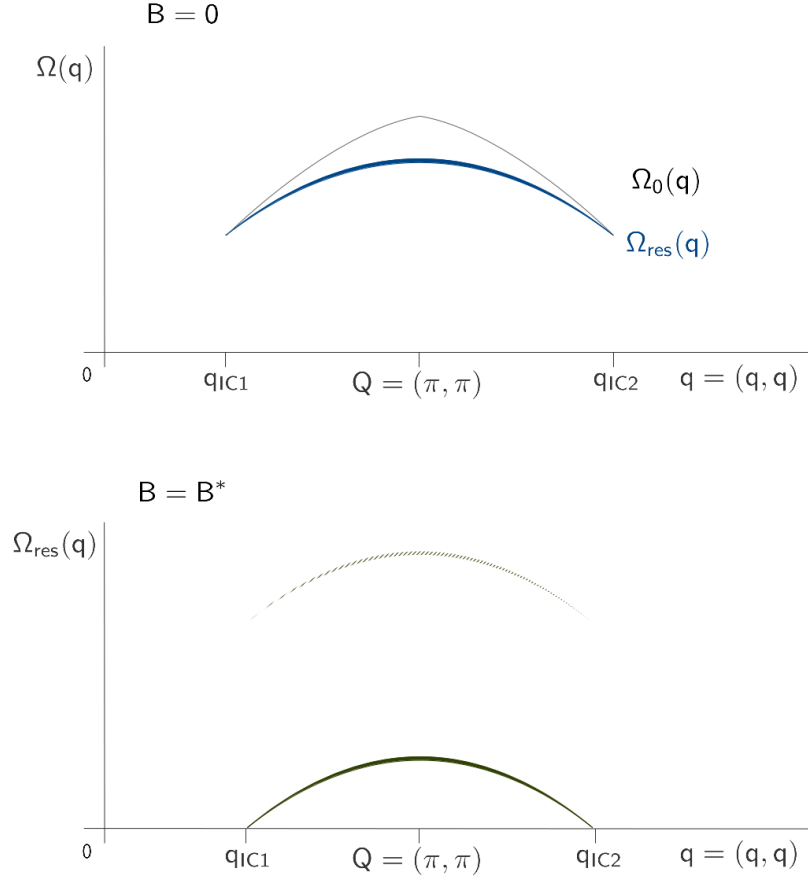


Figure 8.4: Sketch of the predicted resonant mode dispersion and threshold energy at zero field [98], evolution with transverse field in the uniaxial case (the higher energy mode is damped by the particle-hole decay continuum) and criticality at incommensurate wave-vector.

and cutting-off the log-divergence

$$\Pi(\mathbf{q}_{ic}) \approx \gamma_d \Delta_{\min} \ln \left[\frac{\Delta_{\min}}{\max(T, \Lambda)} \right], \quad (8.11)$$

where Λ is an energy cut-off introduced to account for distance from hot-spot and any finite electron lifetime effect on electrons and \mathbf{q}_{ic} the critical

incommensurate wave-vector, we obtain the instability critical temperature dependence on field

$$T^* \sim \mu B \exp\left(-\frac{\xi_m^{-2} + |\mathbf{q}_{\text{ic}} - \mathbf{Q}|^2}{\gamma_d \mu B}\right), \quad (8.12)$$

which emerges starting from the field magnitude B^+ given by

$$\mu B^+ \exp\left(-\frac{\xi_m^{-2} + |\mathbf{q}_{\text{ic}} - \mathbf{Q}|^2}{\gamma_d \mu B^+}\right) \sim \Lambda. \quad (8.13)$$

Notice the temperature-dependence of \mathbf{q}_{ic} which gives complex temperature-dependence of the critical field. Only in the weak coupling limit does this give rise to logarithmic dependence. Instability of the ground state at incommensurate wave-vector yields development of a spin density wave gap close to hot-spots and Fermi surface reconstruction. The spin-fermion model allows account of the feedback effect of the spin collective mode on fermions. In the superconductor both the quasiparticle self energy and the pairing vertex are logarithmic divergent due to the presence of a decay threshold in fermion spectrum [12]. These two effects counteract each other and leads only to a cusp in the gap of the superconductor.

8.2 Numerics

The spin polarisation function Eq. (8.1) is evaluated numerically along the crystal c -axis (x direction of our frame in pseudo-spin space) under magnetic field applied in the crystal basal plane (z -direction). As shown in appendix this goes to

$$\Pi(\mathbf{q}, \Omega) = \frac{1}{2} g^2 \chi_0 \sum_{\mathbf{k}, \sigma, s, s'} c_{ss'}(k, q) \frac{f(sE_k + \sigma\mu B) - f(s'E_{k+q} - \sigma\mu B)}{\Omega + sE_k - s'E_{k+q} + 2\sigma\mu B + i\Gamma}. \quad (8.14)$$

Here $f(z) = 1/[\exp(z/T) + 1]$ is the fermion distribution function at equilibrium, the integral $\sum_{\mathbf{k}} = \int_{B.Z.} d^2k/(2\pi)^2$ is performed over the first Brillouin zone $k_a, k_b \in [-\pi, \pi]$, $s, s' = \pm 1$ are particle-hole indices, $\sigma = \pm 1$ spin index, and Γ is a line broadening constant introduced for computational convenience. Below we take the temperature $T = 4.3085 \times 10^{-3} \text{meV}$ (50mK), and $\Gamma = 5 \times 10^{-3} \text{meV}$. The *coherence factors* are

$$c_{ss'}(k, q) = \frac{1}{2} \left(1 + ss' \frac{\epsilon_k \epsilon_{k+q} + \Delta_k \Delta_{k+q}}{E_k E_{k+q}} \right). \quad (8.15)$$

For superconductor gap with $d_{k_a^2 - k_b^2}$ -wave symmetry, the coherence factor $c_{ss'}(k, q)$ with $\text{sgn}(s) = -\text{sgn}(s')$ which corresponds to singular terms in integrand is close to unity at the points of the Fermi line where $\Delta_k = -\Delta_{k+q}$. The importance of the symmetry of the order parameter was early emphasised [82, 83] for the occurrence of the spin resonance.

We consider the non-superconducting-state two-dimensional electron energy spectrum⁵

$$\begin{aligned} \epsilon_k = & \epsilon + 2t_1[\cos(k_a) + \cos(k_b)] + 4t_2 \cos(k_a) \cos(k_b) \\ & + 2t_3[\cos(2k_a) + \cos(2k_b)], \end{aligned} \quad (8.16)$$

with $t_1 = 1 \text{meV}$, $t_2 = -0.5t_1$, $t_3 = 0.4t_1$ and $\epsilon = 0.6t_1$. A simple choice consists in considering the order parameter

$$\Delta_k = \frac{\Delta_0}{2} [\cos(k_a) - \cos(k_b)], \quad (8.17)$$

which manifestly is not flat at hot-spots. We take the maximal gap magnitude $\Delta_0 = 0.5 \text{meV}$.

The field dependent static spin polarisation function $\Pi(\Omega = 0)$ is shown in Fig. (8.5) for different wave-vectors in both the superconducting and

⁵The energy spectrum was computed in [102] in the mean-field three-dimensional Anderson model and gave a two-band structure including an open corrugated Fermi surface.

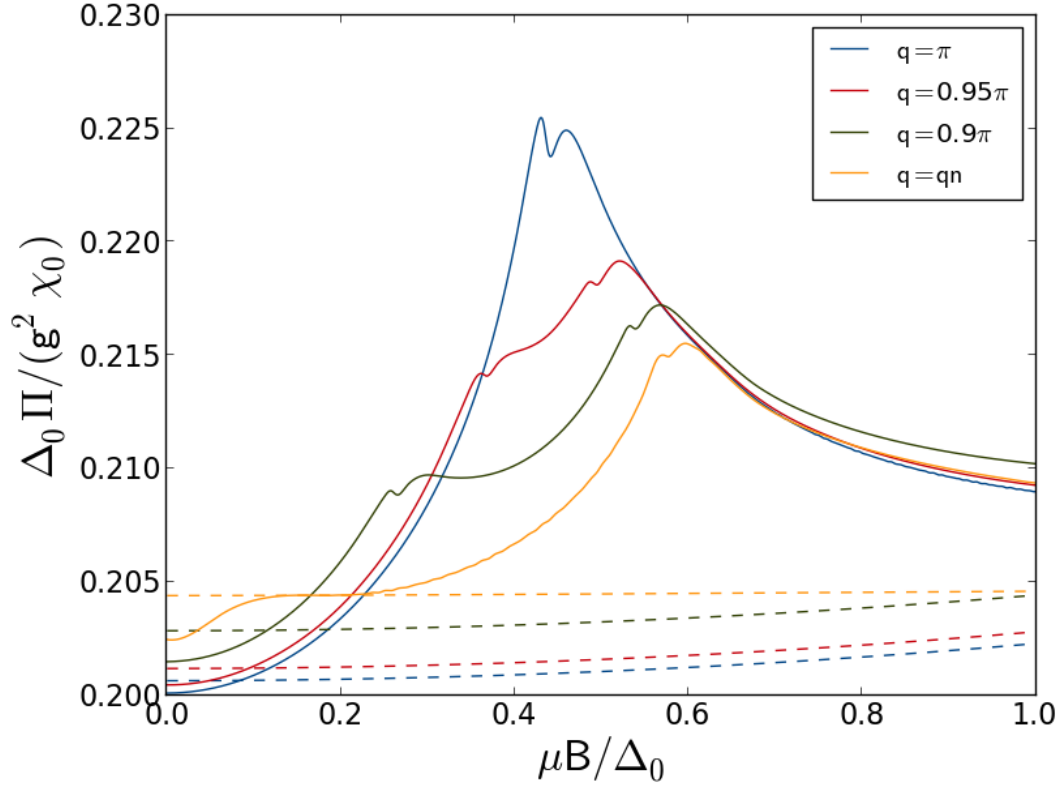


Figure 8.5: Comparison between static spin response functions in the superconductor (full lines) and in the metal (dashed lines). The polarisation function for the metal is $\Pi = \sum_{k\sigma} [f(\epsilon_k + \sigma\mu B) - f(\epsilon_{k+q} - \sigma\mu B)] \times [\epsilon_k - \epsilon_{k+q} + 2\sigma\mu B] / [(\epsilon_k - \epsilon_{k+q} + 2\sigma\mu B)^2 + \Gamma^2]$. These are evaluated for different wave-vectors from commensurate (blue) to nesting (yellow). There is a substantial increase in the superconductor spin polarisation function whereas the corresponding function for the metal remains essentially constant. The two-hump structure follows from umklapp process at incommensurate wave-vector. The maximum in the polarisation function occurs for antiferromagnetic wave-vector. As one moves away from commensuration the first increase occurs at lower field because of the reduction of the gap as one goes towards gap nodes. For nesting wave-vector (that connects gap nodes) we observe no susceptibility enhancement in comparison with the metallic case at low field, only increase occurs at higher field.

metallic phase.⁶ Magnetic transition occurs at some instability field B^* if the Overhauser criterion is fulfilled with $B^* < H_{c2}$. Calculation of H_{c2} in the Pauli limit with the above electron energy dispersion and factorised pairing potential $V(\mathbf{k}, \mathbf{k}') = -V\psi(\mathbf{k})\psi(\mathbf{k}')$ with $\psi(\mathbf{k}) = \cos(k_a) - \cos(k_b)$ yields $\mu H_{c2}^P = 0.37\Delta_0$. The spin polarisation function of the $d_{k_a^2 - k_b^2}$ -wave superconductor increases with field, becomes larger than the normal-state response function and has humps at fields $\mu B = \Delta_k$ and $\Delta_{k'}$, with Δ_k and $\Delta_{k'}$ the gap values at Fermi wave-vectors connected by $\mathbf{q} = (\pi, \pi) \pm (\delta, \delta)$. This two-hump structure is the result of umklapp process at incommensurate wave-vector. In contrast, Π in the metal does not sensibly depend on field. As explained in the legend of Fig. (8.5), the maximum increase in the polarisation function is for the antiferromagnetic wave-vector which is degenerate regarding umklapp. In contrast no low-field enhancement with respect to the metallic phase is yielded for nesting wave-vector. The precise instability wave-vector and critical magnetic field values depend on the magnitude of the coupling parameter $\xi_m^2 g^2 \chi_0 \Delta_0 / v_F^2$.

For arbitrary field direction, the polarisation function writes

$$\Pi^{\varphi\varphi} = \cos^2(\varphi)\Pi^{zz} + \sin^2(\varphi)\Pi^{xx}, \quad (8.18)$$

where φ is the angle between the magnetic field and the c-axis. The longitudinal polarisability Π^{zz} doesn't carry any field dependence in the denominator and therefore for $\mathbf{B}||c$ no magnetic ordering along the c-axis is induced in this uniaxial hypothesis. This point is consistent with experiment [68] where it was found that magnetic ordering disappears as magnetic field is tilted from the crystal plane. Also consistent with experiment is that the wave-vector of the spin density wave is not constrained by the in-plane orientation of the field [48] but by the gapped energy spectrum characteristics (in the condition

⁶The numerically evaluated polarisation function can be expressed as $\Pi^{\text{tot}}(\mathbf{q}, \Omega) = \Pi^{\text{reg}}(\mathbf{q}, \Omega) + \Pi^{\text{sing}}(\mathbf{q}, \Omega)$ where the first [second] term is a regular [singular] contribution. The analysis in the previous section concerns the singular part only.

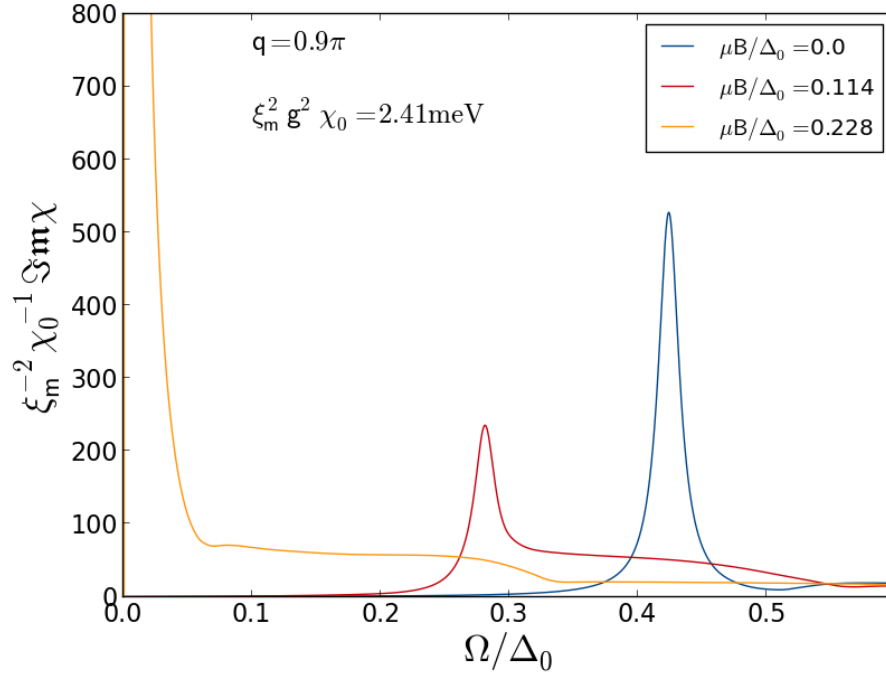


Figure 8.6: Spectral function of the dynamic spin susceptibility computed at magnetic fields $\mu B/\Delta_0 = 0$ (blue), $\mu B^*/(2\Delta_0) = 0.11415$ (red), and $\mu B^*/\Delta_0 = 0.2283$ (yellow), where we recall $\Delta_0 = 0.5 \text{meV}$. We used the interaction parameter value $\xi_m^2 g^2 \chi_0 = 2.41 \text{meV}$.

one can neglect orbital and magnetostriction effects).

Fig. (8.6) shows the evolution of the resonance energy at three different fields and fixed incommensurate wave-vector $\mathbf{q} = (0.9\pi, 0.9\pi)$. The value of the gap at hot-spots is $\Delta_{hs} \approx 0.26\Delta_0$. We note several features: (i) The zero field collective peak appears at energy $\Omega_{res} \approx 0.42\Delta_0 \lesssim 2\Delta_{hs}$. (ii) Under transverse magnetic field a well defined collective peak is shifted to lower energy due to Zeeman splitting of the energy of elementary excitations. The higher energy branch of $\Im \mathbf{m} \Pi(\Omega)$ in the uniaxial approximation does not appear since the excitations are damped by the continuum. This observation is consistent with experiment [79, 103] where it was observed strong reduction of the upper energy mode spectral weight. (iii) The field at which the excita-

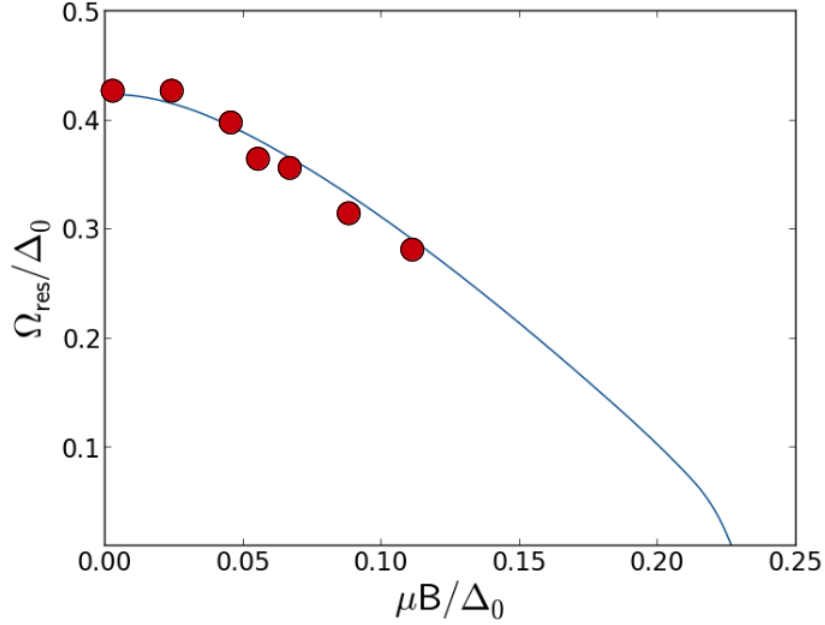


Figure 8.7: Evolution of the resonance energy with magnetic field applied parallel to the crystal plane and comparison with experiment [79]. The value of the condensation field corresponding to vanishing resonance energy is found to be $\mu B^* = 0.2283\Delta_0$.

tion softens to zero energy is $\mu B^* = 0.2283\Delta_0 \lesssim \Omega_{res}/2$, at which point the inelastic resonance translates into the phase instability. The evolution of the resonance energy with applied field is represented in Fig. (8.7). We point out the necessity the transition from superconducting to normal state to be of the first order since a vanishingly small gap would give negligibly small effect. The physics behind the effect described here is reminiscent of the excitonic phases close to a semiconductor/semi-metal transition [104]. Here exciton originates from hot-spot region in a $d_{k_a^2 - k_b^2}$ -wave superconductor under time-dependent perturbation and magnetic ordering represents the zero-energy condensation of the mode at finite wave-vector in transverse magnetic field.

8.3 Discussion

We now discuss some implications of the model and comment further on the assumptions we made. First there is a possibility of a double- \mathbf{q} structure which follows from the mode dispersion [Fig. (8.4)] leading to criticality at four degenerate incommensurate wave-vectors and is consistent with the discussion of Yanase and Sigrist [71] and Y. Kato *et al.* [77], the latter being seen as a consequence of incommensuration of the ordering wave-vector connecting nested pockets. The spin density wave order parameter then has two components

$$\Delta_{\text{SDW}_{\mathbf{q}_1}}(m, n) = \Delta_{\text{SDW}}(-1)^{m+n} \cos[\delta(m+n)], \quad (8.19)$$

and

$$\Delta_{\text{SDW}_{\mathbf{q}_2}}(m, n) = \Delta_{\text{SDW}}(-1)^{m+n} \cos[\delta(m-n)], \quad (8.20)$$

where m, n label lattice sites and δ is the instability wave-vector incommensuration. As emphasised in [77], this degeneracy is however expected to be lifted by small coupling between the electron orbital motion and the magnetic field. On magnetic field orientation effect, we believe lattice symmetry breaking by magnetostriction also plays a part. The most drastic effect however is likely to be the coherence length wave-vector dependence

$$\xi_q = 1/\sqrt{\xi_m^{-2} + f(\mathbf{q})^2}. \quad (8.21)$$

In the spin-fermion model, $f(\mathbf{q}) = |\mathbf{q} - \mathbf{Q}|$, which is symmetric with respect to \mathbf{Q} . In principle non-symmetric contribution is not excluded leading to lifting of incommensurate critical wave-vector degeneracy.

The exact role played by a putative FFLO phase is still unclear⁷. It has been conjectured [75, 76] and derived from numerical computation [70, 71]

⁷A recently published experimental work [105] signals observation of increase in the quasiparticle density consistent with transition to the FFLO phase

the existence of a phase where spin density wave lives (either intrinsically in the first case or extrinsically in the second) with the FFLO state. Because the two orders couple, this should give rise to additional length-scale for space dependence of the spin density wave order parameter with experimental hallmark as Bragg peaks measurable with elastic neutron scattering. Such a prediction pointing out coexistence between FFLO and spin density wave is yet to be experimentally verified.

The fermion energy dispersion we consider is a simplified one. The observed spectrum is known [16] to consist of several bands. We however showed in the analytic treatment that the physics discussed here is determined by the Fermi surface region in the hot-spot vicinity and features of this section persist in case of multiband structure including hot-spots. The model with uniaxial spin fluctuation is of course a limit case. Ongoing experiment [96, 103] is providing information on the actual magnetic anisotropy of the system and is showing deviation from strict uniaxiality.

The picture we advance is related to the problem of understanding collective excitations in d-wave superconductors. As previously said the magnon scenario of Chubukov and Gork'ov [86] is an alternative to the spin-exciton scenario. For their mechanism to stand, the magnon must be Landau-damped in the metal which translates into the condition

$$\gamma_d > \xi_m^{-1}/v_s, \quad (8.22)$$

where v_s is the energy scale introduced in the spin-fermion model section and $\gamma_d \sim 1/E_F$ is the damping coefficient of their three-dimensional system. On the other hand, for the magnon to stand below the superconductor gap one must have

$$v_s^2 < \Delta/\gamma_d. \quad (8.23)$$

The two relations provide the condition for consistence of the magnon sce-

nario

$$E_F/\Delta < \xi_m^2. \quad (8.24)$$

This appears to be an extreme case indeed with quasi long-range order in the metal. For this reason we advocate for the more realistic superconductor spin-exciton scheme. It is still important the dispersion of the collective mode be experimentally studied for knowledge of the physics taking place in the system.

Our physical representation of the spin-fermion approach is localized fraction of spin on cerium site coupling with itinerant electrons. Once in the superconductor, the spin dynamics is determined by the superconductor order parameter and spin susceptibility becomes singular for wave-vector connecting the hot-spot regions. Magnetic field induces fermion quasiparticle pockets and triggers the ground state transition when the quasiparticle energy reaches the gap above hot-spots.

Developments are under way concerning this scenario for field-induced criticality. There actually exists a second logarithmic-divergent response function channel and corresponds to staggered triplet superconductivity (the so-called π -triplet superconductivity) which has to compete with spin density wave ordering. A suitable approach for this problem is given by the patch model [106, 107] developed for cuprates and graphene doped to the fermion energy excitation saddle point. The model inventories channels with logarithmic-diverging response functions. Interactions between patches are introduced and renormalization group flow of these is derived by including singular loop Feynman diagrams. The d-wave superconductor with hot-spots in Zeeman magnetic field can be viewed as a $n = 8$ patch system whose properties are being investigated.

8.4 Addendum: Derivation of the spin polarisation function Eq. (8.14)

We start with Eq. (7.16) for $a = b = x$, equivalently expressed as

$$\Pi(\mathbf{q}, i\Omega_n) = -\frac{1}{2}g^2\chi_0T \sum_{k,\sigma,\omega_m} \text{Tr} \left[\hat{G}_\sigma(\mathbf{k}, i\omega_m) \hat{G}_{-\sigma}(\mathbf{k} + \mathbf{q}, i\omega_m + i\Omega_n) \right], \quad (8.25)$$

with $\Omega_n = 2n\pi T$ the bosonic Matsubara frequency. Once compacted into the Nambu (particle-hole space) notation the Gor'kov Green functions derived in the previous section write

$$\hat{G}_\sigma(\mathbf{k}, i\omega_m) = \frac{(i\omega_m - \sigma\mu B)\tau_0 + \Delta_k\tau_1 + \epsilon_k\tau_3}{[(i\omega_m - \sigma\mu B)^2 - \epsilon_k^2 - \Delta_k^2]}. \quad (8.26)$$

Here $\omega_m = \pi T(2m + 1)$ are fermion Matsubara frequencies. We note $E_k = (\epsilon_k^2 + \Delta_k^2)^{1/2}$ the zero-field energy of excitations in the superconducting state, and the matrices in Nambu space

$$\tau_0 = \begin{pmatrix} 1 & 0 \\ 0 & 1 \end{pmatrix}, \quad \tau_1 = \begin{pmatrix} 0 & 1 \\ 1 & 0 \end{pmatrix}, \quad \text{and} \quad \tau_3 = \begin{pmatrix} 1 & 0 \\ 0 & -1 \end{pmatrix}. \quad (8.27)$$

We make use of the spectral representation

$$\hat{G}_\sigma(\mathbf{k}, i\omega_m) = \int_{-\infty}^{+\infty} \frac{d\omega}{\pi} \frac{\Im \hat{G}_\sigma(\mathbf{k}, \omega + i0^+)}{\omega - i\omega_m}, \quad (8.28)$$

which yields

$$\begin{aligned} \Pi(\mathbf{q}, i\Omega_n) &= -\frac{1}{2}g^2\chi_0T \sum_{k,\sigma,\omega_m} \int_{-\infty}^{+\infty} \frac{d\omega}{\pi} \int_{-\infty}^{+\infty} \frac{d\tilde{\omega}}{\pi} \\ &\times \frac{\text{Tr}[\Im \hat{G}_\sigma(\mathbf{k}, \omega + i0^+) \Im \hat{G}_{-\sigma}(\mathbf{k} + \mathbf{q}, \tilde{\omega} + i0^+)]}{(\omega - i\omega_m)(\tilde{\omega} - i\omega_m - i\Omega_n)}. \end{aligned} \quad (8.29)$$

$\hat{G}_\sigma(\mathbf{k}, \omega + i0^+)$ is the fermion retarded Green function whose imaginary part reads

$$\begin{aligned}
\Im \hat{G}_\sigma(\mathbf{k}, \omega + i0^+) &= -\frac{\pi}{2E_k} [(\omega - \sigma\mu B)\tau_0 + \Delta_k\tau_1 + \epsilon_k\tau_3] \\
&\quad \times [\delta(\omega - \sigma\mu B - E_k) - \delta(\omega - \sigma\mu B + E_k)] \\
&= -\frac{\pi}{2} \sum_{s=\pm 1} [\tau_0 + s \frac{\Delta_k\tau_1 + \epsilon_k\tau_3}{E_k}] \\
&\quad \times \delta(\omega - \sigma\mu B - sE_k). \tag{8.30}
\end{aligned}$$

Performing summation over fermion Matsubara frequencies $\omega_m = \pi T(2m + 1)$,

$$T \sum_{\omega_m} \frac{1}{(\omega - i\omega_m)(\tilde{\omega} - i\omega_m - i\Omega_n)} = \frac{f(\omega) - f(\tilde{\omega})}{i\Omega_n + \omega - \tilde{\omega}}, \tag{8.31}$$

with $f(z) = 1/[\exp(z/T) + 1]$ the fermion distribution function at equilibrium and by the relation $\text{Tr}[\tau_\mu\tau_\nu] = 2\delta_{\mu\nu}$ we obtain the trace in particle-hole space

$$\begin{aligned}
&\text{Tr}[\Im \hat{G}_{-\sigma}(\mathbf{k} + \mathbf{q}, \tilde{\omega} + i0^+) \Im \hat{G}_\sigma(\mathbf{k}, \omega + i0^+)] \\
&= \frac{\pi^2}{2} \sum_{s,s'=\pm 1} \left(1 + ss' \frac{\epsilon_k\epsilon_{k+q} + \Delta_k\Delta_{k+q}}{E_k E_{k+q}} \right) \\
&\quad \times \delta(\omega - \sigma\mu B - sE_k) \delta(\tilde{\omega} + \sigma\mu B - s'E_{k+q}). \tag{8.32}
\end{aligned}$$

Together with Eqs. (8.29), (8.31), and analytically continuing $i\Omega_n \rightarrow \Omega + i\Gamma$, we recover the response function Eq. (8.14).

Chapter 9

Conclusion part II

We have presented a mechanism for understanding magnetism that is tied to superconductivity in CeCoIn_5 . The slowing down of the $d_{k_a^2-k_b^2}$ -wave superconductor spin-exciton driven by Zeeman magnetic field constitutes a natural scenario where magnetism is intrinsically stimulated by superconductivity. A physical picture of the spin-fermion approach is related to the two-fluid model for Ce115 heavy electron compounds. Fraction of electrons are localized spins coupled to itinerant fermions which participate to superconductivity. Analysis of the uniaxial spin-fermion model with transverse magnetic field shows that the critical behaviour follows from development of Fermi pockets by Zeeman magnetic field in the nodal superconductor with energy level tuning to proximity to logarithmic divergence in the spin polarisation function. Numerics demonstrates that the ordering wave-vector is almost commensurate connecting Brillouin zone regions close to hot-spots. The computed collective mode resonance energy dependence on magnetic field displays good correspondence with experiment. The specificities of the heavy electron superconductor CeCoIn_5 brings all conditions (first order transition resulting from Pauli limiting, quasi two-dimensionality, $d_{k_a^2-k_b^2}$ -wave pairing symmetry, proximity to antiferromagnetism) for realizing this ground state transition.

Core references

AbramowitzStegun M. Abramowitz and I. A. Stegun, Handbook of mathematical functions, Dover Pub., (1965).

Abrikosov A. A. Abrikosov, Fundamentals of the theory of metals, North-Holland (1988).

AGD A. A. Abrikosov and L. P. Gor'kov and I. E. Dzyaloshinski, Methods of quantum field theory in statistical physics, Dover (1963).

AshcroftMermin N. W. Ashcroft and N. D. Mermin, Solid state physics, Saunders College (1976).

deGennes P. G. de Gennes, Superconductivity of metals and alloys, Advanced Book Program, Perseus Books (1999).

MineevSamokhin V. P. Mineev and K. V. Samokhin, Introduction to unconventional superconductivity, Gordon and Breach Science Publishers (1999).

Bibliography

- [1] Michael R. Norman. The challenge of unconventional superconductivity. *Science*, 332(6026):196–200, 2011.
- [2] A. A. Abrikosov. On the magnetic properties of superconductors of the second group. *Sov. Phys. JETP*, page 1174, 1957.
- [3] Manfred Sigrist and Kazuo Ueda. Phenomenological theory of unconventional superconductivity. *Rev. Mod. Phys.*, 63:239–311, Apr 1991.
- [4] G. E. Volovik and L. P. Gor'kov. Superconductivity classes in the heavy fermion systems. *Sov. Phys.-JETP*, 88:843, 1985.
- [5] C. Petrovic, P. G. Pagliuso, M. F. Hundley, R. Movshovich, J. L. Sarrao, J. D. Thompson, Z. Fisk, and P. Monthoux. Heavy-fermion superconductivity in CeCoIn₅ at 2.3K. *Journal of Physics: Condensed Matter*, 13(17):L337, 2001.
- [6] P. G. Pagliuso, C. Petrovic, R. Movshovich, D. Hall, M. F. Hundley, J. L. Sarrao, J. D. Thompson, and Z. Fisk. Coexistence of magnetism and superconductivity in CeRh_{1-x}Ir_xIn₅. *Phys. Rev. B*, 64:100503, Aug 2001.
- [7] P.G. Pagliuso, R. Movshovich, A.D. Bianchi, M. Nicklas, N.O. Moreno, J.D. Thompson, M.F. Hundley, J.L. Sarrao, and Z. Fisk. Multiple phase transitions in Ce(Rh,Ir,Co)In₅. *Physica B: Condensed Matter*,

- 312313(0):129 – 131, 2002. The International Conference on Strongly Correlated Electron Systems.
- [8] Georg Knebel, Dai Aoki, Jean-Pascal Brison, Ludovic Howald, Gerard Lapertot, Justin Panarin, Stephane Raymond, and Jacques Flouquet. Competition and/or coexistence of antiferromagnetism and superconductivity in CeRhIn₅ and CeCoIn₅. *physica status solidi (b)*, 247(3):557–562, 2010.
- [9] Piers Coleman. *Heavy Fermions: Electrons at the Edge of Magnetism*. John Wiley & Sons, Ltd, 2007.
- [10] Pegor Aynajian, Eduardo H. da Silva Neto, Andras Gyenis, Ryan E. Baumbach, J. D. Thompson, Zachary Fisk, Eric D. Bauer, and Ali Yazdani. Visualizing heavy fermions emerging in a quantum critical Kondo lattice. *Nature*, 486:201 – 206, 2012.
- [11] A. Benlagra, T. Pruschke, and M. Vojta. Finite-temperature spectra and quasiparticle interference in Kondo lattices: from light electrons to coherent heavy quasiparticles. *Phys. Rev. B*, 84:195141, 2011.
- [12] A. V. Chubukov, D. Pines, and J. Schmalian. A spin fluctuation model for d-wave superconductivity. In K. H. Bennemann and John B. Ketterson, editors, *Superconductivity*, pages 1349–1413. Springer Berlin Heidelberg, 2008.
- [13] Hilbert v. Löhneysen, Achim Rosch, Matthias Vojta, and Peter Wölfle. Fermi-liquid instabilities at magnetic quantum phase transitions. *Rev. Mod. Phys.*, 79:1015–1075, Aug 2007.
- [14] Yi-feng Yang, Zachary Fisk, Han-Oh Lee, J. D. Thompson, and David Pines. Scaling the Kondo lattice. *Nature*, 454:611–613, 2008.

- [15] G. Seyfarth, J. P. Brison, G. Knebel, D. Aoki, G. Lapertot, and J. Flouquet. Multigap superconductivity in the heavy-fermion system CeCoIn₅. *Phys. Rev. Lett.*, 101:046401, Jul 2008.
- [16] R. Settai, H. Shishido, S. Ikeda, Y. Murakawa, M. Nakashima, D. Aoki, Y. Haga, H. Harima, and Y. Onuki. Quasi-two-dimensional fermi surfaces and the de Haas-van Alphen oscillation in both the normal and superconducting mixed states of CeCoIn₅. *Journal of Physics: Condensed Matter*, 13(27):L627, 2001.
- [17] Donovan Hall, E. C. Palm, T. P. Murphy, S. W. Tozer, Z. Fisk, U. Alver, R. G. Goodrich, J. L. Sarrao, P. G. Pagliuso, and Takao Ebihara. Fermi surface of the heavy-fermion superconductor CeCoIn₅: The de Haas-van Alphen effect in the normal state. *Phys. Rev. B*, 64:212508, Nov 2001.
- [18] P. Monthoux and G. G. Lonzarich. Magnetically mediated superconductivity in quasi-two and three dimensions. *Phys. Rev. B*, 63:054529, Jan 2001.
- [19] K. Izawa, H. Yamaguchi, Yuji Matsuda, H. Shishido, R. Settai, and Y. Onuki. Angular position of nodes in the superconducting gap of quasi-2D heavy-fermion superconductor CeCoIn₅. *Phys. Rev. Lett.*, 87:057002, Jul 2001.
- [20] A. Vorontsov and I. Vekhter. Nodal structure of quasi-two-dimensional superconductors probed by a magnetic field. *Phys. Rev. Lett.*, 96:237001, Jun 2006.
- [21] K. An, T. Sakakibara, R. Settai, Y. Onuki, M. Hiragi, M. Ichioka, and K. Machida. Sign reversal of field-angle resolved heat capacity oscillations in a heavy fermion superconductor CeCoIn₅ and $d_{x^2-y^2}$ pairing symmetry. *Phys. Rev. Lett.*, 104:037002, Jan 2010.

- [22] M. T. Béal-Monod, C. Bourbonnais, and V. J. Emery. Possible superconductivity in nearly antiferromagnetic itinerant fermion systems. *Phys. Rev. B*, 34:7716–7720, Dec 1986.
- [23] K. Miyake, S. Schmitt-Rink, and C. M. Varma. Spin-fluctuation-mediated even-parity pairing in heavy-fermion superconductors. *Phys. Rev. B*, 34:6554–6556, Nov 1986.
- [24] D. J. Scalapino, E. Loh, and J. E. Hirsch. *d*-wave pairing near a spin-density-wave instability. *Phys. Rev. B*, 34:8190–8192, Dec 1986.
- [25] S. Nakatsuji, S. Yeo, L. Balicas, Z. Fisk, P. Schlottmann, P. G. Pagliuso, N. O. Moreno, J. L. Sarrao, and J. D. Thompson. Intersite coupling effects in a Kondo lattice. *Phys. Rev. Lett.*, 89:106402, Aug 2002.
- [26] Satoru Nakatsuji, David Pines, and Zachary Fisk. Two fluid description of the Kondo lattice. *Phys. Rev. Lett.*, 92:016401, Jan 2004.
- [27] Yi-feng Yang, Ricardo Urbano, Nicholas J. Curro, David Pines, and E. D. Bauer. Magnetic excitations in the Kondo liquid: Superconductivity and hidden magnetic quantum critical fluctuations. *Phys. Rev. Lett.*, 103:197004, Nov 2009.
- [28] Yi feng Yang, N J Curro, Z Fisk, D Pines, and J D Thompson. A predictive standard model for heavy electron systems. *Journal of Physics: Conference Series*, 273(1):012066, 2011.
- [29] Sunil Nair, O. Stockert, U. Witte, M. Nicklas, R. Schedler, K. Kiefer, J. D. Thompson, A. D. Bianchi, Z. Fisk, S. Wirth, and F. Steglich. Magnetism and superconductivity driven by identical 4f states in a heavy-fermion metal. *Proceedings of the National Academy of Sciences*, 2010.

- [30] V. P. Michal and V. P. Mineev. Paramagnetic effects in vortex lattice field distribution in strongly type-II superconductors. *Phys. Rev. B*, 82:104505, Sep 2010.
- [31] V. P. Michal. Muon spin rotation in heavy electron Pauli limited superconductors. *Accepted to JETP*.
- [32] A. D. Bianchi, M. Kenzelmann, L. DeBeer-Schmitt, J. S. White, E. M. Forgan, J. Mesot, M. Zolliker, J. Kohlbrecher, R. Movshovich, E. D. Bauer, J. L. Sarrao, Z. Fisk, C. Petrovi, and M. R. Eskildsen. Superconducting vortices in CeCoIn₅: Toward the pauli-limiting field. *Science*, 319:177–180, 2008.
- [33] J. R. Clem. Simple model for the vortex core in a type II superconductor. *J. Low Temp. Phys.*, 18:427, 1975.
- [34] J. Spehling, R. H. Heffner, J. E. Sonier, N. Curro, C. H. Wang, B. Hitti, G. Morris, E. D. Bauer, J. L. Sarrao, F. J. Litterst, and H.-H. Klauss. Field-induced coupled superconductivity and spin density wave order in the heavy fermion compound CeCoIn₅. *Phys. Rev. Lett.*, 103:237003, Dec 2009.
- [35] L. DeBeer-Schmitt, C. D. Dewhurst, B. W. Hoogenboom, C. Petrovic, and M. R. Eskildsen. Field dependent coherence length in the superclean, high- κ superconductor CeCoIn₅. *Phys. Rev. Lett.*, 97:127001, Sep 2006.
- [36] J. S. White, P. Das, M. R. Eskildsen, L. DeBeer-Schmitt, E. M. Forgan, A. D. Bianchi, M. Kenzelmann, M. Zolliker, S. Gerber, J. L. Gavilano, J. Mesot, R. Movshovich, E. D. Bauer, J. L. Sarrao, and C. Petrovic. Observations of Pauli paramagnetic effects on the flux line lattice in CeCoIn₅. *New Journal of Physics*, 12:023026, 2010.

- [37] A. Bianchi, R. Movshovich, N. Oeschler, P. Gegenwart, F. Steglich, J. D. Thompson, P. G. Pagliuso, and J. L. Sarrao. First-order superconducting phase transition in CeCoIn₅. *Phys. Rev. Lett.*, 89:137002, Sep 2002.
- [38] A. I. Larkin and Yu. N. Ovchinnikov. *Zh. Eksp. Teor. Fiz.*, 47:1136.
- [39] Peter Fulde and Richard A. Ferrell. Superconductivity in a strong spin-exchange field. *Phys. Rev.*, 135:A550–A563, Aug 1964.
- [40] A. Bianchi, R. Movshovich, C. Capan, P. G. Pagliuso, and J. L. Sarrao. Possible Fulde-Ferrell-Larkin-Ovchinnikov superconducting state in CeCoIn₅. *Phys. Rev. Lett.*, 91:187004, Oct 2003.
- [41] A. M. Clogston. Upper limit for the critical field in hard superconductors. *Phys. Rev. Lett.*, 9:266–267, Sep 1962.
- [42] B. S. Chandrasekhar. A note on the maximum critical field of high-field superconductors. *Applied Physics Letters*, 1(1):7–8, 1962.
- [43] M. Houzet and V. P. Mineev. Interplay of paramagnetic, orbital, and impurity effects on the phase transition of a normal metal to the superconducting state. *Phys. Rev. B*, 74:144522, Oct 2006.
- [44] M. Houzet and V. P. Mineev. Electrodynamics of Fulde-Ferrell-Larkin-Ovchinnikov superconducting state. *Phys. Rev. B*, 76:224508, Dec 2007.
- [45] E. H. Brandt. Precision Ginzburg-Landau solution of ideal vortex lattices for any induction and symmetry. *Phys. Rev. Lett.*, 78:2208–2211, Mar 1997.
- [46] A. I. Bouzdine and J. P. Brison. Non-uniform state in 2D superconductors. *Europhys. Lett.*, 35:707–712, 1996.

- [47] A. I. Bouzdine and H. Kachkachi. Generalized Ginzburg-Landau theory for nonuniform FFLO superconductors. *Physics Letters A*, 225:341–348, 1997.
- [48] M. Kenzelmann, Th. Strassel, C. Niedermayer, M. Sigrist, B. Padmanabhan, M. Zolliker, A. D. Bianchi, R. Movshovich, E. D. Bauer, J. L. Sarrao, and J. D. Thompson. Coupled superconducting and magnetic order in CeCoIn₅. *Science*, 321(5896):1652–1654, 2008.
- [49] Masanori Ichioka and Kazushige Machida. Vortex states in superconductors with strong Pauli-paramagnetic effect. *Phys. Rev. B*, 76:064502, Aug 2007.
- [50] M. Ichioka and K. Machida. Flux line lattice form factor and paramagnetic effects in type II superconductors. *Journal of Physics: Conference Series*, 150(5):052074, 2009.
- [51] K. V. Samokhin. Magnetic properties of superconductors with strong spin-orbit coupling. *Phys. Rev. B*, 70:104521, Sep 2004.
- [52] L. DeBeer-Schmitt, M. R. Eskildsen, M. Ichioka, K. Machida, N. Jenkins, C. D. Dewhurst, A. B. Abrahamsen, S. L. Bud’ko, and P. C. Canfield. Pauli paramagnetic effects on vortices in superconducting TmNi₂B₂C. *Phys. Rev. Lett.*, 99:167001, Oct 2007.
- [53] V. H. Dao, D. Denisov, A. Buzdin, and J. P. Brison. On the theory of the vortex state in the Fulde-Ferrell-Larkin-Ovchinnikov (FFLO) phase. *arXiv:1208.1839v1*.
- [54] Y. Haga. Private communication.
- [55] Yusei Shimizu, Yoichi Ikeda, Takumi Wakabayashi, Yoshinori Haga, Kenichi Tenya, Hiroyuki Hidaka, Tatsuya Yanagisawa, and Hiroshi

- Amitsuka. Maki parameter and upper critical field of the heavy-fermion superconductor UBe_{13} . *Journal of the Physical Society of Japan*, 80(9):093701, 2011.
- [56] V. P. Mineev and V. P. Michal. Temperature-dependent Ginzburg-Landau parameter. *Journal of the physical society of Japan*, 81:093701, 2012.
- [57] Shugo Ikeda, Hiroaki Shishido, Miho Nakashima, Rikio Settai, Dai Aoki, Yoshinori Haga, Hisatomo Harima, Yuji Aoki, Takahiro Namiki, Hideyuki Sato, and Yoshichika Ōnuki. Unconventional superconductivity in CeCoIn_5 studied by the specific heat and magnetization measurements. *Journal of the Physical Society of Japan*, 70(8):2248–2251, 2001.
- [58] Hiroto Adachi, Masanori Ichioka, and Kazushige Machida. Mixed-state thermodynamics of superconductors with moderately large paramagnetic effects. *Journal of the Physical Society of Japan*, 74(8):2181–2184, 2005.
- [59] Y. Kasahara, T. Iwasawa, H. Shishido, T. Shibauchi, K. Behnia, Y. Haga, T. D. Matsuda, Y. Onuki, M. Sigrist, and Y. Matsuda. Exotic superconducting properties in the electron-hole-compensated heavy-fermion “semimetal” URu_2Si_2 . *Phys. Rev. Lett.*, 99:116402, Sep 2007.
- [60] Dai Aoki, Yoshinori Haga, Tatsuma D. Matsuda, Naoyuki Tateiwa, Shugo Ikeda, Yoshiya Homma, Hironori Sakai, Yoshinobu Shiokawa, Etsuji Yamamoto, Akio Nakamura, Rikio Settai, and Yoshichika Ōnuki. Unconventional heavy-fermion superconductivity of a new transuranium compound NpPd_5Al_2 . *Journal of the Physical Society of Japan*, 76(6):063701, 2007.
- [61] L. Glémot, J. P. Brison, J. Flouquet, A. I. Buzdin, I. Sheikin, D. Jaccard, C. Thessieu, and F. Thomas. Pressure dependence of the upper

- critical field of the heavy fermion superconductor UBe_{13} . *Phys. Rev. Lett.*, 82:169–172, Jan 1999.
- [62] H. R. Ott, H. Rudigier, Z. Fisk, and J. L. Smith. UBe_{13} : An unconventional actinide superconductor. *Phys. Rev. Lett.*, 50:1595–1598, May 1983.
- [63] T. P. Murphy, Donavan Hall, E. C. Palm, S. W. Tozer, C. Petrovic, Z. Fisk, R. G. Goodrich, P. G. Pagliuso, J. L. Sarrao, and J. D. Thompson. Anomalous superconductivity and field-induced magnetism in $CeCoIn_5$. *Phys. Rev. B*, 65:100514, Mar 2002.
- [64] B.-L. Young, R. R. Urbano, N. J. Curro, J. D. Thompson, J. L. Sarrao, A. B. Vorontsov, and M. J. Graf. Microscopic evidence for field-induced magnetism in $CeCoIn_5$. *Phys. Rev. Lett.*, 98:036402, Jan 2007.
- [65] M. Kenzelmann, S. Gerber, N. Egetenmeyer, J. L. Gavilano, Th. Strässle, A. D. Bianchi, E. Ressouche, R. Movshovich, E. D. Bauer, J. L. Sarrao, and J. D. Thompson. Evidence for a magnetically driven superconducting Q phase of $CeCoIn_5$. *Phys. Rev. Lett.*, 104:127001, Mar 2010.
- [66] G. Koutroulakis, V. F. Mitrović, M. Horvatić, C. Berthier, G. Lapertot, and J. Flouquet. Field dependence of the ground state in the exotic superconductor $CeCoIn_5$: A nuclear magnetic resonance investigation. *Phys. Rev. Lett.*, 101:047004, Jul 2008.
- [67] G. Koutroulakis, M. D. Stewart, V. F. Mitrović, M. Horvatić, C. Berthier, G. Lapertot, and J. Flouquet. Field evolution of coexisting superconducting and magnetic orders in $CeCoIn_5$. *Phys. Rev. Lett.*, 104:087001, Feb 2010.
- [68] E. Blackburn, P. Das, M. R. Eskildsen, E. M. Forgan, M. Laver, C. Niedermayer, C. Petrovic, and J. S. White. Exploring the fragile anti-

- ferromagnetic superconducting phase in CeCoIn_5 . *Phys. Rev. Lett.*, 105:187001, Oct 2010.
- [69] D. F. Agterberg, M. Sigrist, and H. Tsunetsugu. Order parameter and vortices in the superconducting Q phase of CeCoIn_5 . *Phys. Rev. Lett.*, 102:207004, May 2009.
- [70] Youichi Yanase and Manfred Sigrist. Antiferromagnetic order and π -triplet pairing in the Fulde–Ferrell–Larkin–Ovchinnikov state. *Journal of the Physical Society of Japan*, 78(11):114715, 2009.
- [71] Youichi Yanase and Manfred Sigrist. Ginzburg–Landau analysis for the antiferromagnetic order in the fulde–ferrell–larkin–ovchinnikov superconductor. *Journal of the Physical Society of Japan*, 80(9):094702, 2011.
- [72] Kazumasa Miyake. Theory for coupled SDW and superconducting order in FFLO state of CeCoIn_5 . *Journal of the Physical Society of Japan*, 77(12):123703, 2008.
- [73] Alexandros Aperis, Georgios Varelogiannis, and Peter B. Littlewood. Magnetic-field-induced pattern of coexisting condensates in the superconducting state of CeCoIn_5 . *Phys. Rev. Lett.*, 104:216403, May 2010.
- [74] Kenta M. Suzuki, Masanori Ichioka, and Kazushige Machida. Theory of an inherent spin-density-wave instability due to vortices in superconductors with strong Pauli effects. *Phys. Rev. B*, 83:140503, Apr 2011.
- [75] Ryusuke Ikeda, Yuhki Hatakeyama, and Kazushi Aoyama. Antiferromagnetic ordering induced by paramagnetic depairing in unconventional superconductors. *Phys. Rev. B*, 82:060510, Aug 2010.

- [76] Yuhki Hatakeyama and Ryusuke Ikeda. Emergent antiferromagnetism in a d -wave superconductor with strong paramagnetic pair-breaking. *Phys. Rev. B*, 83:224518, Jun 2011.
- [77] Yasuyuki Kato, C. D. Batista, and I. Vekhter. Antiferromagnetic order in Pauli-limited unconventional superconductors. *Phys. Rev. Lett.*, 107:096401, Aug 2011.
- [78] C. Stock, C. Broholm, J. Hudis, H. J. Kang, and C. Petrovic. Spin resonance in the d -wave superconductor CeCoIn_5 . *Phys. Rev. Lett.*, 100:087001, Feb 2008.
- [79] Justin Panarin, Stéphane Raymond, Gérard Lapertot, and Jacques Flouquet. Evolution of the spin resonance in CeCoIn_5 under magnetic field. *Journal of the Physical Society of Japan*, 78(11):113706, 2009.
- [80] I. Eremin, G. Zwicknagl, P. Thalmeier, and P. Fulde. Feedback spin resonance in superconducting CeCu_2Si_2 and CeCoIn_5 . *Phys. Rev. Lett.*, 101:187001, Oct 2008.
- [81] M. Lavagna and G. Stemann. Spin excitations of two-dimensional-lattice electrons: Discussion of neutron-scattering and NMR experiments in high- T_c superconductors. *Phys. Rev. B*, 49:4235–4250, Feb 1994.
- [82] Hung Fai Fong, B. Keimer, P. W. Anderson, D. Reznik, F. Doğan, and I. A. Aksay. Phonon and magnetic neutron scattering at 41 meV in $\text{YBa}_2\text{Cu}_3\text{O}_7$. *Phys. Rev. Lett.*, 75:316–319, Jul 1995.
- [83] N. Bulut and D. J. Scalapino. Neutron scattering from a collective spin fluctuation mode in a CuO_2 bilayer. *Phys. Rev. B*, 53:5149–5152, Mar 1996.

- [84] Patrick A. Lee, Naoto Nagaosa, and Xiao-Gang Wen. Doping a Mott insulator: Physics of high-temperature superconductivity. *Rev. Mod. Phys.*, 78:17–85, Jan 2006.
- [85] Wei-Cheng Lee and A. H. MacDonald. Weak-coupling theory of photoemission and inelastic neutron scattering and the mechanism of superconductivity in the cuprates. *Phys. Rev. B*, 78:174506, Nov 2008.
- [86] A. V. Chubukov and L. P. Gor'kov. Spin resonance in three-dimensional superconductors: The case of CeCoIn₅. *Phys. Rev. Lett.*, 101:147004, Oct 2008.
- [87] V. P. Michal and V. P. Mineev. Field-induced spin-exciton condensation in the $d_{x^2-y^2}$ -wave superconductor CeCoIn₅. *Phys. Rev. B*, 84:052508, Aug 2011.
- [88] Hiroaki Shishido, Rikio Settai, Dai Aoki, Shugo Ikeda, Hirokazu Nakawaki, Noriko Nakamura, Tomoya Iizuka, Yoshihiko Inada, Kiyohiro Sugiyama, Tetsuya Takeuchi, Kouichi Kindo, Tatsuo C. Kobayashi, Yoshinori Haga, Hisatomo Harima, Yuji Aoki, Takahiro Namiki, Hideyuki Sato, and Yoshichika Ōnuki. Fermi surface, magnetic and superconducting properties of LaRhIn₅ and CeTIn₅ (T: Co, Rh and Ir). *Journal of the Physical Society of Japan*, 71(1):162–173, 2002.
- [89] Y. Nakajima, H. Shishido, H. Nakai, T. Shibauchi, K. Behnia, K. Izawa, M. Hedo, Y. Uwatoko, T. Matsumoto, R. Settai, Y. Ōnuki, H. Kontani, and Y. Matsuda. Non-fermi liquid behavior in the magnetotransport of CeMIn₅ (M: Co and Rh): Striking similarity between quasi two-dimensional heavy fermion and high- T_C Cuprates. *Journal of the Physical Society of Japan*, 76(2):024703, 2007.

- [90] I. Vekhter, P. J. Hirschfeld, J. P. Carbotte, and E. J. Nicol. Anisotropic thermodynamics of d -wave superconductors in the vortex state. *Phys. Rev. B*, 59:R9023–R9026, Apr 1999.
- [91] H. Aoki, T. Sakakibara, H. Shishido, R. Settai, Y. Ōnuki, P. Miranovi, and K. Machida. Field-angle dependence of the zero-energy density of states in the unconventional heavy-fermion superconductor CeCoIn₅. *Journal of Physics: Condensed Matter*, 16(3):L13, 2004.
- [92] W. K. Park, J. L. Sarrao, J. D. Thompson, and L. H. Greene. Andreev reflection in heavy-fermion superconductors and order parameter symmetry in CeCoIn₅. *Phys. Rev. Lett.*, 100:177001, Apr 2008.
- [93] Kun Yang and S. L. Sondhi. Response of a $d_{x^2-y^2}$ superconductor to a Zeeman magnetic field. *Phys. Rev. B*, 57:8566–8570, Apr 1998.
- [94] V. P. Michal. Field-induced collective spin-exciton condensation in a quasi-2D $d_{x^2-y^2}$ -wave heavy electron superconductor. *Accepted to J. Phys.: Conf. Series (SCES 2012)*.
- [95] Stéphane Raymond, Justin Panarin, Gérard Lapertot, and Jacques Flouquet. Evolution of the spin resonance of CeCoIn₅ as a function of magnetic field and La substitution. *Journal of the Physical Society of Japan*, 80SB(Supplement B):SB023, 2011.
- [96] S. Raymond. Unpublished.
- [97] M. Eschrig, M. R. Norman, and B. Jankó. Influence of vortices on the magnetic resonance in cuprate superconductors. *Phys. Rev. B*, 64:134509, Sep 2001.
- [98] Andrey V. Chubukov, Boldizsár Jankó, and Oleg Tchernyshyov. Dispersion of the neutron resonance in cuprate superconductors. *Phys. Rev. B*, 63:180507, Apr 2001.

- [99] A. Abanov and A. V. Chubukov. A relation between the resonance neutron peak and ARPES data in cuprates. *Phys. Rev. Lett.*, 83:1652, 1999.
- [100] A. Akbari and P. Thalmeier. Field induced doublet splitting in $d_{x^2-y^2}$ -wave 115-heavy electron superconductors. *arXiv:1208.2897v1*.
- [101] J.-P. Ismer, Ilya Eremin, Enrico Rossi, and Dirk K. Morr. Magnetic resonance in the spin excitation spectrum of electron-doped cuprate superconductors. *Phys. Rev. Lett.*, 99:047005, Jul 2007.
- [102] Kazunori Tanaka, Hiroaki Ikeda, Yunori Nisikawa, and Kosaku Yamada. Theory of superconductivity in CeMIn_5 (M=Co, Rh, Ir) on the basis of the three dimensional periodic Anderson model. *Journal of the Physical Society of Japan*, 75(2):024713, 2006.
- [103] C. Stock, C. Broholm, Y. Zhao, F. Demmel, H. J. Kang, K. C. Rule, and C. Petrovic. Magnetic field splitting of the spin-resonance in CeCoIn_5 . *arXiv:1203.2189v1*, March 2012.
- [104] B. I. Halperin and T. M. Rice. Possible anomalies at a semimetal-semiconductor transition. *Rev. Mod. Phys.*, 40:755–766, Oct 1968.
- [105] K. Kumagai, H. Shishido, T. Shibauchi, and Y. Matsuda. Evolution of paramagnetic quasiparticle excitations emerged in the high-field superconducting phase of CeCoIn_5 . *Phys. Rev. Lett.*, 106:137004, Mar 2011.
- [106] Nobuo Furukawa, T. M. Rice, and Manfred Salmhofer. Truncation of a two-dimensional fermi surface due to quasiparticle gap formation at the saddle points. *Phys. Rev. Lett.*, 81:3195–3198, Oct 1998.
- [107] Rahul Nandkishore, L. S. Levitov, and A. V. Chubukov. Chiral superconductivity from repulsive interactions in doped graphene. *Nat Phys*, 8:158–163, 2012.

Publication list

1. V. P. Michal and V. P. Mineev, Paramagnetic effects in vortex lattice field distribution in strongly type-II superconductors. *Phys. Rev. B* **82**,104505 (2010).
2. V. P. Michal and V. P. Mineev, Field-induced spin-exciton condensation in the $d_{x^2-y^2}$ -wave superconductor CeCoIn₅. *Phys. Rev. B* **84**, 052508 (2011).
3. V. P. Michal, Muon spin rotation in heavy electron Pauli limited superconductors. Accepted to JETP.
4. V. P. Michal, Field-induced collective spin-exciton condensation in a quasi-2D $d_{x^2-y^2}$ -wave heavy electron superconductor. Accepted to *J. Phys.: Conf. Series (SCES 2011)*.
5. V. P. Mineev and V. P. Michal, Temperature-dependent Ginzburg-Landau parameter. *Journal of the physical society of Japan* **81**, 093701 (2012).

Chapter 10

Résumé

Comprendre les propriétés des composés à électrons fortement corrélés nouvellement découverts est un important défi à la fois pour des raisons fondamentales et pour un impact industriel à long terme. Une activité expérimentale sur les métaux et supraconducteurs à électrons lourds a mis en évidence des effets qui dérogent clairement à notre connaissance actuelle sur ces systèmes. Le but de cette thèse est de modéliser les effets de spin spéciaux qui ont été observés en réponse à un champ magnétique dans le supraconducteur CeCoIn_5 . Elle est composée de deux parties.

Dans un premier temps nous avons à faire à la distribution anormale du champ magnétique local dans le réseau de vortex révélé par les expériences de diffraction de neutrons à petits angles et rotation de spin muonique. Sur la base de la théorie de Ginzburg-Landau avec prise en compte de l'effet de spin, nous analysons l'inhomogénéité du champ local dans le réseau de vortex et calculons des expressions pour les facteurs de forme en diffraction neutronique et la largeur de raie statique en rotation de spin muonique. Nous montrons que les données expérimentales anormales sont le résultat de supercourants générés par le spin circulant autour du cœur du vortex et donnent une augmentation de l'inhomogénéité du champ sur une distance de l'ordre de la longueur de corrélation du supraconducteur à partir de l'axe

du vortex. L'importance de l'effet est contrôlée par une seule quantité (le paramètre de Maki).

La seconde partie traite d'une transition d'onde de densité de spin presque commensurable dans un supraconducteur non-conventionnel. Elle est motivée par l'observation du confinement d'un ordre d'onde de densité de spin dans la phase supraconductrice de CeCoIn_5 sous champ magnétique. Dans le cadre de la formulation spin-fermion nous proposons un mécanisme pour la transition de l'état fondamental qui consiste en un ralentissement du mode collectif de fluctuation de densité de spin (exciton de spin) induit par le champ vers un ordre statique. Cela représente un scénario par lequel la transition vers l'ordre de spin est reliée intrinsèquement au supraconducteur.

Chapter 11

Conclusion de la première partie

Sur la base de l'expansion de Ginzburg-Landau pour l'énergie libre du supraconducteur en incluant le couplage entre le champ magnétique interne et à la fois la charge et le spin de l'électron, nous avons étudié la dépendance par rapport au champ externe de l'inhomogénéité anormale du champ magnétique interne local, mesurée par les facteurs de forme du réseau de vortex et la largeur de raie statique de rotation de spin du muon. Dans un premier temps nous avons pris la limite à bas champ avec vortex indépendants proche de la température critique du supraconducteur T_c et dans un deuxième temps nous avons examiné le régime à haut champ proche du champ critique supérieur H_{c2}^p .

Dans le premier cas, en nous fiant à une fonction variationnelle pour la structure du gap d'un vortex isolé nous avons trouvé une expression simple pour les facteurs de forme qui est une fonction du champ interne en unité de champ critique supérieur dans la limite de Pauli et comprend le seul paramètre $\alpha_M = \alpha_{M0} \sqrt{1 - T/T_c}$ avec $\alpha_{M0} = \mu\phi_0 T_c / v_F^2$ le paramètre de Maki à température nulle. Nous avons trouvé une transition continue (*crossover*) réglée par le paramètre α_M . Lorsque l'effet orbital est dominant ($\alpha_M < 1$) la

largeur de raie statique diminue en augmentant le champ magnétique externe (de même pour le facteur de forme F_{10}). D'autre part le régime où la limite de Pauli est dominante ($\alpha_M > 1$) donne une augmentation de la largeur de raie statique (d'abord d'une façon non-analytique et ensuite linéairement) à cause de l'augmentation de l'inhomogénéité du champ local autour du coeur des vortex comme résultat de l'effet Zeeman. La comparaison entre la formule trouvée et les données expérimentales donne un accord satisfaisant.

Dans le régime proche de $H_{c2}^P(T)$ nous avons appliqué la solution d'Abrikosov de la première équation de Ginzburg-Landau linéarisée et déterminé le champ magnétique local dans la limite de Pauli. Nous avons retrouvé l'augmentation linéaire du facteur de forme et trouvé la chute linéaire au champ critique H_{c2}^P . Nous avons décrit l'approche de la transition vers le métal du deuxième ordre vers le premier ordre (ça a lieu à $T/T_c \approx 0.56$ et $\mu H_{c2}^P/T_c \approx 1.07$) avec une augmentation soudaine de la valeur absolue de la pente de $\sigma_s^{VL}(B)$.

Le chapitre supplémentaire discute la dépendance par rapport à la température du paramètre de Ginzburg-Landau effectif au voisinage du champ critique supérieur. Nous avons mis en contraste le comportement attendu dans la limite orbitale ($\alpha_{M0} \ll 1$) menant à un paramètre de Ginzburg-Landau effectif constant, avec la limite de Pauli ($\alpha_{M0} \gg 1$) menant à une augmentation soudaine de ce paramètre lorsque la température est augmentée vers T_c avec $B < T_c/(\mu\alpha_{M0})$ (proximité de T_c). Cela donne une signature additionnelle de la supraconductivité dans la limite de Pauli permettant d'identifier des systèmes expérimentaux tels que URu₂Si₂, NpPd₅Al₂ et possiblement UBe₁₃ comme étant des éléments de cette catégorie.

Chapter 12

Conclusion de la deuxième partie

Nous avons présenté un mécanisme pour comprendre le magnétisme qui est lié à la supraconductivité dans CeCoIn_5 . Le ralentissement de l'exciton de spin du supraconducteur avec fonction d'onde $d_{k_a^2 - k_b^2}$ induit par un champ magnétique Zeeman constitue un scénario naturel où le magnétisme est stimulé par la supraconductivité d'une façon intrinsèque. Une image physique de l'approche spin-fermion est reliée au modèle à deux fluides pour les composés à fermions lourds Ce115 . Une fraction des électrons consiste en des spins localisés couplés à des fermions itinérants qui participent à la supraconductivité.

L'analyse du modèle spin-fermion avec anisotropie magnétique uniaxiale et champ magnétique transverse montre que le comportement critique est une conséquence du développement de poches de Fermi par le champ magnétique Zeeman dans le supraconducteur nodal avec un réglage du niveau d'énergie vers la proximité d'une divergence logarithmique dans la fonction de polarisation en spin. Un calcul numérique démontre que le vecteur d'onde de l'ordre statique est presque commensuré connectant les régions de la zone de Brillouin proche des points chauds. La dépendance par rapport au champ

magnétique de l'énergie de la résonance ainsi calculée est en bonne correspondance avec l'expérience.

Les spécificités du supraconducteur à électrons lourds CeCoIn_5 apportent toutes les conditions (transition du premier ordre comme conséquence de la limitation de Pauli, dimensionnalité proche de deux, symétrie de fonction d'onde du supraconducteur $d_{k_a^2 - k_b^2}$, proximité de l'antiferromagnétisme) pour réaliser cette transition d'état fondamental.